Australian Government
Geoscience Australia

Geoscience Australia Survey 238 Post-cruise Report

Sources and sinks of terrigenous sediments in the Southern Gulf of Carpentaria

RV *Southern Surveyor* 04/2003 May-June 2003

Andrew Heap, Peter Harris, Vicki Passlow, Theodore Wassenberg, Michael Hughes, Laura Sbaffi, Emma Mathews, Melissa Fellows, Leharne Fountain, Rick Porter-Smith, James Daniell, Cameron Buchanan, & Lisette Robertson

Record
2006/11

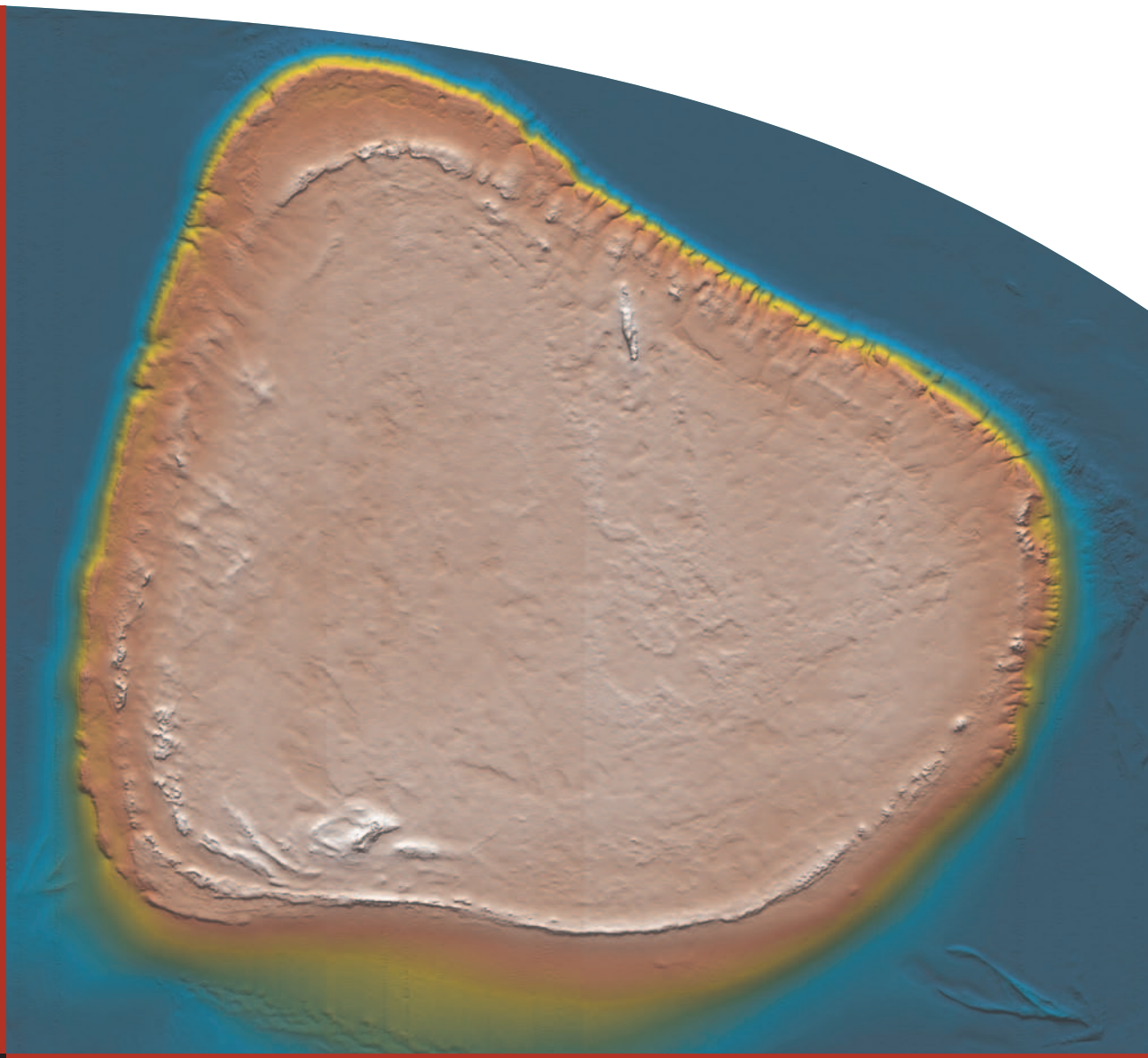

Geoscience Australia Record 2006/11

Geoscience Australia Survey 238

Post-survey Report

Sources and sinks of terrigenous sediments in the Southern Gulf of Carpentaria

RV *Southern Surveyor* Survey 04/2003

May – June 2003

Andrew Heap[1], Peter Harris[1], Vicki Passlow[1], Theodore Wassenberg[2], Michael Hughes[3], Laura Sbaffi[1], Emma Mathews[1], Melissa Fellows[1], Leharne Fountain[1], Rick Porter-Smith[1], James Daniell[1], Cameron Buchanan[1], and Lisette Robertson[4]

[1.] Geoscience Australia, GPO Box 378, Canberra, ACT 2601
[2.] CSIRO – Marine and Atmospheric Research, PO Box 120, Cleveland, QLD 4163
[3.] School of Geosciences, University of Sydney, Sydney, NSW 2006
[4.] Antarctic CRC, University of Tasmania, Hobart, TAS 7001

Australian Government
Geoscience Australia

Department of Industry, Tourism & Resources

Minister for Industry, Tourism & Resources: Senator The Hon. Ian Macfarlane, MP
Parliamentary Secretary: The Hon. Bob Baldwin, MP
Secretary: Mark Paterson

Geoscience Australia

Chief Executive Officer: Dr Neil Williams

ISSN: 1448-2177
ISBN: 1 920871 83 7

GeoCat No. 64162

Bibliographic reference: Heap, A., Harris, P., Passlow, V., Wassenberg, T., Hughes, M., Sbaffi, L., Mathews, E., Fellows, M., Fountain, L., Porter-Smith, R., Daniell, J., Buchanan, C., & Robertson, L. (2006). *Sources and Sinks of Terrigenous Sediments in the Southern Gulf of Carpentaria – post survey report*. Geoscience Australia, Record 2006/11, 106pp.

Correspondence for feedback:
Sales Centre
Geoscience Australia
GPO Box 378
Canberra
ACT 2601

Sales@ga.gov.au

Contents

Page

List of Figures v

List of Tables vii

Executive Summary ix

1. Introduction 1

1.1. Background 1

1.1.1. Regional Setting – Gulf of Carpentaria 1

1.1.2. Research Aims and Survey Objectives 5

1.2. General Survey Itinerary 5

1.3. Survey Participants 7

1.3.1. Scientific Personnel 7

1.3.2. Ship's Crew 7

2. Geophysics 8

2.1. Data Acquisition 8

2.1.1. Multibeam (Swath) Sonar Mapping 8

2.1.2. Shallow Seismic Reflection 8

2.2. Data Processing and Analysis 8

2.2.1. Multibeam (Swath) Sonar Data 8

2.2.2. Shallow Seismic Reflection Data 10

2.3. Results 10

2.3.1. Multibeam (Swath) Sonar 10

2.3.2. Shallow Seismic Reflectors 16

2.3.3. Acoustic Facies 20

3. Oceanography 27

3.1. Data Acquisition 27

3.1.1. BRUCE Deployment 27

3.2. Results 28

3.2.1. Water Levels 28

3.2.2. Tidal Currents 29

3.2.3. Turbidity 31

4. Sedimentology 33

4.1. Sample Acquisition 33

4.1.1. Water Samples 36

4.1.2. Digital Video Footage 36

4.1.3. Surface Sediment Sampling 37

4.1.4. Benthic Biota Sampling 38

4.1.5. Subsurface Sediment Sampling 38

4.2. Sample Processing and Analysis 39

4.2.1. Water Samples 39

4.2.2. *Digital Video Footage* 39
4.2.3. *Surface Sediments* 40
4.2.4. *Subsurface Sediments* 41
4.3. Results 44
4.3.1. *Water Samples* 44
4.3.2. *Digital Video Footage* 55
4.3.3. *Surface Sediments* 61
4.3.4. *Benthic Biota* 73
4.3.5. *Subsurface Sediments* 75

5. Discussion 85
5.1. Sources and Sinks of Terrigenous Sediment 85
5.2. Late Quaternary Evolution 86
5.2.1. *Deposition of Shelf Sequences* 86
5.2.2. *Development of the Submerged Reefs* 89

6. Acknowledgements 93

7. References 94

8. Appendices 97
8.1. Appendix A – Survey Leaders Log 97
8.2. Appendix B – Shallow Seismic Reflection Profiles 101
8.3. Appendix C – Photographs of the BRUCE Mooring 101
8.4. Appendix D – Digital Video Footage 101
8.5. Appendix E – Scheffe's Test Results for CTD Data 101
8.6. Appendix F – Photographs of Benthic Biota 101
8.7. Appendix G – Textural Characteristics of Surface Sediments 101
8.8. Appendix H – Core Logs 104
8.9. Appendix I – Textural Characteristics of Subsurface Sediments 105

List of Figures

Page

1. Introduction 11

Figure 1.1. Regional map of Gulf of Carpentaria. 12
Figure 1.2. Map showing carbonate concentrations for Australian shelf 12
Figure 1.3. Map showing geomorphic features in Gulf of Carpentaria. 14
Figure 1.4. Map showing survey plan and study areas. 16

2. Geophysics 18

Figure 2.1. Map showing bathymetry of Area A: Regional Survey 22
Figure 2.2. Map showing bathymetry of Area B: Bryomol Reef. 23
Figure 2.3. Map showing bathymetry of Area C: Reef R1 23
Figure 2.4. Map showing bathymetry of Area D: Reef R2. 24
Figure 2.5. Map showing bathymetry of Area E: Reef R3. 25
Figure 2.6. Chirp shallow seismic reflection profile of seabed reflector. 26
Figure 2.7. Chirp shallow seismic reflection profiles of: a) pre-Holocene surface, b) widely-space sub-bottom reflections, and c) dipping reflections. 27
Figure 2.8. Sparker shallow seismic reflection profile over Reef R1. 28
Figure 2.9. Chirp shallow seismic reflection profiles of typical nature of sub-surface reflections. 29
Figure 2.10. Chirp shallow seismic reflection profile of: a) infilled channels, and b) infilled depressions of the pre-Holocene surface. 29
Figure 2.11. Maps of: a) acoustic facies, and b) corresponding seabed texture and composition for Area A: Regional Survey. 31
Figure 2.12. Maps of: a) acoustic facies, b) acoustic facies polygons, and c) corresponding seabed texture and composition for Area B: Bryomol Reef. 32
Figure 2.13. Maps of: a) acoustic facies, b) acoustic facies polygons, and c) corresponding seabed texture and composition for Area C: Reef R1. 33
Figure 2.14. Maps of: a) acoustic facies, b) acoustic facies polygons, and c) corresponding seabed texture and composition for Area D: Reef R2. 35
Figure 2.15. Maps of: a) acoustic facies, b) acoustic facies polygons, and c) corresponding seabed texture and composition for Area E: Reef R3 36

3. Oceanography 37

Figure 3.1. Map showing location of BRUCE oceanographic mooring. 37
Figure 3.2. Graph of tidal heights measured at the BRUCE mooring. 39
Figure 3.3. Graphs of: a) burst-averaged current speed, and b) current direction measured at the BRUCE mooring. 40
Figure 3.4. Progressive vector plot of tidal excursion at the BRUCE mooring. 41
Figure 3.5. Graph of turbidity recorded by the OBS sensors at the BRUCE mooring. 41
Figure 3.6. Graph of detail turbidity record at the BRUCE mooring. 42

4. Sedimentology 43

Figure 4.1. Photograph of CTD rosette. 46
Figure 4.2. Photograph of underwater digital video camera system. 47
Figure 4.3. Photograph of Smith-McIntyre grab sampler. 48
Figure 4.4. Photograph of benthic sled. 48
Figure 4.5. Photograph of vibrocorer. 49

Figure 4.6. Photograph of water filtering system. 50
Figure 4.7. Graphs of: a) temperature, b) salinity, and c) transmission for waters in Area A: Regional Survey. 55
Figure 4.8. Graph of near-bed and surface SSC from Area A: Regional Survey. 56
Figure 4.9. Graphs of: a) temperature, b) salinity, and c) transmission for waters in Area B: Bryomol Reef. 57
Figure 4.10. Graph of near-bed and surface SSC from Area B: Bryomol Reef. 59
Figure 4.11. Graphs of: a) temperature, b) salinity, and c) transmission for waters in Area C: Reef R1. 60
Figure 4.12. Graph of near-bed and surface SSC from Area C: Reef R1. 61
Figure 4.13. Graphs of: a) temperature, b) salinity, c) transmission, d) salinity v transmission, e) temperature v transmission, and e) temperature v salinity for Area D: Reef R2. 62
Figure 4.14. Graphs of: a) temperature, b) salinity, and c) transmission for a N-S transect in the southern Gulf of Carpentaria. 64
Figure 4.15. Map of camera stations for Area A: Regional Survey. 67
Figure 4.16. Map of camera stations for Area B: Bryomol Reef. 68
Figure 4.17. Map of camera stations for Area C: Reef R1. 69
Figure 4.18. Map of camera stations for Area D: Reef R2. 69
Figure 4.19. Map of camera stations for Area E: Reef R3. 70
Figure 4.20. Maps of: a) mean grain size, b) %Gravel, c) %Sand, and d) %Mud for surface sediments in Area A: Regional Survey. 72
Figure 4.21. Maps of: a) %$CaCO_3$(Bulk), b) %$CaCO_3$(Sand), c)$CaCO_3$(Mud) for surface sediments in Area A: Regional Survey. 74
Figure 4.22. Maps of: a) mean grain size, b) %Gravel, c) %Sand, and d) %Mud for surface sediments in Area B: Bryomol Reef. 75
Figure 4.23. Maps of: a) %$CaCO_3$(Bulk), b) %$CaCO_3$(Sand), c)$CaCO_3$(Mud) for surface sediments in Area B: Bryomol Reef. 77
Figure 4.24. Maps of: a) mean grain size, b) %Gravel, c) %Sand, and d) %Mud for surface sediments in Area C: Reef R1. 78
Figure 4.25. Maps of: a) %$CaCO_3$(Bulk), b) %$CaCO_3$(Sand), c)$CaCO_3$(Mud) for surface sediments in Area C: Reef R1. 79
Figure 4.26. Maps of: a) Gravel:Sand:Mud, and b) %$CaCO_3$(Bulk), %$CaCO_3$(Sand) and %$CaCO_3$(Mud) for surface sediments in Area D: Reef R2. 80
Figure 4.27. Maps of: a) Gravel:Sand:Mud, and b) %$CaCO_3$(Bulk), %$CaCO_3$(Sand) and %$CaCO_3$(Mud) for surface sediments in Area E: Reef R3. 82
Figure 4.28. Graph of composition of benthic biota in the southern Gulf of Carpentaria. 84
Figure 4.29. Graph of fossil composition for surface sediments in southern Gulf of Carpentaria. 85
Figure 4.30. Graph of fossil biota taxa for surface sediments in southern Gulf of Carpentaria. 86

5. Discussion 95
Figure 5.1. Generalized facies diagram for the southern Gulf of Carpentaria. 97
Figure 5.2. Late Quaternary eustatic sea level curve for northeast Australia and PNG. 98
Figure 5.3. Graph of radiocarbon ages <40 kyr BP from northeast Australia. 98
Figure 5.4. Hypsometric curves for Reefs R1, R2 and R3. 100
Figure 5.5. Sea level curve showing times of reef development in southern Gulf of Carpentaria. 101

List of Tables

Page

1. Introduction 11

Table 1.1. Geomorphic features of the Gulf of Carpentaria. 13

2. Geophysics 18

Table 2.1. Summary details of multibeam (swath) sonar surveys. 21
Table 2.2. Acoustic facies and sediment composition for Area A: Regional Survey. 32
Table 2.3. Acoustic facies and sediment composition for Area B: Bryomol Reef. 33
Table 2.4. Acoustic facies and sediment composition for Area C: Reef R1. 34
Table 2.5. Acoustic facies and sediment composition for Area D: Reef R2. 35
Table 2.6. Acoustic facies and sediment composition for Area E: Reef R3. 36

3. Oceanography 37

Table 3.1. Tidal constituents for the BRUCE mooring. 39

4. Sedimentology 43

Table 4.1. Summary details of operations undertake at: a) Area A: Regional Survey, b) Area B: Bryomol Reef, c) Area C: Reef R1, d) Area D: Reef R2, and e) Area E: Reef R3. 43
Table 4.2. List of grab samples analysed for fossil content of surface sediments. 51
Table 4.3. Summary details of analyses undertaken on vibrocores. 52
Table 4.4. Results of a one-way Analysis of Variance (ANOVA) for water properties from Area A: Regional Survey. 55
Table 4.5. a) Descriptive statistics for near-bed and surface SSC's, and b) z-test results for difference between means for SSC's. 56
Table 4.6. Results of a one-way Analysis of Variance (ANOVA) for water properties from Area B: Bryomol Reef. 58
Table 4.7. Results of a one-way Analysis of Variance (ANOVA) for water properties from Area C: Reef R1. 61
Table 4.8. Results of a one-way Analysis of Variance (ANOVA) for water properties from a N-S transect of the southern Gulf of Carpentaria. 64
Table 4.9. Results of a Scheffe's post-hoc comparison test for water properties from a N-S transect of the southern Gulf of Carpentaria. 65
Table 4.10. Results of a one-way Analysis of Variance (ANOVA) for near-bed and surface SSC's. 66
Table 4.11. Number of benthic biota species collected by different sampling devices. 84
Table 4.12.. Major sources of bioclastic material in surface sediments of southern Gulf of Carpentaria. 86
Table 4.13. AMS radiocarbon and calibrated age determinations for vibrocore samples. 88
Table 4.14. Summary details of physical properties for sub-surface facies in Area A: Regional Survey 92
Table 4.15. Summary details of physical properties for sub-surface facies in Area B: Bryomol Reef. 93
Table 4.16. Summary details of physical properties for sub-surface facies in Area C: Reef R1. 94

5. Discussion **95**
Table 5.1. Water depths of reefal features from multibeam sonar data. 100

8. Appendices **107**
Table 8.1. Texture and composition of surface sediment samples collected in: a) Area A: Regional Survey, b) Area B: Bryomol Reef, c) Area C: Reef R1, d) Area D: Reef R2, and e) Area E: Reef R3. 111

Executive Summary

This report contains the preliminary results of Geoscience Australia survey 238 to the southern Gulf of Carpentaria. The survey was completed to provide fundamental geoscience information on the nature of key shallow seabed environments in northern Australia. The survey has led to an improved understanding of the Late Quaternary sources and sinks of terrigenous sediments in the southern gulf, and in particular increased our knowledge of the geologic evolution of the region. The data have also allowed an examination of the relationships between oceanographic processes, marine geology, geomorphology, and benthic habitats and biota. Data and knowledge gained from the survey will support sustainable use of Australia's marine environment by addressing the need for information about deciding how to provide adequate protection for the marine environment where detailed seabed information is lacking. The principal research aims of the survey were to: 1) identify and quantify terrigenous sediment sources and sinks and the Late Quaternary evolution of the southern Gulf, and 2) identify and characterise the benthic habitats.

The southern Gulf of Carpentaria is a unique study site as it is the largest area of terrigenous dominated sedimentation on Australia's continental shelf. Notwithstanding biogenic sources, approximately two thirds of the modern shelf sediment in the southern Gulf of Carpentaria (>100,000 km^2) is composed of terrigenous material. This region of the gulf is characterised by a range of sedimentary environments including: shallow shelf (open marine), reefal platforms (and their associated deposits and biota), transgressive fluvial-deltas, river beds, as well as the last glacial land surface.

A total of five study areas were investigated. Initially, a regional survey of the southern gulf was undertaken to provide data on the different sedimentary environments. Four smaller areas were then studied in detail to characterise smaller-spatial scale differences in seabed environments. These four smaller areas were selected from the regional survey and comprise high-standing carbonate platforms on the gulf floor that represent distinctive reefal environments.

The investigation of the four reefal platforms revealed three to be newly discovered submerged coral reefs. The reefs contain distinctive morphologies including: marginal ridges (representing multiple phases of reef growth), reef crests, talus slopes, spur and grooves on the fore-reef slope, flat central platforms (lagoons), and eroded terraces. Overall reef morphology indicates that they developed during the Late Quaternary, with modern growth forming a thin mantle over an older reef framework. Reef-associated biota is common to inner-shelf reefs in northern Australia. A small (but healthy) modern coral factory has prevented them reaching present level. The discovery of these well-developed submerged reefs is significant because the southern Gulf is a region not previously recognised as being suitable for coral reef growth. The implication of the presence of the submerged reefs is that reef development was much more extensive in northern Australia in the past.

The seabed in the southern Gulf of Carpentaria is characterised by moderately- to poorly-sorted muddy sands and gravels. The modern seabed sediment is patchy and generally forms a thin (<2 m) veneer over the last glacial land surface. Hard-grounds are also common, with the last glacial land surface cropping out on the seabed. These sub-crops form complicated crescent-shaped patterns on the seabed and form substrates for a variety of benthic organisms.

Benthic biota is very diverse, with 569 individual taxa identified within 64 major taxonomic groups. Crustaceans were most abundant followed by bivalves, sponges and soft corals. Sediment composition showed trends between the different seabed habitats, with sites in the central gulf containing higher abundances and diversity than those near the coast. This pattern reflects the presence of terrigenous dominated sediments in the southern gulf inner-shelf regions.

Water properties (temperature, salinity and transmission) are very similar throughout the southern Gulf; greatest differences were observed at sites from the deeper central regions compared with those of the shallower inner-shelf regions in the south. Tides in the southern gulf are diurnal. Near-bed currents attained 0.6 m s^{-1} during spring tides and <0.25 m s^{-1} during neap tides. Measured near-bed turbidity was <5.6 FTU throughout the survey. These results indicate that the waters in the southern Gulf of Carpentaria are relatively well mixed and clear during the survey.

Terrigenous sediment in the southern gulf is derived from local rivers with significant input from reworking of terrigenous grains from the gulf floor during the latest post-glacial sea level rise. Concentrations of terrigenous sediment are high in the southern gulf because the transgressing shoreline eroded a vast area (>400,000 km^2) during the Holocene post-glacial sea-level rise, and a large proportion of this material has been deposited in the southern gulf. The Holocene evolution of the southern Gulf of Carpentaria has thus been characterised by backfilling of channels and shoreline reworking of terrigenous sediments across the gulf floor, followed by reef development and contemporaneous carbonate-dominated deposition in a shallow tropical shelf environment.

1. Introduction

This record contains the preliminary results of Geoscience Australia marine survey 238 (SS04/2003) to southeast Gulf of Carpentaria. The survey was completed between 9 May and 10 June 2003 using Australia's national facility research vessel *Southern Surveyor*. The survey included Geoscience Australia and CSIRO – Marine and Atmospheric Research scientists.

Geoscience Australia undertook the survey to provide fundamental geoscience information on the nature of key shallow seabed environments in northern Australia. Major drivers for the survey were to develop an improved understanding of the Late Quaternary sources and sinks of terrigenous sediments in the southern Gulf to increase our knowledge of the geologic evolution of the region, and to examine the relationships between oceanographic processes, marine geology, geomorphology, and benthic habitats and biota. One of the biggest challenges facing marine managers is deciding how to provide adequate protection for the marine environment in regions where detailed seabed information is lacking. This work supports the federal government's designated national research priority of an "Environmentally sustainable Australia" by assisting with the sustainable use of Australia's marine environment.

A second survey by Geoscience Australia to the southern Gulf of Carpentaria is planned for March-April 2005. This second survey is designed to investigate potential submerged reefs in the southern Gulf to provide crucial information on the nature of seabed habitats in the southern gulf in support of regional marine planning in northern Australia.

1.1. BACKGROUND

The northern margin of Australia is one of the largest tropical shallow shelf regions on Earth, and the Gulf of Carpentaria is the largest modern example of a tropical epicontinental seaway that forms a broad shallow basin extending from Cape Wessel in the west to the top of the Cape York Peninsula in the east (Fig. 1.1). The gulf and adjacent shallow shelf regions form part of a modern analogue for the large tropical shallow seas that occurred over North America in the Carboniferous Period approximately 286-320 million years ago (Edgar et al., 2003). The gulf represents the best modern analogue for these ancient cratonic basins where the geology, oceanography and climate are reasonably well-known compared with these ancient systems (Dott & Batten, 1976; Baldwin & Butler, 1982).

The Gulf of Carpentaria also contains Australia's largest shelf province of terrigenous dominated sedimentation (Fig. 1.2). This region covers an area of >100,000 km^2 where surface sediments have an average siliciclastic content of >50%. The adjacent coastline is characterised by prograding depositional environments (deltas and chenier plains), indicative of large sediment discharge from the hinterland to the coast throughout the Holocene. A principal aim of the survey is to identify and quantify sediment sources, sinks and the Late Quaternary history of terrigenous sedimentation in the region.

This information is of fundamental importance for understanding the evolution, processes and seabed environments of this unique shelf province, and for the successful management of regional river catchments and the adjacent offshore environment.

1.1.1. Regional Setting – Gulf of Carpentaria

Most of the Gulf of Carpentaria forms a shallow (<70 m) low-gradient basin that covers an area of >400,000 km^2 (Fig. 1.3; Table 1.1). In the northwest, it is connected to the Arafura Shelf

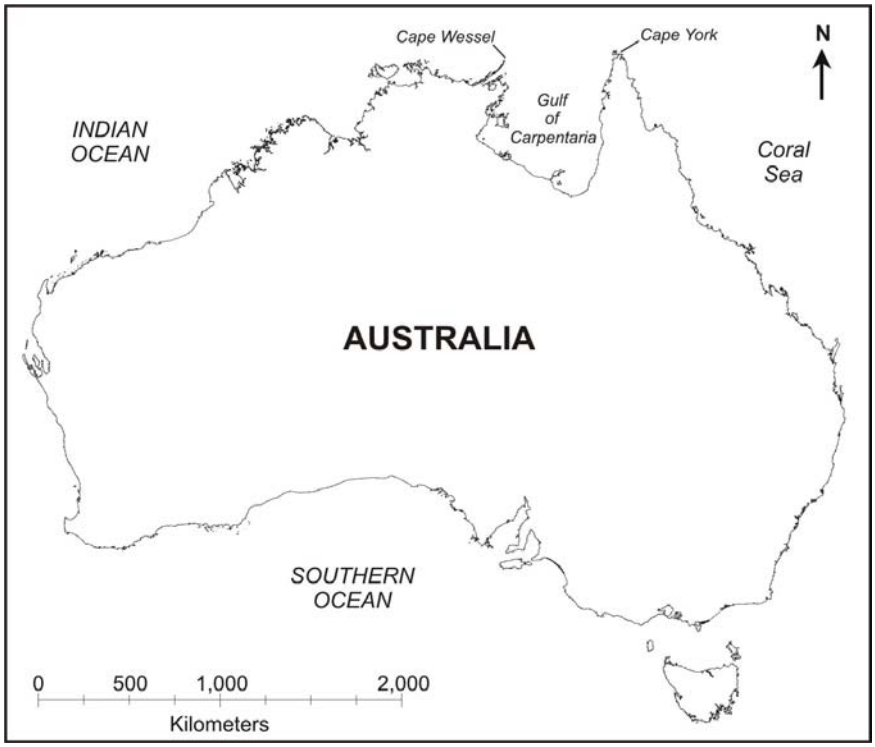

Figure 1.1. Map showing location of Gulf of Carpentaria. The gulf forms a 400,000 km^2 epicontinental seaway on the tropical northern margin of Australia.

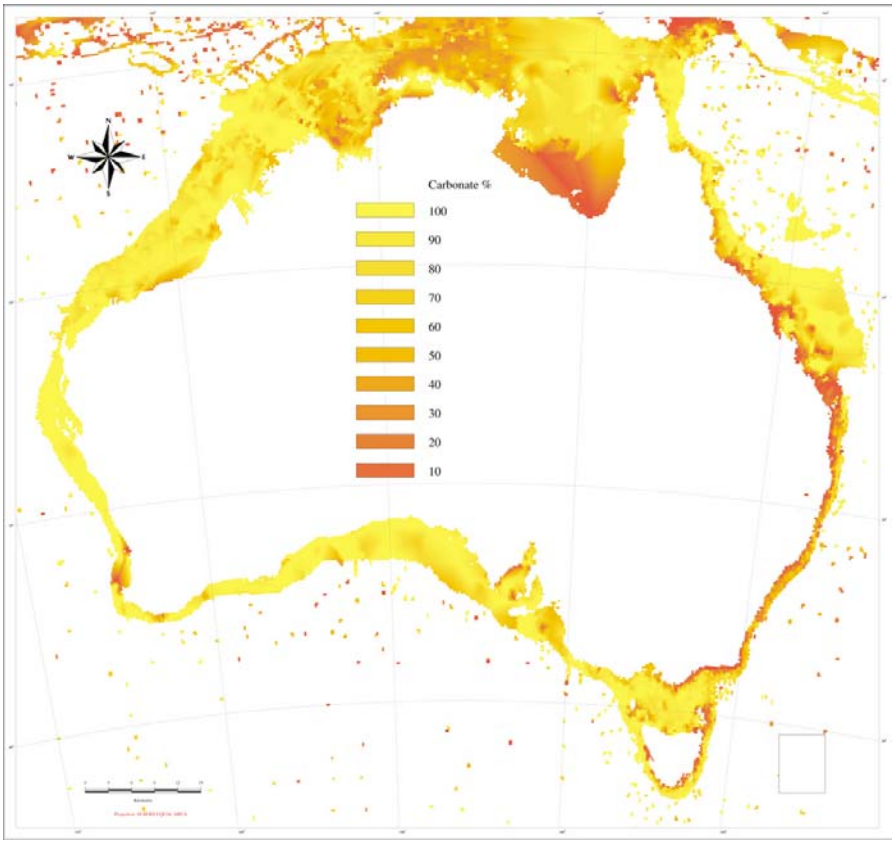

Figure 1.2. Map showing carbonate concentrations around Australia. The southern Gulf of Carpentaria represents the largest area of terrigenous-dominated sedimentation on the Australian margin. The area of the Gulf of Carpentaria where concentrations of siliciclastic sediment attain >50% is approximately 100,000 km^2. Data from Geoscience Australia's MARS sediment database (www.ga.gov.au/oracle/mars).

across the 53 m deep Arafrua Sill (Harris et al., 1991; Chivas et al., 2001). This sill has greatly influenced sedimentation and the nature of sedimentary environments in the gulf and adjacent Arafura Shelf by regulating the transport of water and sediments between the two regions over glacial cycles.

Table 1.1. Geomorphic features of the Gulf of Carpentaria.

Geomorphic Feature	Area (km^2)	Percent
Shelf*	178,113	42.95
Bank/shoal	2,102	0.51
Deep/hole/valley	1,322	0.32
Basin	206,953	49.90
Reef	141	0.03
Ridge	599	0.14
Pinnacle	250	0.06
Plateau	5,078	1.22
Saddle	501	0.12
Sill	10,988	2.65
Terrace	7,435	1.79
Sandwave/sand bank	1,233	0.29
Total	414,715	100

* Shelf area is less the surface areas of superimposed features.

The seabed over most of the Gulf of Carpentaria forms a low-gradient (<1:18,000) plain (Harris et al., 2004). Deepest parts of the gulf are located in the east, where water depths are 70 m, but over most of the gulf water depths are between 50 to 60 m, with deviations of <2 m (Chivas et al., 2001). The Arafura Sill, which formed the northwest drainage boundary of the gulf during periods of low sea level, covers an area of >10,000 km^2 with a relief of <2 m (Torgersen et al., 1983). During the Late Quaternary, during sea level lowstands, the Gulf of Carpentaria contained a freshwater to brackish lake called Lake Carpentaria (Torgersen et al., 1983, 1988; Chivas et al., 2001). At its greatest extent, Lake Carpentaria would have covered an area of 165,000 km^2 and attained a maximum depth of 15 m (Jones & Torgersen, 1988). Palaeo-shorelines have been reported from around the basin margins, recognised from erosional unconformities of regional extent in shallow seismic profiles and bathymetric surveys (Torgersen et al., 1983; Edgar et al., 1994, 2003).

In the south, in the region of high terrigenous sedimentation, the seabed is more variable and contains small rounded pinnacles and broad, flat-topped plateaus (Fig. 1.3). These pinnacles and high points are inferred to be submerged continental rocks, protruding through nearshore and pelagic sediments on the seabed. They represent unique seabed habitats compared to the surrounding relatively flat seabed. They likely formed islands when Lake Carpentaria existed. Offshore-trending shelf channels up to several hundred metres wide and several tens of metres deep occur in water depths of 30 m (Jones, 1986). These channels, which typically have surface expression as sinuous depressions in the seabed, appear to be the continuation of onshore drainage features that were presumably more active during periods of lower sea level.

The surface sediments of the Gulf of Carpentaria are reasonably well studied (e.g., Phipps, 1970, 1980; Jones, 1986, 1987; Jones & Torgersen, 1988; Harris 1994) and the distribution of seabed facies is reasonably well-established. Of major interest in the present survey is the high concentration of siliciclastic sediments in the southern gulf. Large prograding delta and strandplain/beach ridge deposits contain significant amounts of terrigenous sediment. Because the discharge of coastal rivers is very large during the

summer monsoon, the terrigenous sediments are transported offshore. If (and how) these sediments contribute to the modern sediment budget in the southern gulf is not clear.

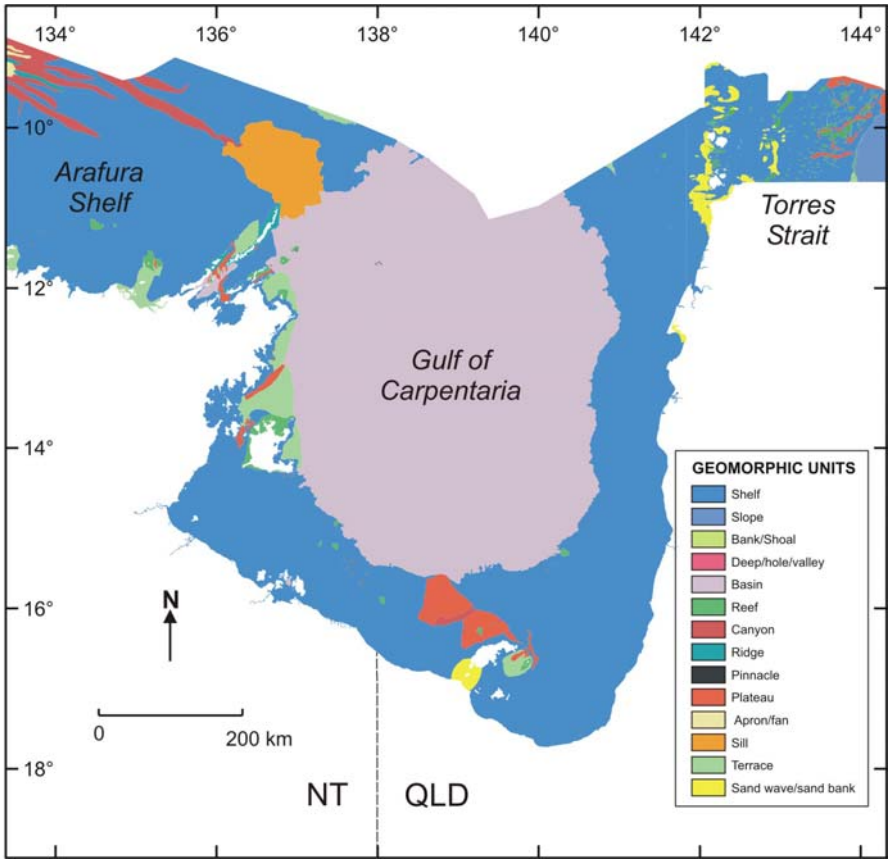

Figure 1.3. Map showing the major geomorphic features in the Gulf of Carpentaria. A total of 12 geomorphic features occur in the gulf, dominated by a broad, low-gradient basin. High standing terraces, plateaus and reef features occur in the southern and western regions of the gulf.

The Gulf of Carpentaria has been subjected to erosional and depositional processes in fluvial, lacustrine and marine environments throughout the Late Quaternary. Inter-bedded marine, coastal and lacustrine deposits have been recovered to a depth of 14 m in shallow cores from the central gulf (Phipps, 1980; Chivas et al., 2001). Laminated mud about 1 m thick occurs in cores recovered from the inferred confines of Lake Carpentaria. The mud is overlain by a unit of marine sandy mud up to 1 m thick, and unconformably overlies subaerially weathered cohesive clay of marine/estuarine origin. Analyses of $\delta^{13}C$ and C/N ratios indicate that the lowstand gulf plain was covered by C_4 savannah grasslands and not C_3 woodland, mangrove and tropical rainforest vegetation which borders the gulf today (Chivas et al., 2001). Shallow seismic sections reveal that the upper-most 150 m of sediment has been incised by numerous channels (Edgar et al., 2003). The largest of these channels are >70 m deep and >10 km wide. The channels are widely distributed and point to Late Quaternary periods when large river systems crossed the lowstand gulf plain. No major river incision is thought to have occurred around the present-day gulf margins because the onshore and offshore gradients are similar (Jones et al., 2003). Smaller deeply-incised channels on the inner-shelf have been interpreted as tidally-incised and inferred to be filled with Holocene sediments (Jones, 1986). Despite this previous work, the nature of the Late Quaternary evolution of the southern Gulf of Carpentaria is poorly resolved and the timing relatively un-constrained.

1.1.2. Research Aims and Survey Objectives

The principal research aims of the survey to the southern Gulf of Carpentaria were to: 1) identify and quantify sediment sources, sinks and the Late Quaternary history of terrigenous sedimentation, and 2) identify and characterise benthic habitats. These research objectives were designed to gain a better understanding of the terrigenous and carbonate sediment budgets for the region. The southern Gulf of Carpentaria was selected because it contains the largest area of terrigenous dominated sediment on the Australian shelf and thus represents a unique environment. To address these aims the following objectives were formulated:

- Identify and quantify sediment sources, sinks and the Late Quaternary history of terrigenous and carbonate sedimentation in the southern Gulf of Carpentaria;
- Locate and map areas on the shelf characterised by modern terrigenous and carbonate deposition;
- Derive sediment budgets representative of the main depositional environments;
- Date the onset of Holocene, pro-deltaic to distal deltaic/open shelf terrigenous sediment deposition as a function of distance from the coast; and
- Validate Geoscience Australia's GEOMAT sediment mobility model and its prediction of southward oriented maximum tidal current vectors adjacent to Mornington Island.

A selection of geoscience techniques was applied to realise the research aims of the study, including: intensive multibeam (swath) sonar and high-resolution shallow seismic reflection surveys; capture of high-resolution digital video footage of the seabed; and an extensive program of seabed sampling and shallow coring. All of the data collected on this survey are contained in Geoscience Australia's marine samples database (MARS) which can be interrogated over the web at http://www.ga.gov.au/oracle/mars.

1.2. GENERAL SURVEY ITINERARY

The RV *Southern Surveyor* arrived in the south-central Gulf of Carpentaria and proceeded to steam to the south along a regional survey grid collecting multibeam (swath) sonar and shallow seismic reflection data (Fig. 1.4). The regional survey was designed to provide a broad overview of the seabed morphology, surface sediment facies and sub-surface stratigraphy, and facilitate the identification of major sub-surface features in seismic profiles. Specifically, the regional survey lines were positioned so as to intercept low-stand river channels that were expected to extend out into the gulf, directly seawards of the present-day Norman River (Fig. 1.1).

At 20 nautical mile intervals the ship was stopped and CTD, surface grab sample, underwater video, and benthic sled samples were collected. This continued until station 21, after which 18 vibrocores (VC1-18) were collected at 18 sites (stations 22-29) selected from the shallow seismic reflection data. The vibrocore sites were chosen to sample representative modern-day depositional environments and intersect late-Quaternary deposits, specifically filling palaeo-channels. At station 9, Geoscience Australia's oceanographic mooring BRUCE was deployed (see section 3.1.1 for details).

The regional survey grid was also used to select sites for detailed multibeam (swath) mapping along close-spaced parallel lines. The first of these (Area A; Fig. 1.4) was conducted in a region where the CSIRO had established three control sites used to assess the impacts of trawling on the seabed. Trawl boards are known to plough the seabed, disturbing the seabed biota and leaving large parallel grooves. The sites under investigation included areas that

had been trawled and control areas that were used to assess the impacts of trawling. The multibeam (swath) mapping revealed the seabed in Area A to be relatively flat and featureless, and no trawl marks could be detected in the sonar or bathymetry data.

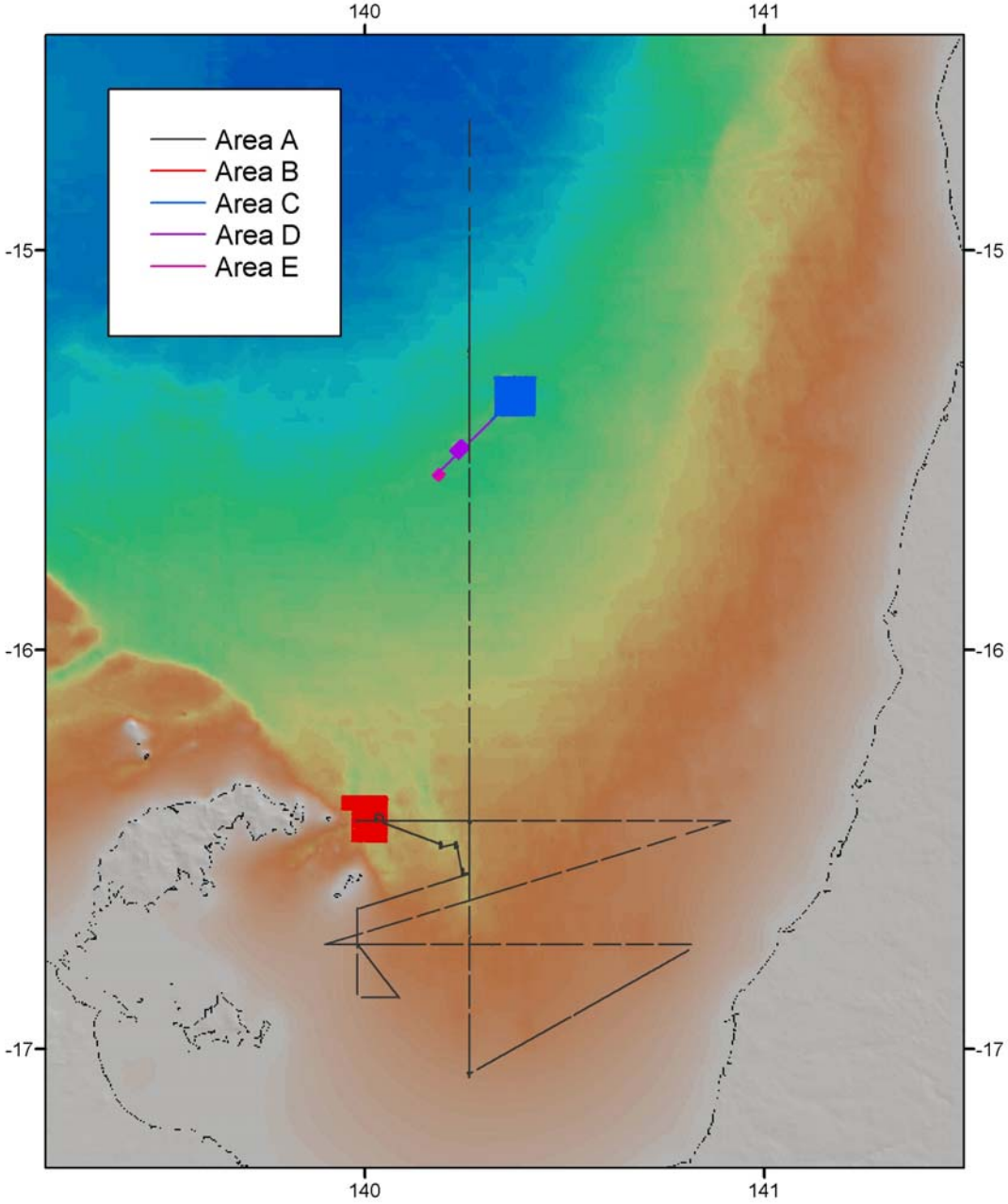

Figure 1.4. Map showing the general survey plan. The long survey lines represent the regional survey (Area A). This survey was designed to provide a regional picture of the seabed sedimentology of the southern Gulf. The smaller surveys (Areas B, C, D, and E) focussed on individual features that were revealed by the regional survey. The sampling programs designed for each of the study areas was tailored to the size and objectives for each area.

Multibeam (swath) mapping and sampling of Areas B, C, D, and E (Fig. 1.4) were completed in succession. Mapping of Area C was interrupted for several days while the ship refuelled at Weipa. Line spacing and orientation in the sampling grids was adjusted in each area to account for water depth and the bathymetry. In each area, stations were sampled to capture a representative suite of modern-day sedimentary environments, seabed habitats, and sub-surface facies. The survey leaders log is detailed in Appendix A.

1.3. SURVEY PARTICIPANTS

1.3.1. Scientific Personnel

Dr Peter Harris (GA) – Cruise Leader
Dr Andrew Heap (GA) – Co-Cruise Leader
Dr Vicki Passlow (GA) – Sedimentology, biological sampling
Dr Ted Wassenberg (CSIRO) – Biological sampling
Mr Rick Smith (GA) – Computer support, water sample analysis
Mr James Daniell (GA) – Computer support, multibeam (swath) bathymetry
Mr Cameron Buchanan (GA) – Computer support, multibeam (swath) bathymetry
Mr Jon Stratton (GA) – Technician (sediment sampling, video/corer operations)
Mr Lyndon O'Grady (GA) – Technician (sediment sampling, video/corer operations)
Mr Kevin Hooper (JCU) – Electronics technician (multibeam and Chirper operations)
Ms Pamela Brodie (CSIRO) – Computer support
Mr Steven Thomas (CSIRO) – Electronics technician

1.3.2. Ship's Crew

Mr Neil Cheshire – Master
Mr John Boyes – 1st Mate
Mr Chris McGuire – 2nd Mate
Mr John Morton – Chief Engineer
Mr David Jonkers – 1st Engineer
Mr Jim Gaffey – 2nd Engineer
Mr Mal McDougall – Bosun
Mr Tony Hearne – IR
Mr Graham McDougall – IR
Mr Paul O'Neill – IR
Mr Mathew Carden – IR
Mr Gary Phillips – Chief Cook
Ms Angie Zutt – 2nd Cook
Mr David Wilcox – Chief Steward

2. Geophysics

A comprehensive geophysical survey was conducted to determine seabed morphology and the composition of the seabed features. The survey consisted of a regional reconnaissance survey followed by intensive multibeam (swath) mapping of the study areas. In each of the study areas, both multibeam sonar and shallow seismic reflection data were collected. The geophysical surveys were used as the basis for determining the location of the oceanographic moorings (Section 3) and to design a sediment sampling strategy (Section 4).

2.1. DATA ACQUISITION

2.1.1. Multibeam (Swath) Sonar Mapping

A Reson™ 240 kHz swath system (model no. 8101) was hired from the School of Earth Sciences at James Cook University for the purposes of gathering high-resolution bathymetry and sonar (backscatter) images of the study areas. The transducer head was fixed to a "trolley" located in the vessel's moon-pool, which was located approximately 4 m to starboard of the centre line. This configuration ensured that the transducer head projected approximately 0.5 m below the hull. The motion sensor was mounted on the centre line. The Reson™ 8101 multibeam system was operated at 9 km hr^{-1} (5 knots) in smooth to slight seas. A total of 3,275 line-km of data (70 GB) was recorded using 6042 Ver. 7.2 format software. The acoustic signals were corrected for temperature and salinity of the seawater using an Applied Microsystems Ltd SV PLUS™ acoustic velocity profiler, which measured an acoustic velocity of seawater of 1542-1546 m s^{-1} in the study area.

2.1.2. Shallow Seismic Reflection

A Datasonics™ 3.5 kHz Chirp sub-bottom profiler (recorder model no. DSP661/66; tow fish model TTV170S) was towed approximately 50 m behind the vessel at 9 km hr^{-1} (5 knots) in smooth to slight seas. The tow-fish was towed approximately 6 m below the sea surface and the trigger interval was 0.5 to 0.25 seconds (0.25 s ≤180 m water depth; 0.5 s >180 m water depth). A total of 3,505 line-km of shallow seismic data (30 GB) were collected over the survey area. At select locations an EG&G™ Sparker system was also deployed in conjunction with the Chirper to provide sub-bottom information where greater penetration was required to image underlying sedimentary strata. Approximately 400 line-km of Sparker data was collected from the study area.

2.2. DATA PROCESSING AND ANALYSIS

Processing of the multi-beam sonar data was a priority. This is because it was necessary to monitor the data to assist with site selection and in improving the survey plan (line spacings, line lengths, etc.). All of the post-processing of the multibeam (swath) sonar data, including data editing, tide corrections and sound velocity profile corrections were undertaken using the Caris™ HIPS/SIPS v5.3 processing software. Data from the sub-bottom profiler was not processed or interpreted during the survey.

2.2.1. Multibeam (Swath) Sonar Data

The multibeam (swath) sonar data were initially acquired in the proprietary Reson™ *.db format. Each line consisted of a separate file to keep the file sizes manageable. The data for

each line were converted to Extended Triton-Elics (XTF) format using the *ExportXTF* module supplied with the Reson™ 6024v7 software. This conversion allowed the data to be imported into the Caris™ HIPS/SIPS processing software.

2.2.1.1. General Processing Procedure

The acoustic signals were corrected for temperature and salinity of the seawater using an Applied Microsystems Ltd SV PLUS™ acoustic velocity profiler. As expected, the sound velocity profiles showed very little variation through the water column, which is well mixed. The acoustic velocity of seawater was measured at 1,542-1,546 m s^{-1}.

A pressure sensor on the current meter deployed in Area B: Bryomol Reef recorded tidal heights during the survey. These heights were used to correct the data to mean sea level. Finally, individual soundings were visually inspected using the Caris™ HIPS/SIPS processing software and bad data were removed to create a level and clean dataset relative to mean sea level.

2.2.1.2. Data Analysis and Presentation

Data were then gridded at 1 m cell size. This spatial resolution was considered appropriate for the size of the survey areas, and given the quality and density of the data. Data density was estimated by calculating the number of soundings per hour, then calculating the area covered per hour and the average number of pings per m^2. The number of soundings per hour (S) is calculated as follows:

$$S = r * n \quad (1)$$

where r is the ping rate per hour and n is the number of beams (101). Then the area covered by the sonar per hour (A) is calculated:

$$A = v * (h * \tan(w/2))*2 \quad (2)$$

where v is average ship speed (m s^{-1}), h is the average water depth (m) and w is the swath width (m). Finally, the number of pings per square meter (P), which is an estimate of the data density, is calculated from Equations 1 and 2, as follows:

$$P = \text{Eq 1} / \text{Eq 2}. \quad (3)$$

Initial estimates with a ping rate of 20 sec^{-1}, velocity of 10 km hr^{-1} (~5 knots), and an average water depth of 7 m yielded approximately 14 pings per m^2. This value is only an estimate of the data density because the calculations assume a flat seabed, and the actual ping density varies with distance from the central beam (due to the angular offsets of the beams) and the true water depth at each location.

Attempts to grid the data at higher resolutions (e.g., 0.5 m cell size) did not significantly improve the quality of the bathymetry grid. In fact, gridding the data at higher than 1 m^2 highlighted artefacts caused by vibrations of the transducer head, which were resolved as ~10 times per second at <0.5 degree. Smaller grid sizes also resulted in data gaps between pings of the outermost beams.

2.2.1.3. Data Quality and Errors

The shallow water depths in the study area allowed for a high rate of data acquisition, and a ping rate of 20 times per second was used. The shallow water depths also produced accurate bathymetric soundings. Data quality varied during the survey. In particular, there

was a refraction artefact on the port side from beam 1 to beam 30. It is not certain why the artefact is present, but it is possible that it was caused by reflections off the hull, engine and/or other noise, or by bubbles under the hull. This may be avoided in the future by placing the transducer at a greater distance below the keel. The data quality was also degraded to variable degrees by ocean waves and strong tidal currents. The overall quality was adequate for the purpose of the study.

During ideal conditions, the multibeam (swath) sonar survey was able to delineate small features (0.2 m high). However, these subtle features were not discernible when ocean waves of up to 1.5 m were present. Strong tidal currents also affected the ability of the boat to maintain a constant heading along each of the survey lines. In effect, this caused roll artefacts at a lower frequency than could be measured with the motion sensor. A model was developed to remove these low-frequency motions.

2.2.2. Shallow Seismic Reflection Data

Data from the Datasonics™ 3.5 kHz Chirp sub-bottom profiler was processed using the following standard procedure:

1. data from the two recorded channels were stacked to reduce the signal to noise ratio,
2. the signal was then de-biased, and
3. the data were then converted to standard 32 bit Seg-Y format.

The data were then viewed in the seismic processing software package SeisVU (www.phoenixdatasolutions.co.uk) where salient features were resolved. The profiles were saved as bitmaps (.bmp) and a hard-copy printed for interpretation.

The acoustic character of the reflections in the Chirp profiles was then interpreted based on a classification devised by Damuth (1980). This scheme classifies the reflections based on their clarity, continuity and morphology into three major echo-types, namely: Echo-type I: distinct; Echo-type II: indistinct – prolonged; and Echo-type III: indistinct – hyperbolae. These echo-types are then further sub-divided based on presence or absence of sub-bottom reflectors, degree of prolongation, and relationship of hyperbolae to the seabed. Polygons were drawn by eye around the interpreted echo-types along each line with reference to bathymetry. The acoustic facies maps are available to ground-truth against data collected in the area.

2.3. RESULTS

2.3.1. Multibeam (Swath) Sonar

In total, including the transit lines, the multibeam mapping survey comprised 227 lines and 3,505 line-km of data. Data were acquired over 16 days with a total volume of 35 gigabytes. The regional survey consisted of 922 line-km and the detailed mapping surveys of Areas B, C, D and E consisted of 1,197, 1,194, 137 and 55 line-km, respectively (Table 2.1). This equated to a surveyed area of 152, 149, 17.4, and 7.0 km^2 for Areas B, C, D and E, respectively.

2.3.1.1. Area A: Regional Survey

The regional survey revealed that most of the southeast Gulf of Carpentaria is characterised by a relatively flat and sedimented seabed (Fig. 2.1). Water depths range from

Table 2.1. Summary details of multibeam (swath) sonar surveys.

		Lines		
Study Area	Direction	Number	Length (km)	Spacing (m)
Area A: Regional Survey	-	5	<300	-
Area B: Bryomol Reef	E-W / N-S	139 / 29	10 / 3	150 / 100
Area C: Reef R1	N-S	113	12	120 - 150
Area D: Reef R2	NE-SW	33	5	120
Area E: Reef R3	NE-SW	21	3	120

~70 m in the north to <20 m in the south and east. The seabed slopes gently upwards towards the margins of the gulf and in the west the seabed has more local relief with numerous small ridges and depressions. Seabed features are sparsely distributed and include: small (<0.5 m) diameter pock marks, low-relief (<0.5 m) and widely-spaced (>1 km) undulations, and poorly-developed shallow ridges (sandwaves?). Shallow seismic sections indicate that some of the subtle variations in the topography coincide with the partially-filled channels that still have surface expression at the seabed (see section 2.3.2). Due to the wide spacing of the survey lines, the channels could not be traced over the entire study area.

2.3.1.2. Area B: Bryomol Reef

Area B is characterised by an area of hard-grounds surrounding a high-standing platform (Fig. 2.2). Two elongate depressions also flank the north, west and east margins of the platform. Water depths range from >50 m in the depressions to <20 m on the platform.

The seabed surrounding the platform contains extensive hard-grounds characterised by a rugged surface that is locally interspersed with relatively flat sedimented regions. The variations in the seabed morphology form a complex arrangement of curved and linear ridges of up to 2 m in height. The ridges form concentric half-circles in many places, and have the appearance of scroll-bars, characteristic of meandering fluvial systems. The exact origin of the ridges is unknown, although they are associated with the underlying lithified sediment.

Two depressions whose axes bifurcate to the north of the flat-topped platform are characterised by a rugged surface of complex sinuous-crested ridges and adjacent hollows. The overall trend of the depressions is to the NW-SE. The thalweg of the depressions is >50 m deep and the gross morphology forms a "blind" channel with enclosed contours.

The platform has an irregular shape and relatively flat top, with numerous indentations and talus slopes (slumps?) bordering the margins. The morphology of the surface indicates that it is a partially-eroded karst surface, containing numerous steep-sided circular depressions up to 2.5 m deep. The floors of the depression are mostly smooth due to sediment deposition.

2.3.1.2. Area C: Reef R1

Area C is characterised by relatively flat seabed surrounding a high-standing irregularly-shaped shallow platform (Fig. 2.3). Water depths range from 45-50 m on the surrounding seabed to 18 m on the shallowest parts of the platform. The platform mostly forms a surface at 27 m water depth with variations of the local topography of <1.5 m.

The seabed surrounding the platform is mostly flat but contains several irregular features on the north, southeast and south margins. On the north margin, at the base of the

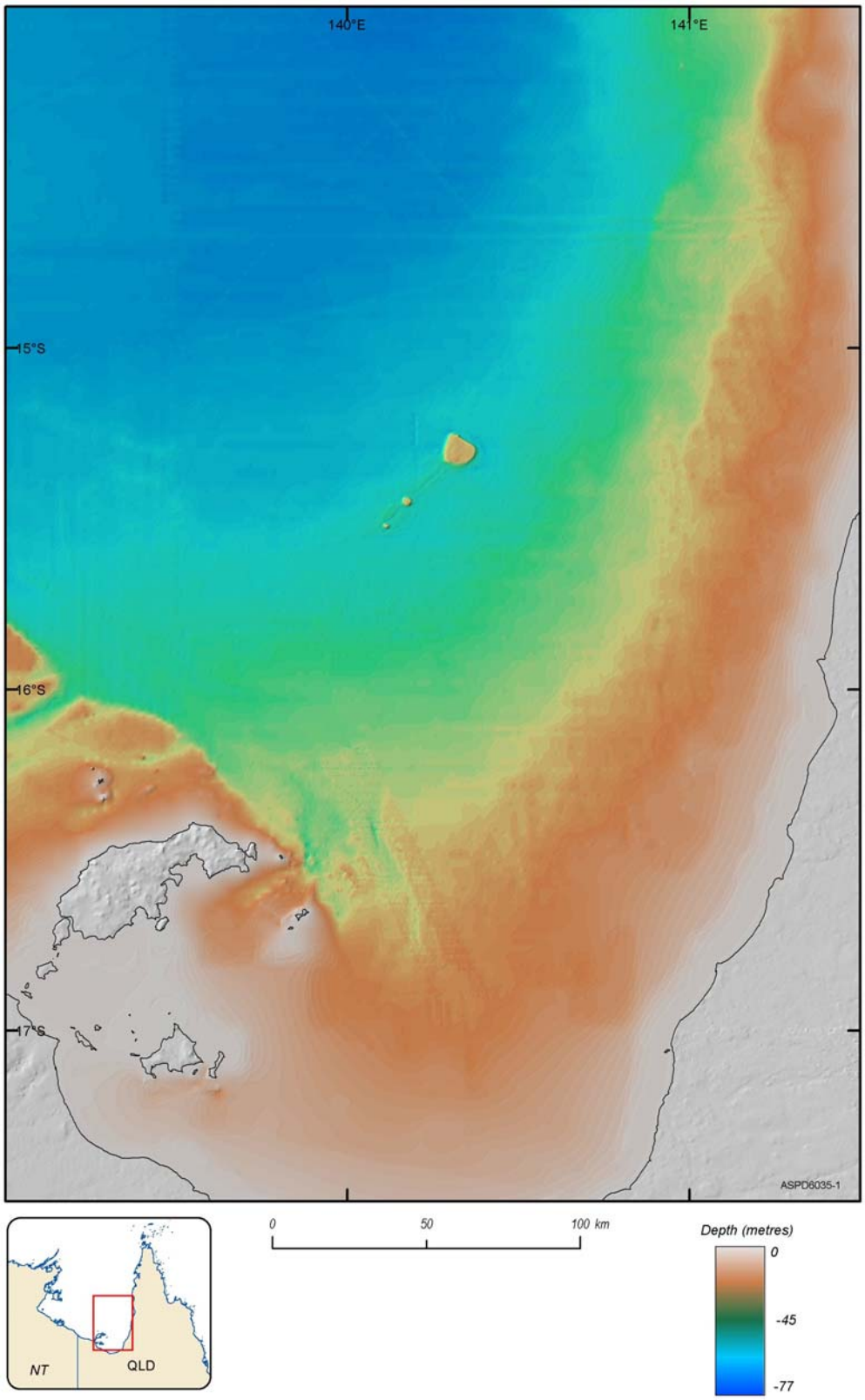

Figure 2.1. Map showing bathymetry derived from multi-beam sonar and Geoscience Australia's 250 m bathymetry grid for Area A: Regional Survey. The southern Gulf of Carpentaria is a shallow tropical shelf environment with a relatively flat and sedimented seabed. The seabed inclines gently towards the margins and water depths range from 70 m in the north of the study area to <20 m in the south and east. Three high-standing carbonate platforms occur in the north of the study area. The platforms rise from >45 m water depth to within 20 m of the water surface.

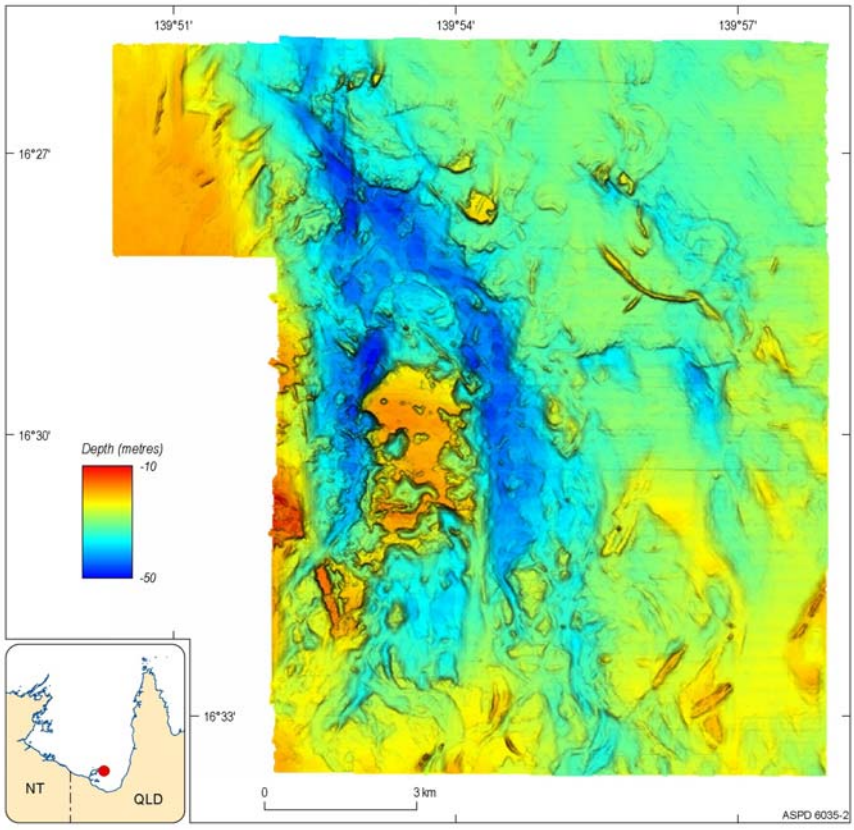

Figure 2.2. Map showing bathymetry derived from multi-beam sonar for Area B: Bryomol Reef. This area consists of a rugged seabed with a high-standing platform. The seabed surrounding the platform is characterised by hard-grounds that form curved and linear ridges up to 2 m high. The morphology of the platform indicates that it has been partially eroded and has a karst-like appearance. Sediment lopes (talus slopes) border the platform margins. Two "blind" depressions >50 m deep occur on either side of the platform.

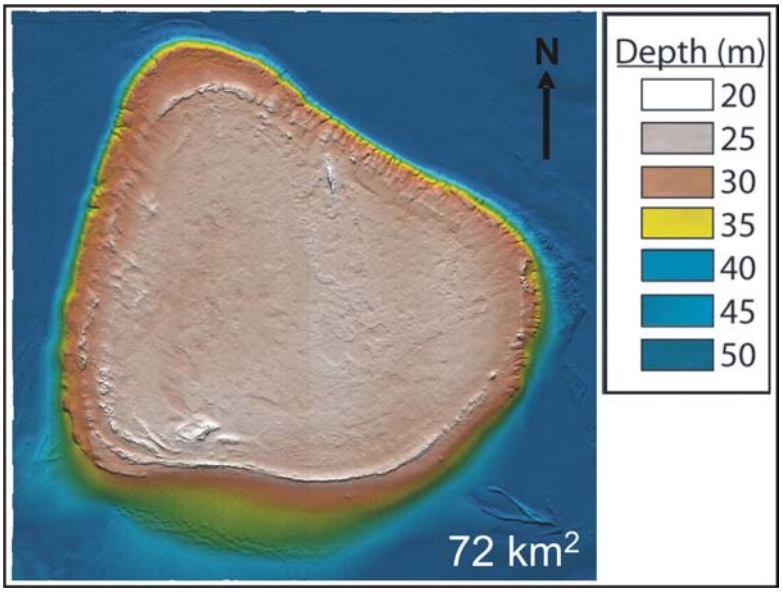

Figure 2.3. Map showing bathymetry derived from multi-beam sonar for Area C: Reef R1. This area consists of a relatively flat seabed surrounding a high-standing irregularly-shaped platform. The morphology of the platform indicates that is a submerged platform reef.

fore-reef slope, the seabed is rugged and elevated by 3-4 m above the surrounding areas. This area appears to be a hard, eroded substrate that where the underlying lithified rocks crop out on the seabed.

A curious feature on the southeast margin forms a 2 m high and ~1.8 km long "wishbone" shape comprising two bifurcating, sinuous-crested ridges. From this distinctive morphology and the cemented carbonate nature of the surface sediments sampled here (105GR97) it is inferred that the ridges are remnant beach ridges, possibly formed during the post-glacial transgression.

The platform contains morphology that is typical of platform reefs, including: a reef lagoon (platform), reef crest and marginal ridges. The windward (northern) marginal ridge contains well-developed spur and groove morphology at the top of the fore-reef slope. On the marginal ridges, which attain 2 m in height above the main platform, the crests are well rounded and incised implying that they have been exposed in the past. The leeward (southern) margin contains a well-developed talus deposit that forms a gently sloping surface extending away from the reef platform. Shallow seismic data revealed that this talus deposit is up to 8 m thick (section 2.3.2) and a core recovered from this deposit (238/104VC40) indicates that it mostly comprises poorly-sorted calcareous muddy sand and sand made up of fragments of molluscs and hard corals, and benthic foraminifera tests (section 4.3.5). On the surface of the talus slope is a series of NW-SE oriented, rounded and sinuous-crested ridges. These ridges are up to 1 m in height and are sandwaves that are likely moving down the talus slope.

2.3.1.2. Area D: Reef R2

Area D is characterised by relatively flat seabed surrounding an oval-shaped high-standing platform (Fig. 2.4). Water depths range from 45-50 m on the surrounding seabed to 18 m on the shallowest parts of the platform located on the SE margin. The platform is divided into two distinct areas by a roughly oval-shaped ridge up to 3 m high. The outer platform surface occurs at a water depth of 30 m and the inner platform surface occurs at a depth of 27 m, with the ridge at 24 m, and crest at 18-20 m.

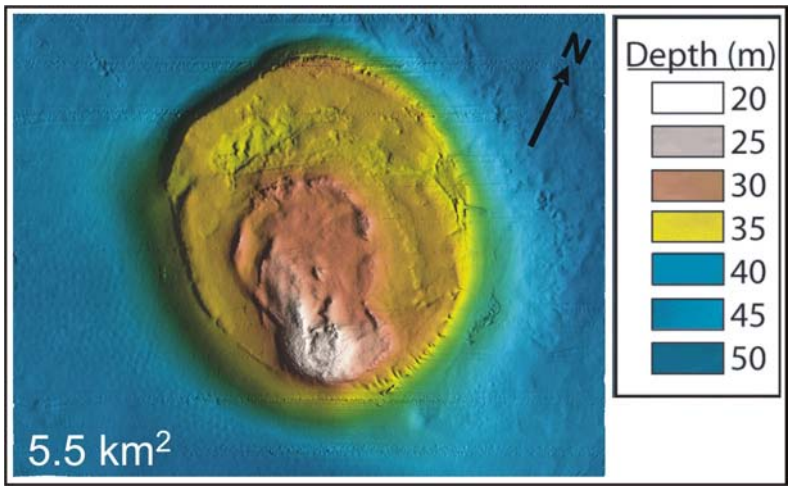

Figure 2.4. Map showing bathymetry derived from multi-beam sonar for Area D: Reef R2. This area consists of a relatively flat seabed surrounding a high-standing oval-shaped platform. The morphology of the platform indicates that is a submerged platform reef. Numerous broad, circular mounds of unknown origin occur to the southwest of the reef.

The seabed surrounding the high-standing platform is generally flat and smooth. To the south are numerous broad (<0.5 m) circular mounds. The mounds are regular in shape and distribution. The origin of the mounds is unknown but their regular distribution and shape suggests they may be the surface expression of interference patterns caused by water

movements around the high-standing reef. Very shallow (<0.2 m) irregularly-shaped depressions also occur on the north and northeast margins. These features do not show the same regular spacing and are probably related to variations in the underlying sediments.

The high-standing platform contains morphologic features that are typical of platform reefs. These features include reef lagoons, a reef crest, talus slope and marginal ridges. The overall morphology of the platform indicates that there are two distinct marginal ridges enclosing two reef lagoons. The surface of the outer lagoon covers an area of ~0.4 km^2, is uneven, and appears to be eroded with incised channels and numerous irregularly-shaped depressions. The marginal ridge bordering the outer lagoon contains numerous grooves and indentations, particularly on the east and north margins. Some of the indentations connect to the depressions on the lagoon surface, indicating that they may be outlets for water; this could either be meteoric water when the platform was subaerially exposed or seawater when the platform is submerged. The surface of the inner lagoon covers an area of ~0.2 km^2 and contains ridges and pinnacles interspersed with gentle topography. The marginal ridge bordering the inner lagoon is discontinuous and generally has a rounded crest. The reef crest covers an area of ~0.02 km^2 and has an irregular surface that slopes gently downwards to the inner lagoon. The leeward (southern) margin contains a well-developed talus deposit that forms a gently sloping surface extending away from the reef platform.

2.3.1.2. Area E: Reef R3

Area E is characterised by relatively flat seabed surrounding an oval-shaped high-standing platform (Fig. 2.5). Water depths range from 45-50 m on the surrounding seabed to 20 m on the shallowest parts of the platform located on the south margin. The platform has three surfaces. The deepest surface occurs at a water depth of ~31 m, the largest surface occurs at a water depth of ~30 m, and the smallest surface at a water depth of ~18-20 m.

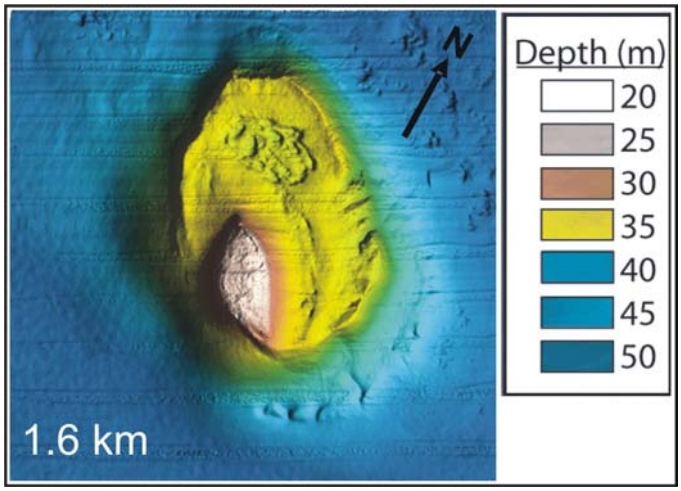

Figure 2.5. Map showing bathymetry derived from multi-beam sonar for Area E: Reef R3. This area consists of a relatively flat seabed surrounding a high-standing oval-shaped platform. The morphology of the platform indicates that is a submerged platform reef. The morphology also shows that there has been significant dissolution on the platform. The reef appears to have formed on antecedent high of the underlying rocks.

The seabed surrounding the high-standing platform is generally flat and smooth. To the south are numerous broad (<0.5 m) circular mounds. The mounds are regular in shape and distribution. The origin of the mounds is unknown but their distribution and shape suggests they may be the surface expression of interference patterns caused by water

movements around the high-standing reef. Several irregularly-shaped and shallow (<0.2 m) depressions occur to the north of the platform. These features do not show the same regular spacing and may be related to the underlying sediments.

To the north and east of the platform, the seabed is raised between 3-5 m forming an irregular surface containing narrow grooves and indentations that extend down to the surrounding seabed. This surface probably traces the surface of the underlying lithified rocks that are cropping out on the seabed of the gulf.

The high-standing platform contains morphologic features that are typical of platform reefs. These features include a reef lagoon, a reef crest, talus slope and a marginal ridge. The reef lagoon surface covers an area of 0.16 km^2 and contains a prominent circular depression with an irregular surface comprising semi-circular holes. The surface is bounded by a steep-sided marginal ridge up to 2-3 m high. The ridge is discontinuous and contains grooves and depressions that occur on the north margin. The oval-shaped reef crest covers an area of ~0.02 km^2 and has an irregular surface that slopes steeply downwards to the lagoon. The leeward (southern) margin contains a well-developed talus deposit that forms a gently sloping surface extending away from the reef platform.

2.3.2. Shallow Seismic Reflectors

A total of 3,505 line-km of digital shallow seismic reflection data (~14 GB) were collected. Sub-surface penetration was limited to <10 ms (~7.5 m) due to the coarse and cemented nature of the seabed sediments in the study area. Examples of the profiles are contained in Appendix B as bitmap (.bmp) files on the accompanying DVD.

2.3.2.1. Seabed Reflector

The seabed is distinguished as the first strong, continuous reflector of regional extent below the water surface (Fig. 2.6). This surface occurs at water depths between -70 m and -18 m, and shoals over the platforms and close to the islands and mainland coasts. The reflector is typically distinct (<3 ms) but in places becomes prolonged (<8 ms). Over most of the southeast Gulf of Carpentaria the seabed reflector forms a relatively flat surface. Near the platforms the reflector becomes rugged with variable topography. Over the reef crests the reflector becomes very distinct with minimal sub-bottom penetration and multiples are observed indicating a very hard (cemented) seabed. The seabed as mapped by the shallow seismic profiles is broadly consistent with previous bathymetric studies in the region.

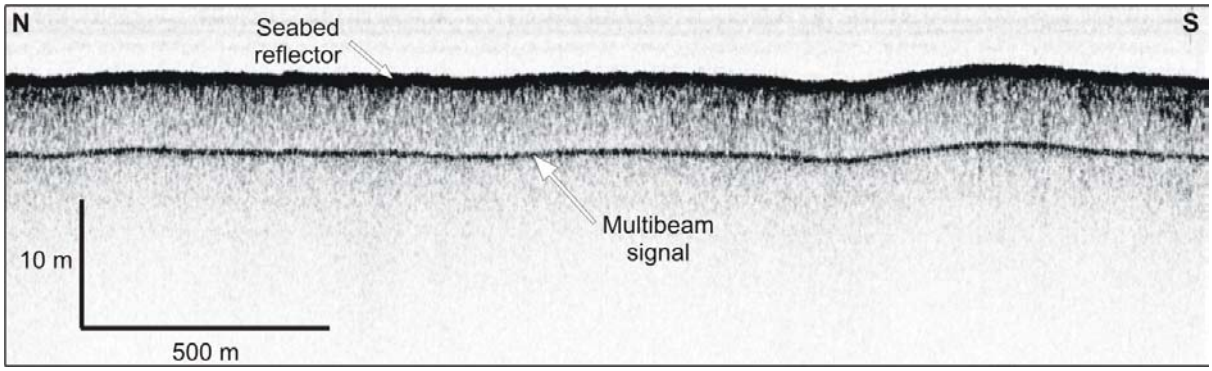

Figure 2.6. Chirp shallow seismic profile showing character of the seabed reflector. The seabed reflector occurs as the first strong, continuous reflector of regional extent below the water surface. Over most of the gulf the reflector traces a relatively flat surface. Near the platforms, the surface becomes rugged with variable topography.

2.3.2.2. *Pre-Holocene Surface*

A strong, distinct and continuous sub-bottom reflector occurs throughout the region between -70 m and -25 m water depth (Fig. 2.7a). This reflector is an irregularly incised surface that truncates underlying units. Throughout the southern gulf the reflector is horizontal but inclines gently towards the mainland and island coasts at an average gradient of ~4 m km^{-1}. In all cases the gradient steepens towards the high-standing platforms and islands. Over most of the gulf, this reflector forms the acoustic basement for the Chirp profiles, except at a few places where strata from the underlying rocks are observed.

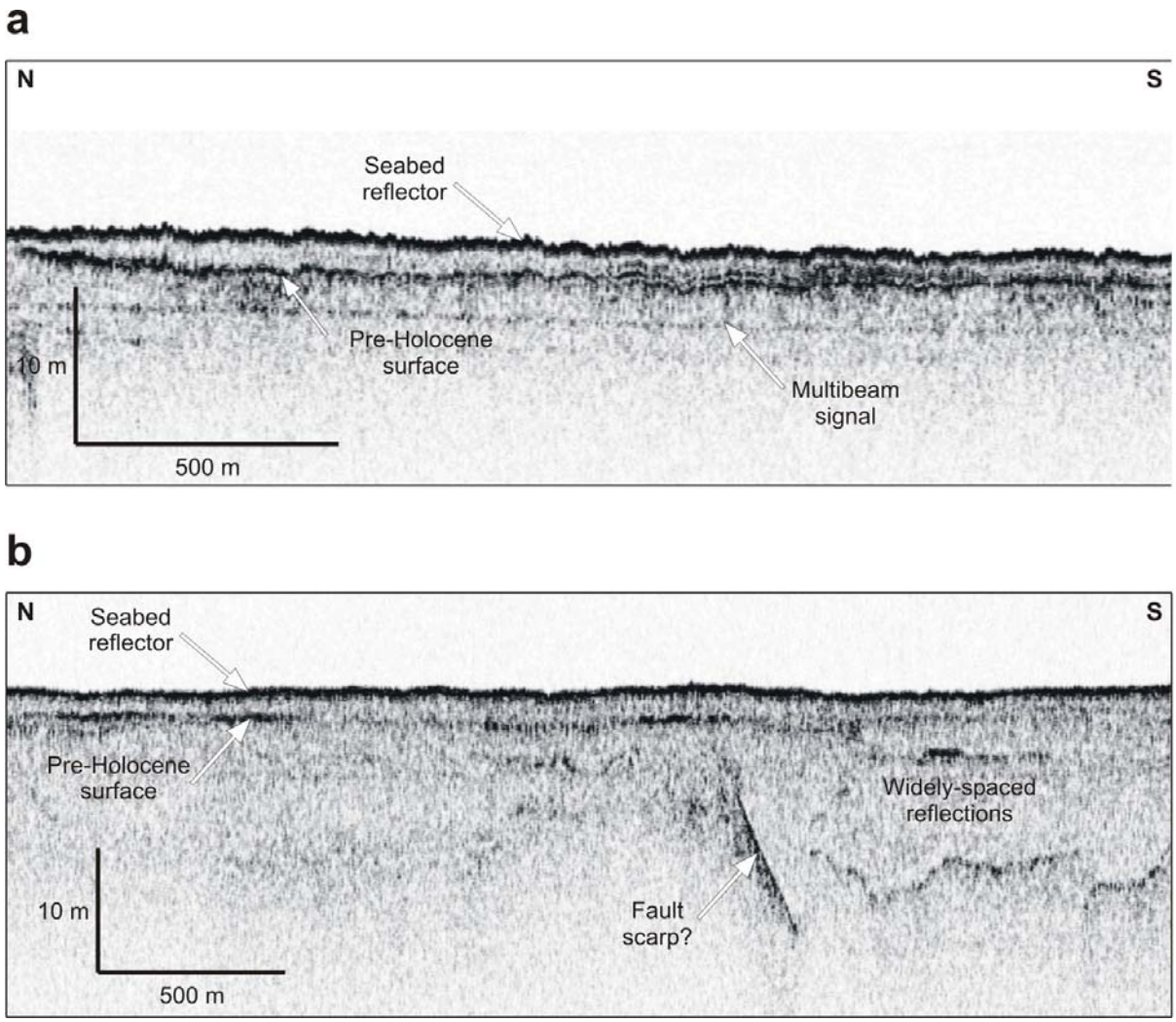

Figure 2.7. Chirp shallow seismic profiles showing: a) pre-Holocene reflector, and b) pre-Holocene reflector and underlying sub-surface reflections. The pre-Holocene reflector occurs throughout the study area and truncates underlying units. Sequences beneath the pre-Holocene reflector are characterised by widely-space, inclined and confused reflections of the underling lithified rocks. The pre-Holocene reflector represents the land surface exposed during the last glacial.

The surface of this reflector has several key characteristics that indicate that it is the pre-Holocene surface that was exposed when the Gulf of Carpentaria was emergent before the last post-glacial marine transgression. First, where sub-bottom reflectors are observed, it separates sequences of different seismic character. Overlying sequences are relatively transparent and opaque or thinly bedded comprising a marine sediment drape of generally <2 ms (<1.5 m) that attains 8 ms (6 m) on the southern margins of the reefs. Underlying sequences contain widely-spaced, inclined or confused reflections (Fig. 2.7b). Second, the surface gently slopes downwards away from the coast and islands. The reflector could not be traced beneath the reefs with the Chirp system. However, the Sparker profiles over Reef R1

reveal an elevated flat-topped sub-surface reflector beneath the seabed reflector that separates a seismically homogenous and transparent overlying sequence from a thinly bedded underlying sequence (Fig. 2.8). The pre-Holocene reflector formed when bedrock, fluvial and coastal sediments were subaerially exposed and weathered during the last glacial maximum and other earlier Pleistocene sea level lowstands.

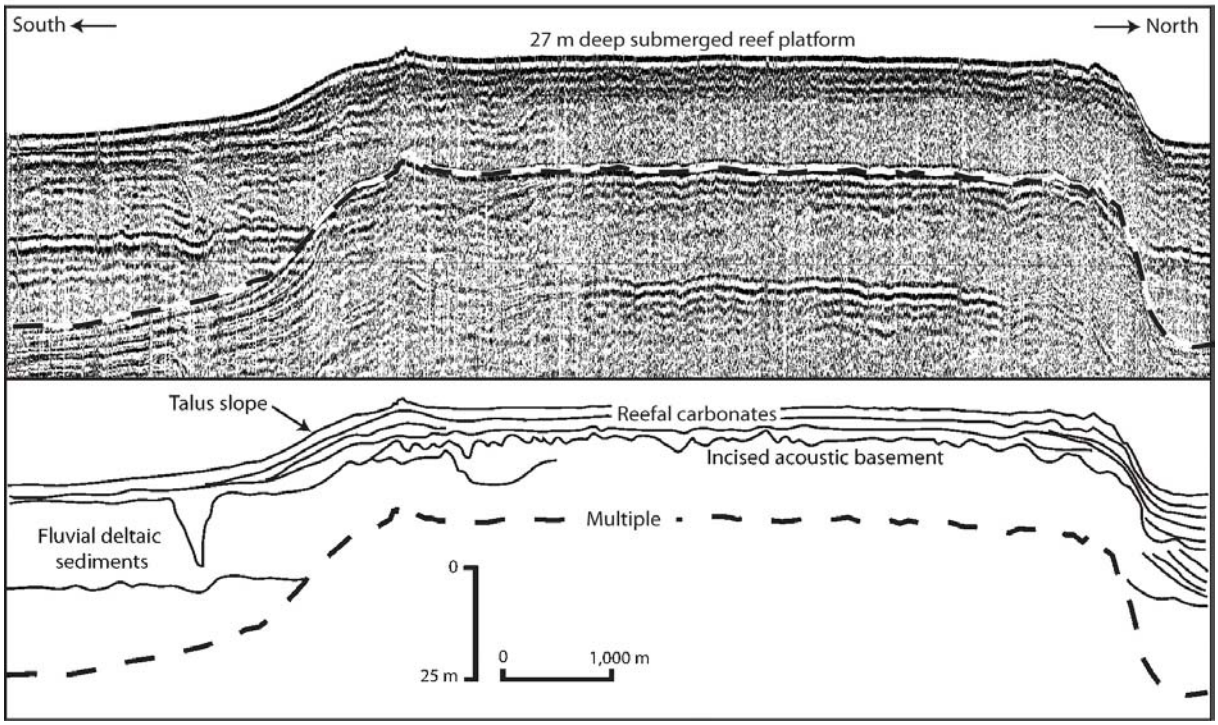

Figure 2.8. Sparker shallow seismic reflection profile over Reef R1 showing reefal carbonates overlying incised acoustic basement having positive relief. The horizontal reflections and talus deposits indicate that reef growth has taken place over numerous sea level cycles.

2.3.2.3. Sub-surface Reflectors

The low power of the Chirp system and sea conditions precluded significant penetration of the subsurface sediments. Sub-bottom reflections occur locally in the Chirp profiles. They are generally indistinct and discontinuous with variable amplitudes (Fig. 2.9). Their origin could not be determined from the seismic profiles. Presumably these reflectors define strata of the underlying acoustic basement. The most numerous features observed in the sub-surface are infilled channels. The channels are characterised by sequences of concave-up distinct (0.9 ms) and discontinuous reflections sometimes contained in a distinct basal reflector of the pre-Holocene surface (Fig. 2.10a). Individual concave-up reflections taper up towards the first reflector and pinch out at the edges of the channel. The channel sequences attain 10 ms (~7.5 m) thickness and are most well developed in the shallow southern gulf. Channels occur locally on each of the regional survey lines (Area A). Due to the wide line spacing the paths of the channels could not be traced across the southern gulf. In all cases, the channel deposits are overlain by the seismically homogenous and transparent marine sediments. A poorly-developed channel also containing concave-up reflections occurs next to Reef R1. Well-bedded channel sediments also occur in depressions of the underlying acoustic basement (Fig. 2.10b). Reflections in the depressions are strong, continuous and gently inclined towards the margins. The sub-surface reflections on lap the irregular morphology of the acoustic basement and in places appear truncated. This geometry indicates that the channel sediments were deposited into the depressions. A wave-

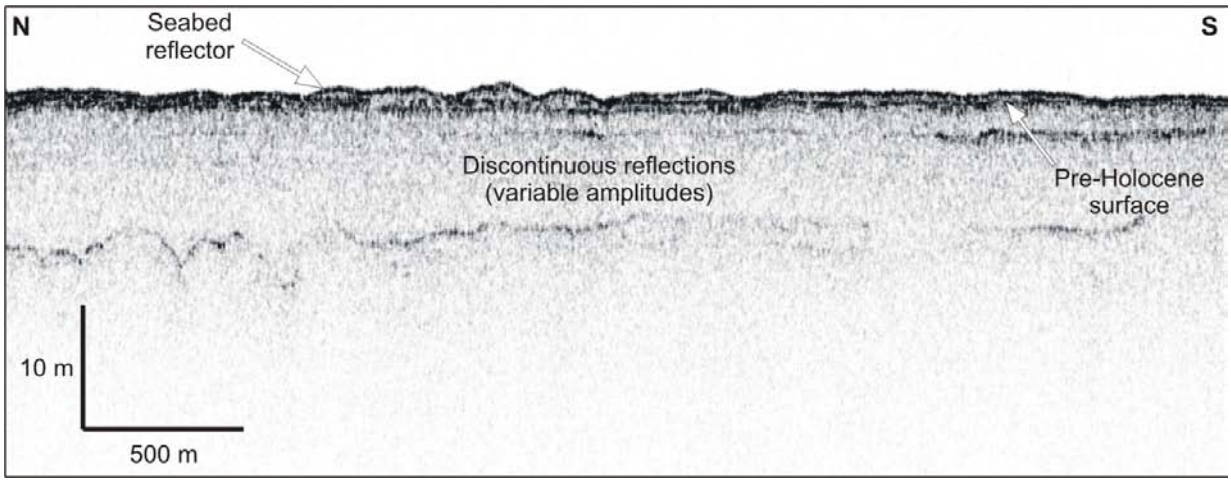

Figure 2.9. Chirp shallow seismic profile showing the typical nature of sub-surface reflections. Sub-surface reflections occur locally and are commonly discontinuous with variable amplitudes. These reflections trace underlying surfaces characterised by variable morphology, which are in contrast to the relatively flat pre-Holocene and seabed reflector. While the origin of these reflections is unknown, they presumably trace the deformed strata of the underlying acoustic basement.

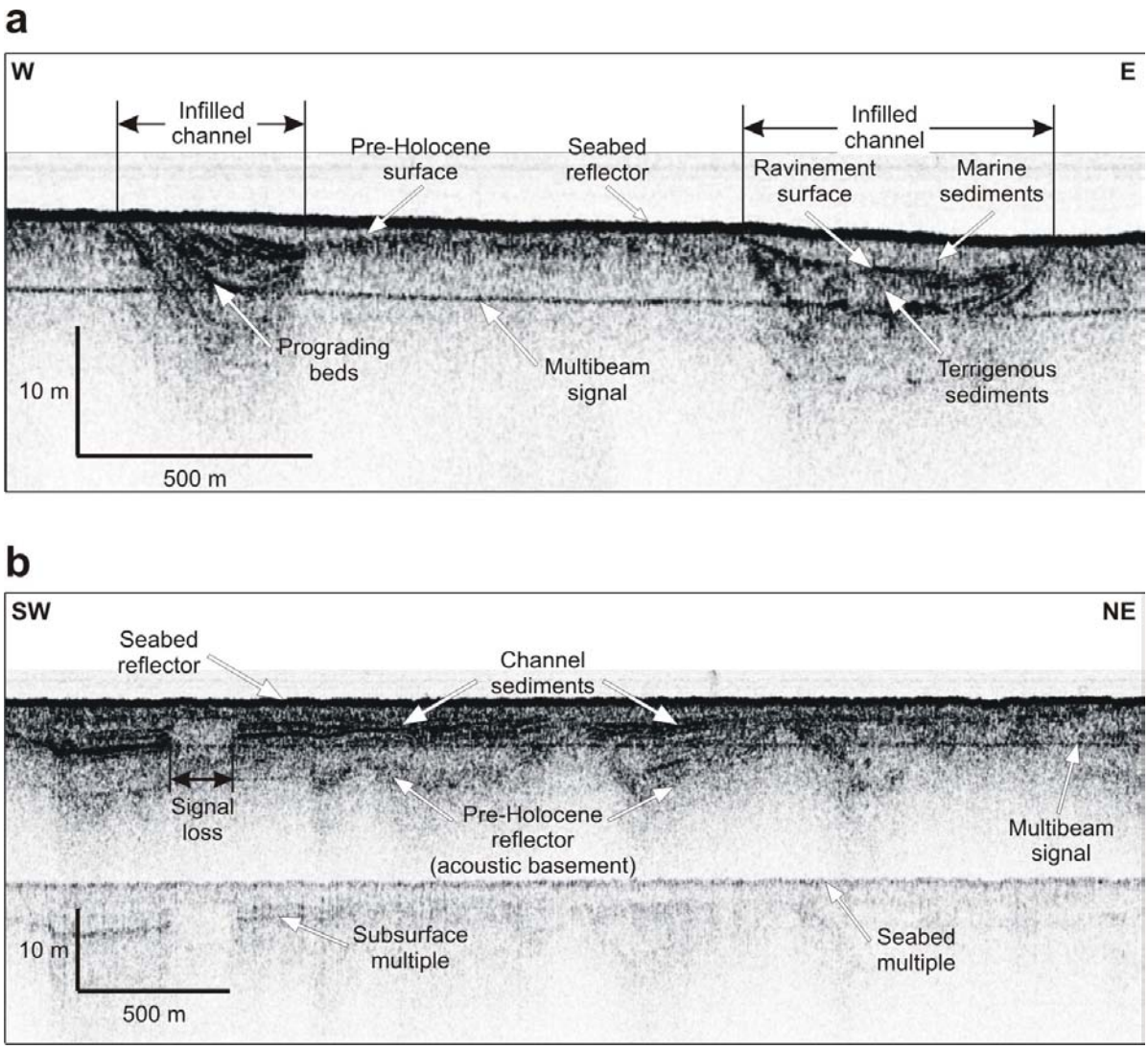

Figure 2.10. Chirp shallow seismic profiles showing: a) infilled channels, and b) infilled depressions of the pre-Holocene surface. The channels are the most numerous sub-surface features observed in the shallow seismic profiles; however they could not be traced across the study area. Channel (fluvial-deltaic) sediments have also infilled depressions of the underlying acoustic basement. These well-bedded deposits have been preserved in the depressions. A wave- or tidal-ravinement surface occurs at the top of these fluvial-deltaic sequences and separates them from the overlying marine (shallow shelf) sequence.

or tidal-ravinement surface occurs at the top of the reflections and separates the channel deposits from the overlying marine (shallow shelf) deposits.

2.3.3. Acoustic Facies

2.3.3.1. Area A: Regional Survey

In Area A, echo-types were mapped along each of the survey lines (Fig. 2.11a). Because of the wide spacing of the lines it was not possible to construct polygons between the lines to cover all of the survey area. Thus, acoustic facies were only interpreted for each line. Interpretation of the acoustic echo-types from Lines 1, 3 and 5 was undertaken to examine the nature of sedimentary environments between the deeper central basin regions and the shallow inner-shelf regions and to highlight any trends or patterns. While broad patterns were observed in the echo-types, no distinct trends were observed in the character of the echo-types between the central basin and inner-shelf environments. Echo-types occur locally along each of the lines.

Echo-type IIA is the most common echo-type identified in the region occurring throughout the study area. It occurs in the north and south at the start and towards the end of Line A, and at the junction with the east-west oriented Line 5 (Fig. 2.11a). Echo-type IA occurs mainly in the central regions and at the junction with the east-west oriented Line 3. Echo-types IC and IIB occur locally along the Line 1. Echo-type IA is the most common echo-type along Line 3 occurring along the entire length. Echo-type IIB occurs mainly in the shallower eastern regions. Echo-types IC and IIA occur locally along the entire length of the line. Echo-type IA is the most common echo-type along Line 5 occurring along the entire length but mostly near the junction with Line 1. As with Line 3, echo-type IIB occurs mostly in the shallow waters environments on the east end of the Line 5. On Line 5, echo-types IIA and IC are relatively scarce occurring only sparsely along the line and in two small areas at the junction with Line 1, respectively.

Each echo-type was compared with textural and compositional information of the surface sediments to highlight correlations between sediment/habitat type and acoustic facies (Fig. 2.11b; Table 2.2). Broadly, in the southeast gulf, differences in the echo-type do not correspond to any observed change in the texture and composition of the surfaces sediments, with all samples comprising mostly calcareous sand. No major changes in sedimentary environments are observed in the regional survey. This result is not unexpected given the relatively small number of samples collected and the relative similarity of the seabed environments surveyed.

2.3.3.2. Area B: Bryomol Reef

In Area B, echo-types were mapped along all of the survey lines (Fig. 2.12a). Because of the close spacing of the lines the echo-types could be transformed into polygons across the study area (Fig. 2.12b). Echo-type IA was the most common echo-types. The distribution of echo-types IC, IIA, IIB and IIIC was patchy across the study area. The distribution of echo-types reflects the variable topography of the area. In the northwest echo-type IIB mainly occurs in shallower regions while echo-types IA and IC occur mainly in deeper water. In the north, the presence of echo-type IIIC corresponds with the location of steep seafloor features in the channels next to the reef. Elsewhere, echo-type IIB commonly occurs in regions of shallow water (e.g., reef platform) and echo-type IA occurs in the channels and hard-

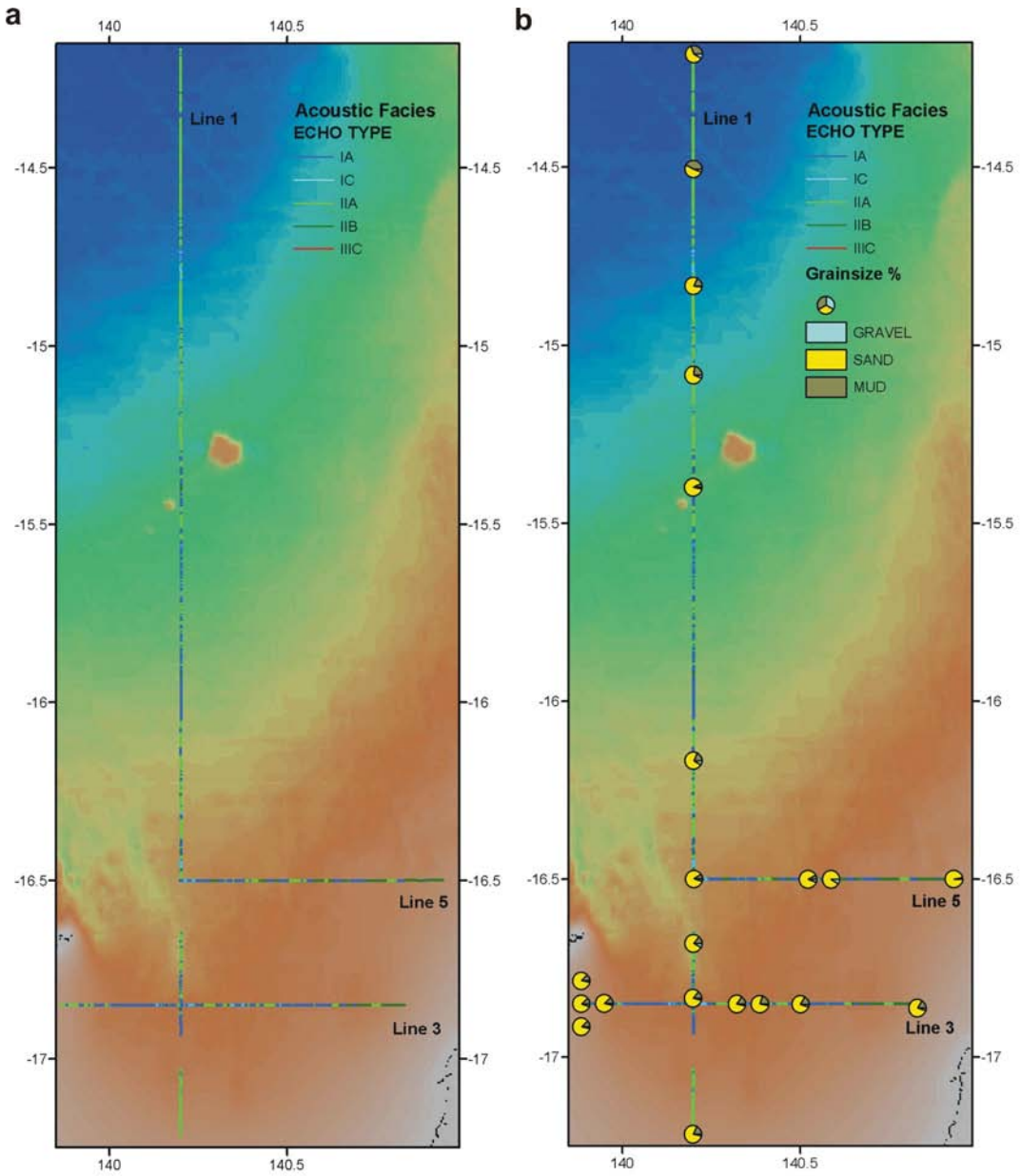

Figure 2.11. Maps showing: a) acoustic facies classification of the seabed from the Chirp sub-bottom profiler records, and b) corresponding texture and composition of seabed sediments. Broadly, major changes in echo-type do not correspond to changes in the texture and composition of the seabed.

grounds. Echo-type IA also occurs in association with the depressions on the reef platform.

Each echo-type was compared with textural and compositional information of the surface sediments to highlight correlations between sediment/habitat type and acoustic facies (Fig. 2.12c; Table 2.3). Differences in the echo-types do not correspond to any distinct differences in the gross texture and composition of the surfaces sediments, with all samples comprising mostly calcareous gravelly sand.

2.3.3.3. Area C: Reef R1

In Area C, echo-types were mapped along all of the survey lines (Fig. 2.13a). Because of the close spacing of the lines the echo-types could be transformed into polygons across the study area (Fig. 2.13b). Echo-type IA is the dominant echo-type on the seabed regions

Table 2.2. Acoustic facies type and corresponding sediment composition for Area A: Regional Survey.

Echo-type	No. of Samples	Grainsize	Average%	Minimum%	Maximum%
IA	3	Gravel	5.8	3.7	8.8
		Sand	83.9	79.1	90.6
		Mud	10.3	0.6	16.0
IC	1	Gravel	5.8		
		Sand	77.6		
		Mud	19.7		
IIA	14	Gravel	5.1	2.4	8.5
		Sand	77.5	50.8	86.5
		Mud	17.6	7.8	42.5
IIB	3	Gravel	2.6	0.1	3.0
		Sand	88.6	78.1	97.6
		Mud	8.8	2.3	17.1
IIIC	0				

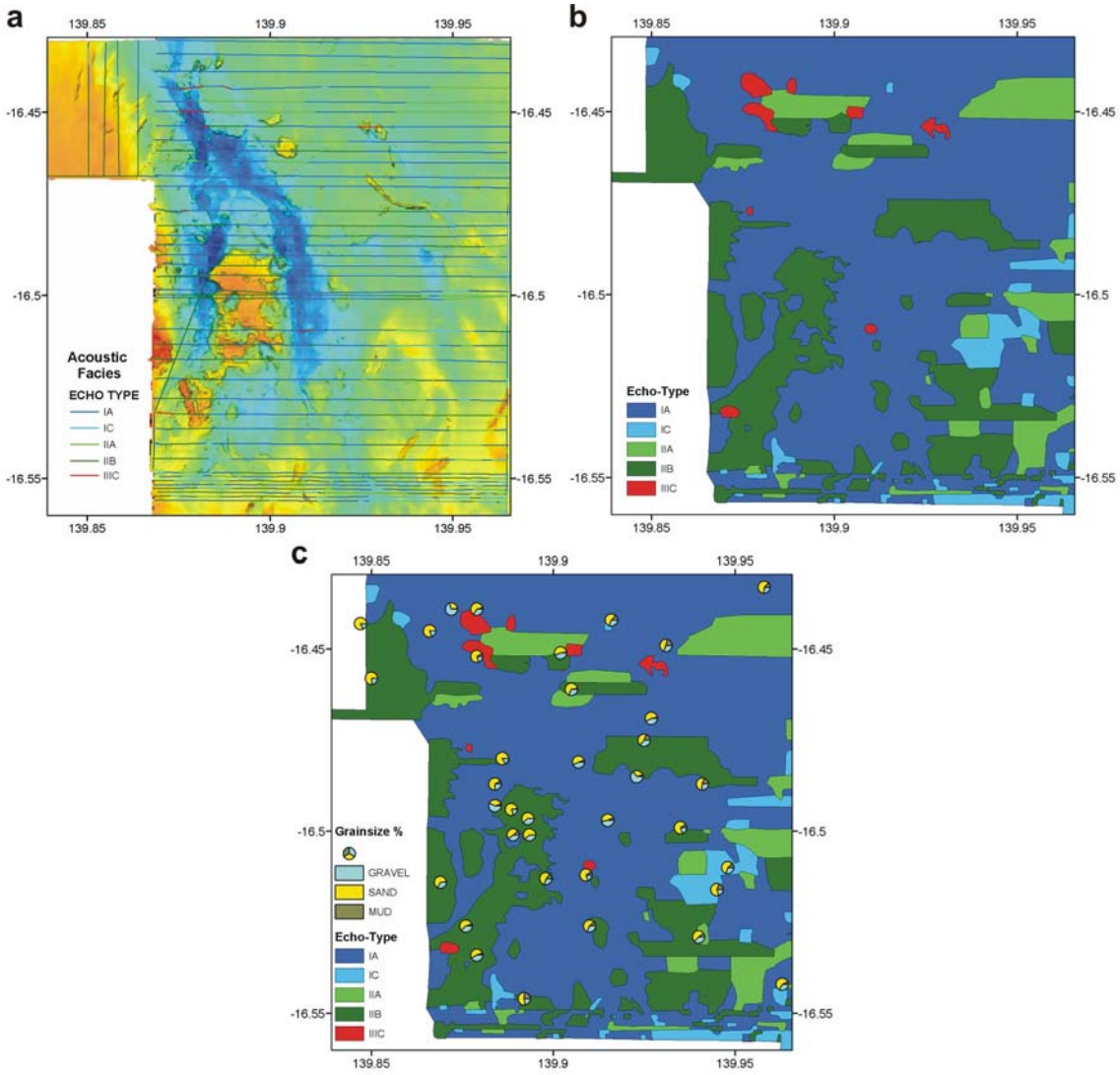

Figure 2.12. Maps showing: a) acoustic facies classification of the seabed from the Chirp sub-bottom profiler records, b) acoustic facies polygons, and c) corresponding textural and composition of seabed sediments. Broadly, major changes in echo-type do not correspond to changes in the texture and composition of the seabed.

Table 2.3. Acoustic facies type and corresponding sediment composition for Area B: Bryomol Reef.

Echo-type	No. of Samples	Grainsize	Average%	Minimum%	Maximum%
IA	19	Gravel	33.3	17.2	70.1
		Sand	58.4	27.9	82.7
		Mud	8.3	0.1	21.1
IC	3	Gravel	27.3	19.9	31.5
		Sand	57.7	55.0	60.6
		Mud	15.0	12.1	19.5
IIA	1	Gravel	27.3		
		Sand	57.7		
		Mud	15.0		
IIB	12	Gravel	35.9	19.9	64.3
		Sand	58.5	31.9	78.2
		Mud	5.6	0.29	24.3
IIIC	0				

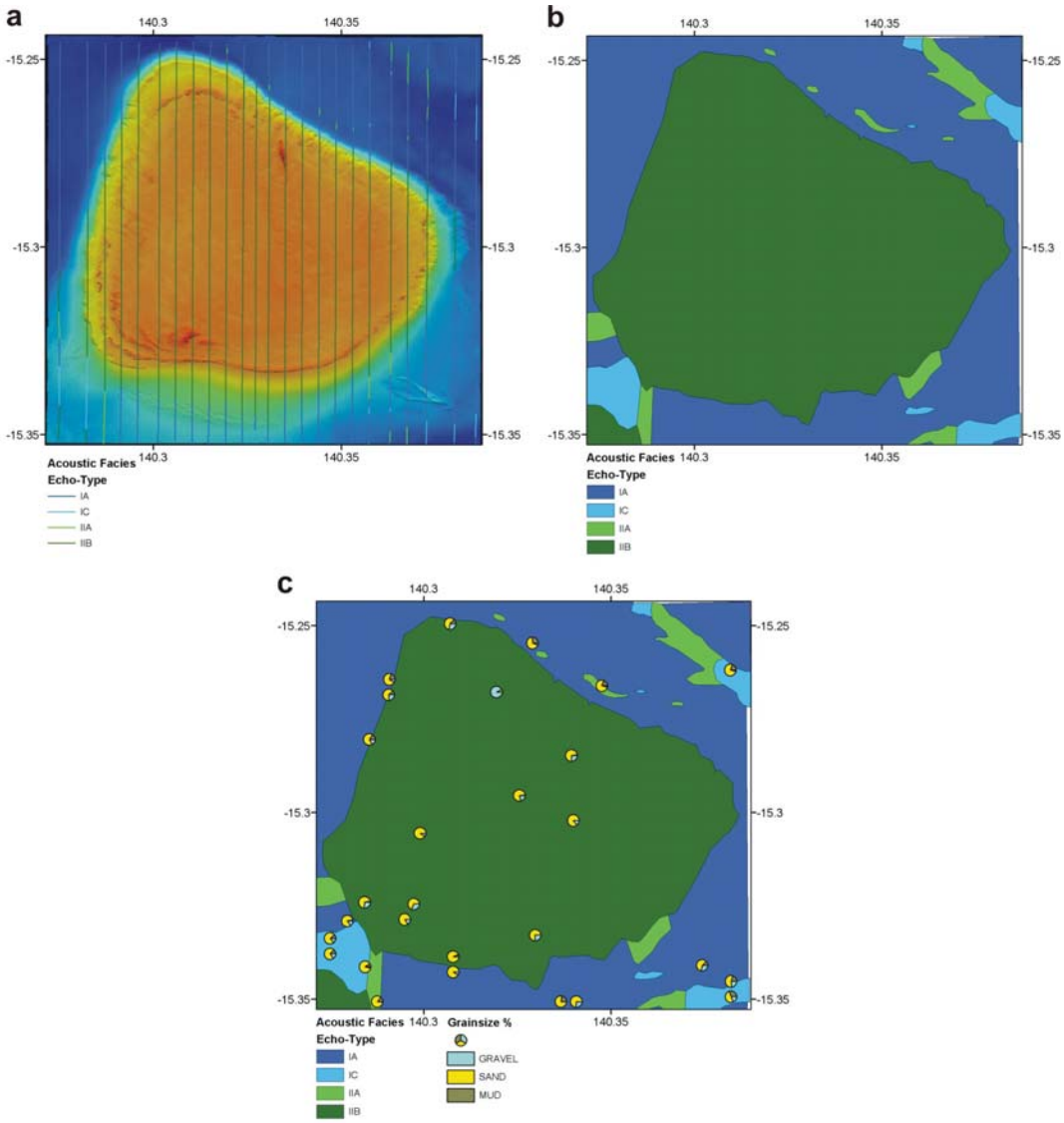

Figure 2.13. Maps showing: a) acoustic facies classification of the seabed from the Chirp sub-bottom profiler records, b) acoustic facies polygons, and c) corresponding textural and composition of seabed sediments. Broadly, echo-type IIA corresponds to sediments with relatively high sand concentrations.

Table 2.4. Acoustic facies type and corresponding sediment composition for Area C: Reef R1.

Echo-type	No. of Samples	Grainsize	Average%	Minimum%	Maximum%
IA	10	Gravel	13.6	0.3	28.5
		Sand	74.6	59	93.7
		Mud	11.8	0	25.6
IC	6	Gravel	13.8	3.5	23.8
		Sand	68.7	50	86.9
		Mud	17.5	8.8	30.3
IIA	2	Gravel	2.7	1.2	4.2
		Sand	80.6	76.7	84.6
		Mud	16.7	14.2	19.1
IIB	11	Gravel	28.9	9.7	91.3
		Sand	68.9	7.9	89.5
		Mud	2.2	0.4	12.6
IIIC	N/A				

surrounding Reef R1. Echo-types IIA and IC occur locally associated with in-filled palaeo-channels and sedimented regions. Echo-type IIB is the dominant echo-type on the reef platform. In addition, echo-type IIB occurs on the talus slope on the southern reef margin and spurs on the west and east margins.

Each echo-type was compared with textural and compositional information of the surface sediments to highlight correlations between sediment/habitat type and acoustic facies (Fig. 2.13c; Table 2.4). On average, echo-type IIA corresponds to sediment comprising relatively low gravel concentrations and relatively high sand concentrations. In all other cases differences in the echo-types was not associated with distinct changes in the texture and composition of the surface sediments.

2.3.3.4. Area D: Reef R2

In Area D, echo-types were mapped along all of the survey lines (Fig. 2.14a). Because of the close spacing of the lines the echo-types could be transformed into polygons across the study area (Fig. 2.14b). Echo-type IIB is the dominant echo-type on the reef platform and also characterises the surrounding seabed to the north and west of the reef. Echo-type IIA is the dominant echo-type on the surrounding seabed to the south and east of the reef, and occurs locally in the north. The occurrence of echo-type IA is restricted to small patches on the south and north reef margins.

Each echo-type was compared with textural and compositional information of the surface sediments to highlight correlations between sediment/habitat type and acoustic facies (Fig. 2.14c; Table 2.5.). The small number of samples precluded a detailed comparison between the acoustic facies and sediment types. However, echo-type IIA corresponded to a sample comprising muddy sand, while echo-type IIIB corresponded to samples comprising gravelly sand.

2.3.3.5. Area E: Reef R3

In Area E, echo-types were mapped along all of the survey lines (Fig. 2.15a). Because of the close spacing of the lines the echo-types could be transformed into polygons across the study area (Fig. 2.15b). Echo-type IIB is the dominant echo-type on the reef platform. It also

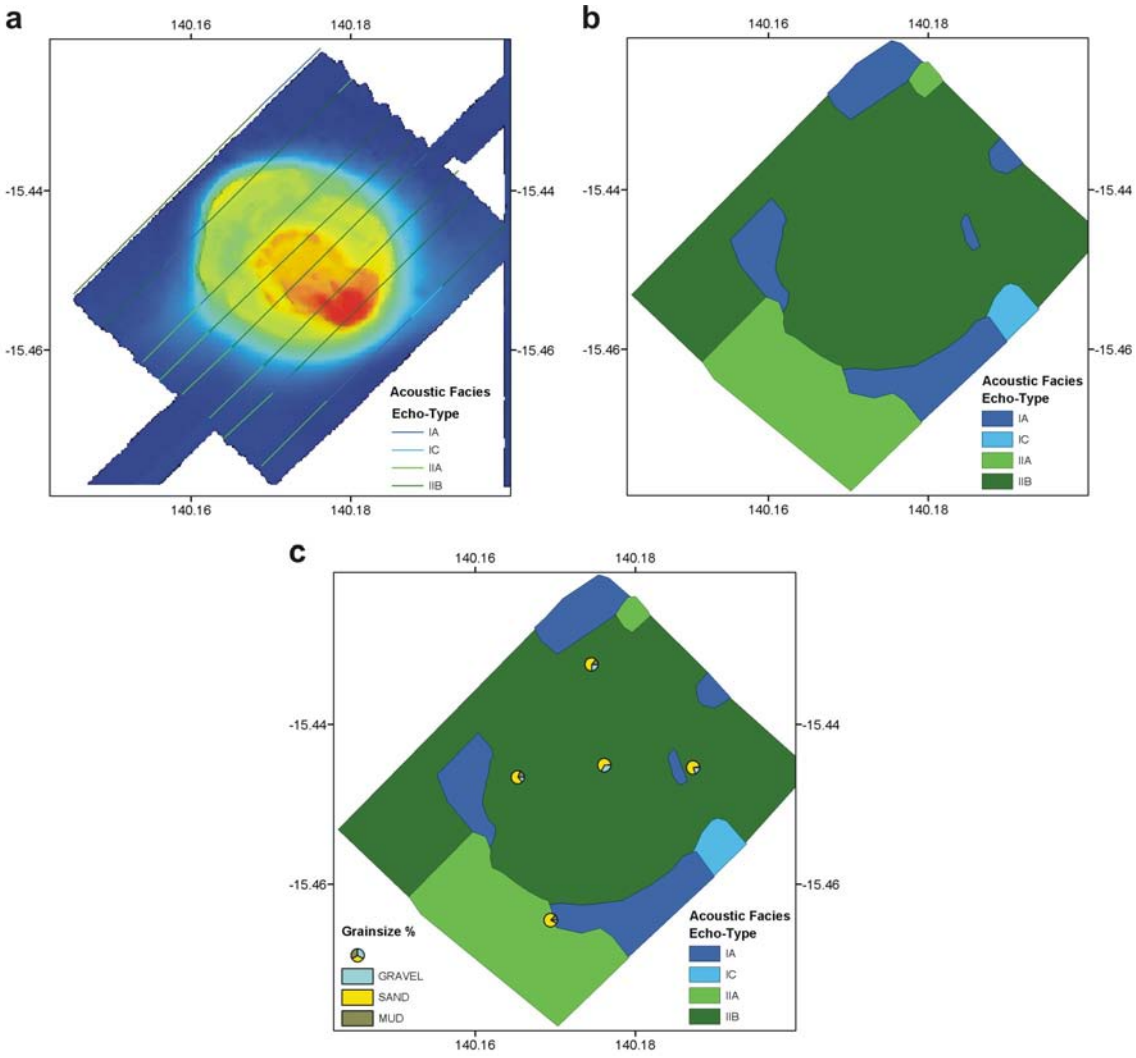

Figure 2.14. Maps showing: a) acoustic facies classification of the seabed from the Chirp sub-bottom profiler records, b) acoustic facies polygons, and c) corresponding textural and composition of seabed sediments. Despite the small number of samples, echo-type IIA corresponds to muddy sand and echo-type IIIB corresponds to gravelly sand.

Table 2.5. Acoustic facies type and corresponding sediment composition for Area D: Reef R2.

Echo-type	No. of Samples	Grainsize	Average%	Minimum%	Maximum%
IA	0				
IC	0				
IIA	1	Gravel	7.7		
		Sand	79.3		
		Mud	13.0		
IIB	4	Gravel	22.6	14.1	32.5
		Sand	68.0	61.8	78.0
		Mud	9.4	1.3	20.0
IIIC	N/A				

occurs on the surrounding seabed on the north and west margins of the reef. Echo-type IA is the dominant echo-type on the other margins and occurs locally on the platform. Echo-type IIA occurs locally in the southwest containing faint sub-bottom reflections. The presence of a strong multiple in this area prevented any further discrimination of the echo-types.

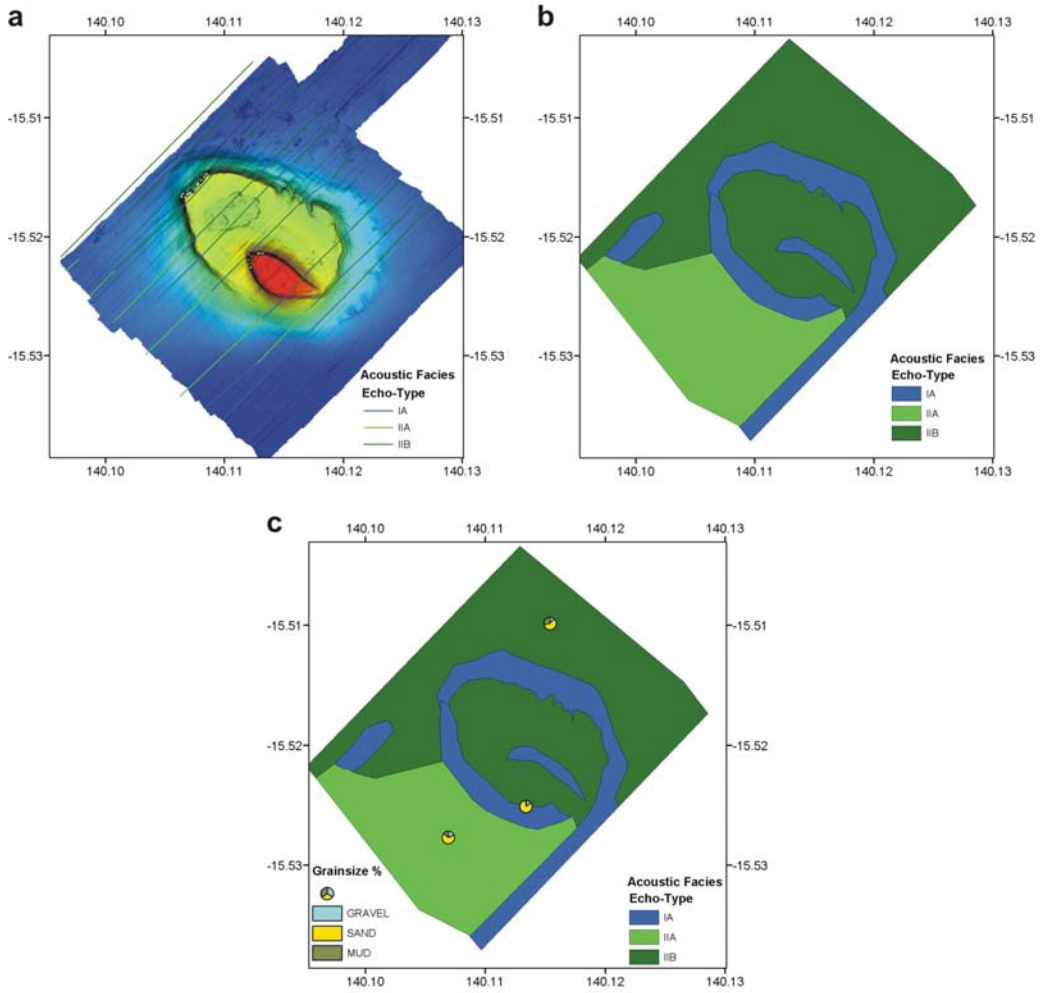

Figure 2.15. Maps showing: a) acoustic facies classification of the seabed from the Chirp sub-bottom profiler records, b) acoustic facies polygons, and c) corresponding textural and composition of seabed sediments. Despite the small number of samples, echo-type IA corresponds gravelly sand and echo-types IIA and IIB correspond to muddy gravelly sand.

Table 2.6. Acoustic facies type and corresponding sediment composition for Area E: Reef R3.

Echo-type	No. of Samples	Grainsize	Average%
IA	1	Gravel	14.6
		Sand	83.9
		Mud	1.5
IIA	1	Gravel	17.9
		Sand	68.0
		Mud	14.1
IIB	1	Gravel	12.4
		Sand	59.9
		Mud	27.7

Each echo-type was compared with textural and compositional information of the surface sediments to highlight correlations between sediment/habitat type and acoustic facies (Fig. 2.15c; Table 2.6). The small number of samples precluded a detailed comparison between the acoustic facies and sediment types. Echo-type IA corresponded to a sample comprising gravelly sand and echo-types IIA and IIB correspond to samples comprising muddy gravelly sand.

3. Oceanography

A preliminary analysis of the oceanographic data from the BRUCE mooring has been undertaken to compute the major tidal features and associated turbidity for the survey. A more detail analysis still needs to be completed to reveal the sediment transport pathways. Data from the BRUCE mooring are available directly from Geoscience Australia.

3.1. DATA ACQUISITION

3.1.1. BRUCE Deployment

The hydrodynamic conditions at Area B were recorded with an array of instruments designed to measure currents, temperature, salinity, and turbidity. The *Benthic Research for Underwater sediment Concentration Experiment* (BRUCE) was constructed at Geoscience Australia, and comprises a Nortek™ acoustic current meter, two Benthos™ optical backscatter sensors (OBS), a Sequoia™ LISST-100 transmissometer/laser particle sizer, and a Seabird™ CTD (conductivity, temperature, depth) probe (see Appendix C for photos of mooring set up). BRUCE was deployed in 34 m water depth at location 16° 29.995′ S, 139° 55.961′ E from 09:45 13/05/03 GMT to 10:41 27/05/03 GMT (Fig. 3.1).

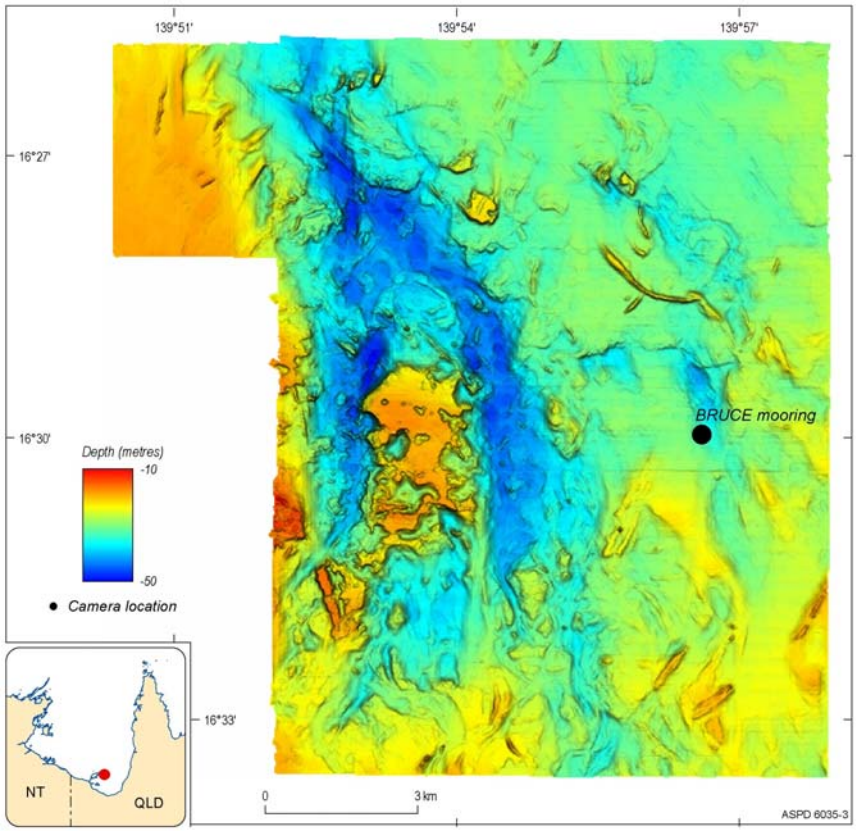

Figure 3.1. Map showing the location of the Benthic Research Underwater sediment Concentration Experiment (BRUCE) oceanographic mooring. BRUCE was deployed on the hard-grounds to the east of the Bryomol Reef in Area B in 34 m water depth. The total length of the deployment was approximately 14 days. BRUCE contains an acoustic current meter, two optical backscatter sensors, an in-situ laser particle sizer, and CTD (conductivity, temperature, depth) probe.

The Nortek™ acoustic current meter (ADV #4103) recorded currents at 1 m above the seabed. Samples were collected for 60 s at 2 Hz every 20 minutes in order to resolve

turbulence. The 3 dimensional velocity components (east, north, and up) and temperature were logged internally and downloaded to a PC upon recovery.

Two Benthos™ optical backscatter sensors (OBS #897) recorded turbidity at 0.3 m and 0.60 m above the seabed. Each sensor was oriented towards the centre of the frame. The sensors were powered by the ADV and thus collected samples at the same frequency and resolution as the current meter. The output of the OBS is recorded in counts as an analogue input to the ADV. This is then converted to volts (0.5 V = 65,535 counts) and then turbidity in fluorometric turbidity units (ftu) as follows:

$$\text{Turbidity (ftu)} = 356.7\times(x+0.002) \tag{4}$$

where x = volts. Samples were logged by the ADV and downloaded to a PC upon recovery.

The Sequoia™ LISST-100 transmissometer/laser particle sizer (LISST #104579) recorded transmissivity and battery voltage, and volume concentrations for 32 particle size "bins" at 0.27 m above the seabed. Samples were collected for 60 s at 2 Hz every 20 minutes.

The Seabird™ CTD (CTD #1620) recorded salinity, temperature and pressure (water depth) at 0.27 m above the seabed. Samples were collected for 60 s at 2 Hz every 20 minutes to resolve wave height and periods from the pressure data. Data were logged to the same files as transmissivity, battery voltage and volume concentrations from the LISST-100. Data from both instruments were then stored to the LISST-100 memory in daylong segments and then the entire dataset was downloaded to a PC upon recovery.

To calibrate each OBS, two sediment traps made of 0.20 m long 0.09 m diameter cylindrical PVC pipe were fixed vertically to the steel frame at 0.30 m and 1 m above the seabed.

3.2. RESULTS

3.2.1. Water Levels

A tidal water level record with a sampling interval of 20 minutes was obtained by extracting burst-averages of the water depth (Fig. 3.2). The length of record is 13.97 days. A harmonic analysis of this record was performed based on the method of Foreman (1977) and the amplitudes and phases of the calculated harmonic constituents are listed in Table 3.1. With a record length of less than 15 days it was not possible to resolve all of the most commonly calculated constituents, in particular, the S2 constituent. In order to obtain an estimate of the common constituents, the results in Table 3.1 were used to forecast tidal water levels for 24.3 hours beyond the end of the measured record. The harmonic analysis was then repeated on this combined measured and forecast record (Table 3.2). Note that the forecasted length of the time series is only 9.5% of the combined time series length. Mean sea level was 33.7 m above the acoustic current meter (i.e., Nortek).

The tidal form factor (F), which is frequently used to classify tides as semi-diurnal, mixed or diurnal, is defined as:

$$F = \frac{a_{O1} + a_{K1}}{a_{M2} + a_{S2}} \tag{5}$$

where a is the amplitude of the subscripted harmonic constituent (O1, K1, M2, S2). Based on the constituent amplitudes listed in Table 3.2 the value of F is 31.8, which indicates a strongly diurnal tide in the southern Gulf of Carpentaria.

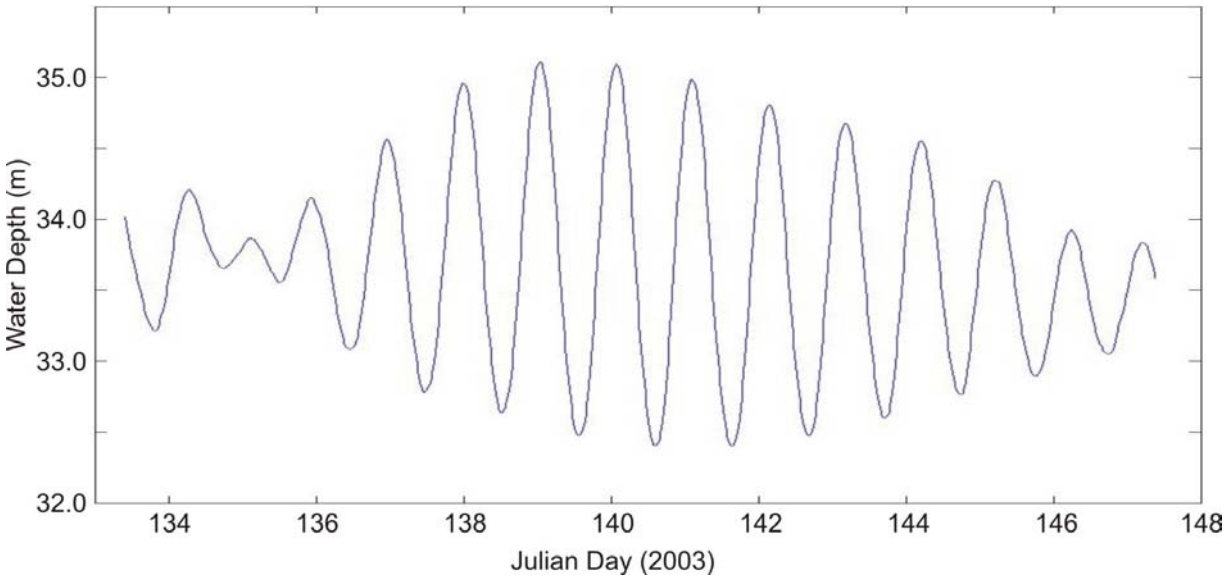

Figure 3.2. Tidal heights as measured by the BRUCE mooring for the period of the survey. Note that the measurements begin and end during neap tides. Measurements were recorded every 20 mins.

Table 3.1. Tidal constituents from the BRUCE mooring located at Area B: Bryomol Reef.

Constituent	Frequency (cycles hr^{-1})	Amplitude (m)	Amplitude Error (m)	Phase (deg.)	Phase error (deg.)
O1	0.038731	0.5806	0.081	135.69	9.44
K1	0.041781	0.6435	0.102	182.5	8.38
M2	0.080511	0.0214	0.017	253.37	47.48
M3	0.120767	0.0142	0.008	78.82	31.78
M4	0.161023	0.0029	0.003	123.59	56.74
2MK5	0.202804	0.0041	0.004	346.42	54.37
2SK5	0.208447	0.0025	0.003	269.87	77.63
M6	0.241534	0.0024	0.003	334.25	66.32
3MK7	0.283315	0.0011	0.001	309.6	51.39
M8	0.322046	0.0007	0.001	176.9	62.47

3.2.2. Tidal Currents

Burst-averaged North-East velocity components of the horizontal current were calculated for the entire record along with burst-averaged current speeds and directions (Fig. 3.3a-b.). The current velocity record is dominated by the diurnal tides. Maximum near-bed current speeds reach 0.6 m s^{-1} during springs and are less than 0.25 m s^{-1} during neaps. The current during the flooding tide is directed toward approximately 220° magnetic and during the ebbing tide it is toward approximately 30° magnetic. Water level and current speed are approximately 90° out of phase, with maximum current speeds occurring approximately midway through the rising and falling tides.

A progressive vector plot of the current (Fig. 3.4) indicates a predominantly northwest directed residual current. The maximum tidal excursion length during springs reached approximately 17 km, which is large, but not unexpected given the diurnal nature of the tide. Excursion lengths during neaps are generally less than 8 km (Fig. 3.4).

Table 3.2. Re-calculated tidal constituents from the BRUCE mooring located at Area B: Bryomol Reef including forecast water levels.

Constituent	Frequency (cycles hr^{-1})	Amplitude (m)	Amplitude Error (m)	Phase (deg.)	Phase error (deg.)
MSF	0.002822	0.1442	0.113	47.39	46.59
O1	0.038731	0.5629	0.095	134.87	10.92
K1	0.041781	0.6619	0.121	182.99	9.32
M2	0.080511	0.0219	0.007	251.96	21.03
S2	0.083333	0.0166	0.009	56.83	24.2
M3	0.120767	0.0128	0.006	76.54	30.51
SK3	0.125114	0.0069	0.006	33.47	53.62
M4	0.161023	0.0018	0.002	129.58	76.53
MS4	0.163845	0.0039	0.002	251.02	29.94
S4	0.166667	0.0011	0.002	215.91	110.25
2MK5	0.202804	0.0046	0.004	334.06	41.85
2SK5	0.208447	0.0022	0.003	267.55	90.08
M6	0.241534	0.0029	0.003	325.96	59.86
2MS6	0.244356	0.0026	0.003	24.94	74.9
2SM6	0.247178	0.0013	0.002	279.46	134.87
3MK7	0.283315	0.0016	0.001	298.34	34.95
M8	0.322046	0.0002	0.001	225.18	179.29

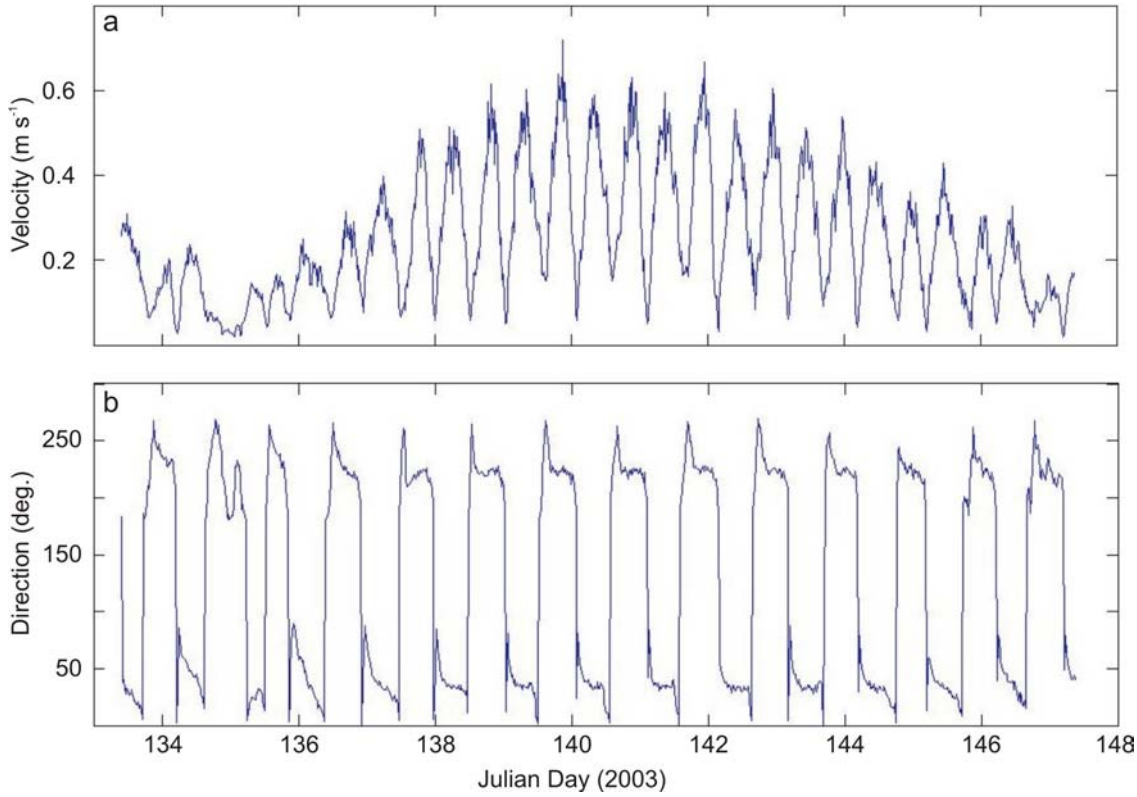

Figure 3.3. Graphs showing: a) burst-averaged current speed, and b) current direction for the deployment. Greatest velocities of >0.5 m s^{-1} occur during spring tides and there is a strong correlation between tidal height and current velocity. Velocities are slightly faster on the flood stage.

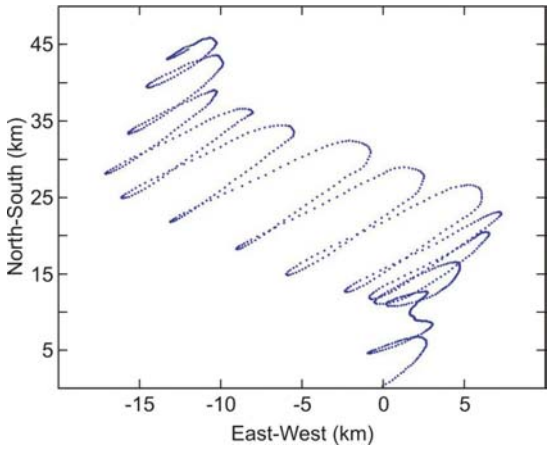

Figure 3.4. Progressive vector plot of tidal excursion recorded during the survey. During the deployment the residual tidal current direction was towards the northwest. Largest excursions were recorded during spring tides in the middle of the record.

3.2.3. Turbidity

The burst-averaged turbidity recorded at 0.30 m and 0.60 m above the seabed is shown in Fig 3.5. For most of the deployment turbidity was low (<5.6 FTU at both depths). There is a short-lived event of elevated turbidity clearly evident at 0.30 m above the seabed on Julian Day 143. The trend of increasing turbidity recorded at 0.60 m above the seabed during the last 3 days of the deployment is almost certainly due to bio-fouling of the sensor.

The records have been re-plotted in Fig 3.6 to show detailed sections of the near-bed turbidity record. There are two peaks (spikes) in turbidity at 0.30 m above the seabed on Julian Days 135 and 136. These are very short-lived (one burst), do not correspond to any consistent stage of the tide and are probably erroneous data. On Julian Day 143, however, there is a sustained elevation in turbidity recorded at both 0.30 m and 0.60 m above the seabed that lasts for 6 hours. Turbidity at 0.30 m above the seabed peaked at 600 FTU during this event. The event is probably real and coincided with maximum ebb current speeds during that day. Further analysis of the turbidity data is required to ascertain whether this event was associated with any wind (wave) events.

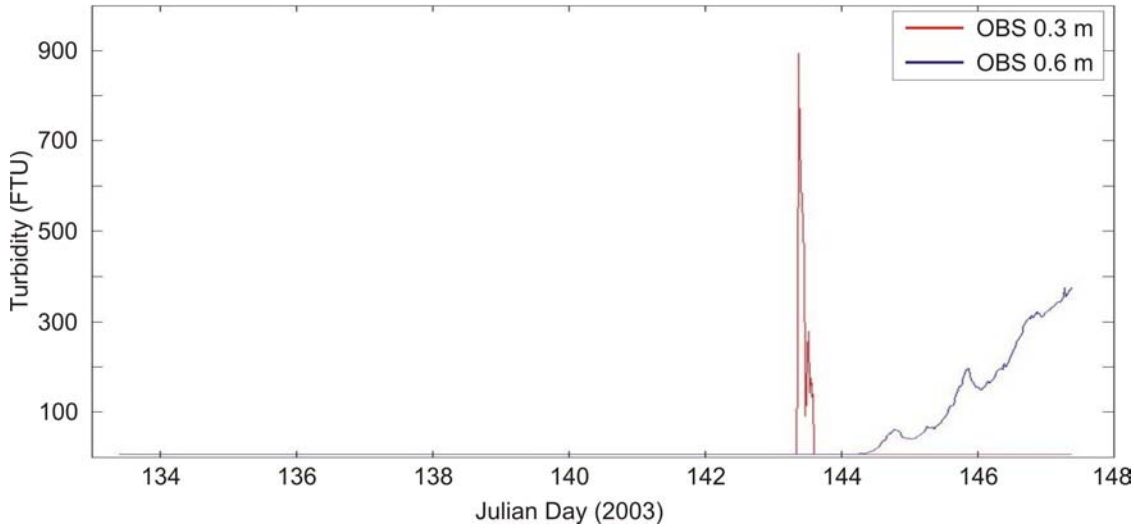

Figure 3.5. Graph showing near-bed turbidity records recorded at the BRUCE mooring during the survey. Sensors were placed at 0.3 m and 0.6 m above the bed. Near-bed turbidity is low throughout the deployment except for a significant spike on Julian Day 143 and an increasing trend at 0.6 m which is probably due to biofouling of the sensor.

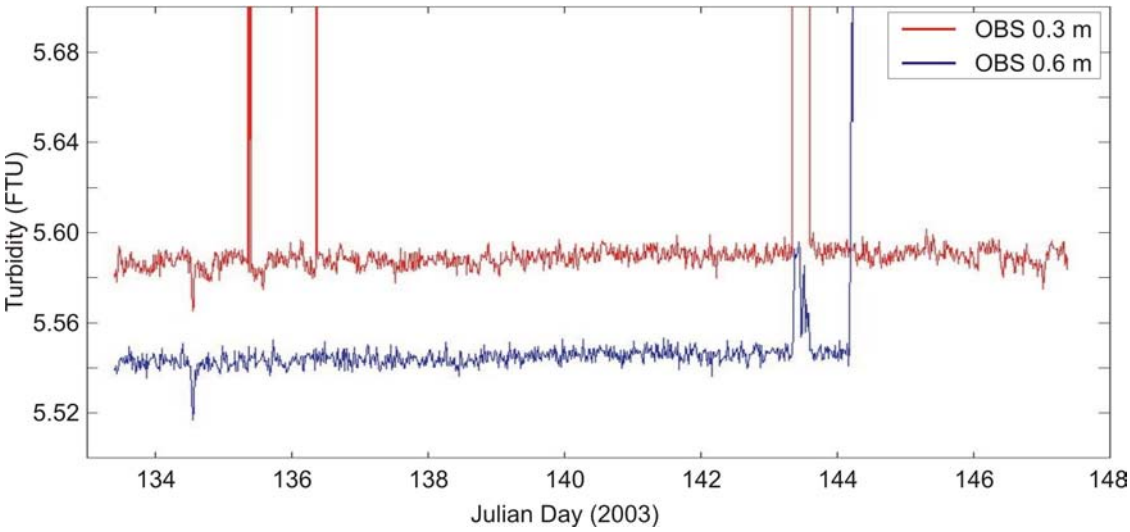

Figure 3.6. Graph showing detailed near-bed turbidity records during the survey. For most of the deployment near-bed turbidity was very low (<5.6 FTU) with daily variations of <0.02 FTU at both 0.3 m and 0.6 m positions. Elevated turbidity is recorded on Julian Day 143 by both sensors.

4. Sedimentology

4.1. SAMPLE ACQUISITION

A total of 117 stations were occupied during the survey. The locations of the stations were designed to capture the full spectrum of sedimentary environments and seabed habitats. A variety of operations were undertaken at each station to characterise the seabed sediments, sedimentary processes, and biota and habitats (Table 4.1a-e).

Table 4.1a. Summary details of operations undertaken at each sample station for Area A: Regional Survey.

Area A: Regional Survey									
Stn	**Lat.**	**Long.**	**Depth (m)**	**Operations**					
1	-14.164	140.200	65.0	CTD01	CAM01	GR01	-	BS01	-
2	-14.501	140.201	63.4	CTD02	CAM02	GR02	-	BS02	-
3	-14.833	140.199	59.0	CTD03	CAM03	GR03	-	BS03	-
4	-15.165	140.200	51.0	CTD04	CAM04	GR04	-	BS04	-
5	-15.398	140.199	43.5	CTD05	CAM05	GR05	-	BS05	-
6	-15.832	140.201	40.0	CTD06	CAM06	GR06	-	BS06	-
7	-16.170	140.203	33.0	-	CAM07	GR07	-	BS07	-
8	-16.500	140.200	29.0	CTD07	CAM08	GR08	-	BS08	-
9	-16.497	139.934	35.0	CTD08	CAM09	GR09	-	BS09	-
10	-16.833	140.199	23.0	CTD09	CAM10	GR10	-	BS10	-
11	-17.217	140.200	16.0	CTD10	CAM11	GR11	-	BS11	-
12	-17.047	140.500	17.5	CTD11	CAM12	GR12	-	BS12	-
13	-16.864	140.827	14.0	CTD12	CAM13	GR13	-	BS13	-
14	-16.849	140.500	19.5	CTD13	CAM14	GR14	-	BS14	-
15	-16.850	139.791	15.5	CTD14	CAM15	GR15	-	BS15	-
16	-16.712	140.249	24.5	CTD15	CAM16	GR16	-	BS16	-
17	-16.613	140.567	22.0	CTD16	CAM17	GR17	-	BS17	-
18	-16.500	140.932	15.0	CTD17	CAM18	GR18	-	BS18	-
19	-16.500	140.567	21.0	CTD18	CAM19	GR19	-	BS19	-
20	-17.000	139.883	16.5	CTD19	CAM20	GR20	-	BS20	-
21	-16.999	139.881	16.5	CTD20	CAM21	GR21	-	BS21	-
22	-16.850	139.885	19.0	CTD21	CAM22	GR22	VC01	BS22	-
23	-16.850	139.909	19.0	-	-	GR23	VC02	-	-
24	-17.204	140.221	15.5	CTD22	CAM23	GR24	VC03	BS23	-
25	-17.206	140.215	15.0	-	-	GR25	VC04	-	-
26	-17.107	140.396	18.0	CTD23	CAM24	GR26	VC05	BS24	-
27	-17.101	140.403	17.5	-	-	GR27	VC06	-	-
28	-17.098	140.411	18.0	-	-	GR28	VC07	-	-
29	-16.851	140.322	23.0	CTD24	CAM25	GR29	VC08	BS25	-
30	-16.851	140.336	24.0	-	-	GR30	VC09	-	-
31	-16.851	140.751	17.5	CTD25	CAM26	-	VC10	BS26	-
32	-16.556	140.751	16.5	CTD26	CAM27	GR31	VC11	BS27	-
33	-16.501	140.522	23.0	CTD27	CAM28	GR32	VC12	BS28	-
34	-16.615	140.562	20.0	CTD28	CAM29	GR33	VC13	BS29	-

35	-16.708	140.260	24.5	CTD29	-	GR34	VC14	BS30	-
36	-16.710	140.251	27.0	-	-	GR35	VC15	-	-
37	-16.681	140.200	33.0	CTD30	CAM30	GR36	VC16	BS31	-
38	-16.808	139.928	22.0	CTD31	-	GR37	VC17	BS32	-
39	-16.818	139.897	20.0	-	-	GR38	VC18	-	-
40	-16.499	139.965	31.0	CTD32	-	-	-	-	-

Table 4.1b. Summary details of operations undertaken at each sample station for Area B: Bryomol Reef.

Area B: Bryomol Reef									
Stn	**Lat.**	**Long.**	**Depth (m)**			**Operations**			
41	-16.512	139.909	41.0	CTD33	CAM31	GR39	-	-	-
42	-16.513	139.898	28.5	CTD34	CAM32	GR40	-	-	-
43	-16.497	139.916	32.5	CTD35	CAM33	GR41	-	-	DR01
44	-16.485	139.923	34.5	CTD36	CAM34	GR42	-	-	-
45	-16.510	139.948	35.0	CTD37	CAM35	GR43	VC19	BS33	-
46	-16.516	139.945	33.0	CTD38	CAM36	GR44	VC20	BS34	-
47	-16.487	139.941	38.5	CTD39	CAM37	GR45	-	BS35	-
48	-16.480	139.886	37.5	CTD40	CAM38	GR46	-	BS36	-
49	-16.497	139.893	26.0	CTD41	CAM39	GR47,48	-	-	-
50	-16.501	139.889	35.0	CTD42	CAM40	GR49	-	-	DR02
51	-16.527	139.876	25.0	-	CAM41	GR50	-	-	DR03
52	-16.534	139.879	25.0	-	CAM42	GR51	VC21	-	-
53	-16.546	139.892	31.5	-	CAM43	GR52	VC22	BS37	-
54	-16.514	139.869	26.5	CTD43	CAM44	GR53	-	-	DR04
55	-16.488	139.887	42.5	-	CAM45	GR54	-	BS38	-
56	-16.501	139.890	36.0	-	-	-	VC23	-	-
57	-16.528	139.940	32.0	-	-	-	VC24	-	-
58	-16.542	139.963	28.0	CTD44	CAM46	GR55	VC25	BS39	-
59	-16.530	139.940	31.5	-	CAM47	GR56	-	BS40	-
60	-16.469	139.927	29.0	-	CAM48	GR57	VC26	-	-
61	-16.475	139.925	33.0	-	CAM49	GR58	-	BS42	-
62	-16.451	139.902	30.5	CTD45	CAM50	GR59	VC27	-	-
63	-16.433	139.958	32.0	-	CAM51	GR60	-	BS43	-
64	-16.449	139.931	33.0	-	CAM52	GR61	-	BS44	-
65	-16.442	139.916	33.5	-	CAM53	GR62	-	BS45	-
66	-16.494	139.871	30.5	CTD46	CAM54	GR63	-	-	-
67	-16.439	139.879	34.5	-	CAM55	GR64,65	-	-	-
68	-16.443	139.847	26.5	-	CAM56	GR66	-	BS46	-
69	-16.445	139.866	33.5	-	CAM57	GR67	-	BS47	-
70	-16.452	139.879	42.5	CTD47	CAM58	GR68	-	BS48	-
71	-16.461	139.905	28.0	-	CAM59	GR69	-	-	-
72	-16.493	139.884	34.5	-	CAM60	GR70	-	-	DR05
73	-16.458	139.850	26.5	-	CAM61	GR71	-	BS49	-
74	-16.481	139.907	41.5	CTD48	CAM62	GR72	-	BS50	-
75	-16.526	139.910	33.5	-	CAM63	GR73	-	BS51	-
76	-16.499	139.932	33.5	CTD49	-	-	-	-	-

Table 4.1c. Summary details of operations undertaken at each sample station for Area C: Reef R1.

Area C: Reef R1									
Stn	**Lat.**	**Long.**	**Depth (m)**	**Operations**					
77	-15.251	140.327	48.5	CTD50	-	-	-	-	-
78	-15.245	140.303	50.5	CTD51	-	-	-	-	-
79	-15.262	140.382	49.0	CTD52	CAM64	GR74	VC28	BS52	-
80	-15.349	140.382	48.0	-	CAM65	GR75	VC29	BS53	-
81	-15.351	140.341	43.5	-	CAM66	GR76	VC30	BS54	-
82	-15.333	140.330	26.0	-	CAM67	GR77	-	-	DR06
83	-15.302	140.340	26.5	CTD53	CAM68	GR78	-	BS55	-
84	-15.276	140.334	22.5	-	CAM69	-	-	-	DR07
85	-15.266	140.347	47.5	-	CAM70	GR79	VC31	BS56	-
86	-15.284	140.339	27.5	-	CAM71	GR80	-	-	DR08
87	-15.295	140.325	27.0	-	CAM72	GR81	-	-	-
88	-15.268	140.319	27.0	-	CAM73	GR82	-	-	-
89	-15.255	140.329	47.5	CTD54	CAM74	GR83	VC32	BS57	-
90	-15.265	140.291	43.0	-	CAM75	GR84	VC33,34	BS58	-
91	-15.281	140.286	40.0	-	CAM76	GR85	VC35	BS59	-
92	-15.258	140.310	24.0	-	CAM77	-	-	-	-
93	-15.249	140.307	35.5	-	CAM78	GR86,87	-	-	DR09
94	-15.305	140.299	26.0	CTD55	CAM79	GR88	-	-	-
95	-15.324	140.309	20.5	-	CAM80	-	-	-	-
96	-15.326	140.297	24.0	-	CAM81	GR89	-	-	-
97	-15.329	140.295	25.5	-	CAM82	GR90	-	-	-
98	-15.324	140.284	30.5	-	CAM83	GR91	-	-	-
99	-15.329	140.280	39.5	-	CAM84	GR92	VC36	-	-
100	-15.338	140.275	43.0	CTD56	CAM85	GR93	VC37	-	-
101	-15.329	140.313	40.0	-	-	-	-	-	DR10
102	-15.341	140.284	43.5	-	CAM86	GR94	VC38	BS60	-
103	-15.353	140.288	43.5	-	CAM87	GR95	VC39	BS61	-
104	-15.343	140.308	37.0	-	CAM88	GR96	VC40	BS62	-
105	-15.341	140.375	41.5	CTD57	CAM89	GR97	-	-	DR11

Table 4.1d. Summary details of operations undertaken at each sample station for Area D: Reef R2.

Area D: Reef R2									
Stn	**Lat.**	**Long.**	**Depth (m)**	**Operations**					
112	-15.464	140.169	42.00	-	CAM96	GR104	-	-	-
113	-15.453	140.180	19.50	-	CAM97	-	-	-	-
114	-15.445	140.176	27.50	-	CAM98	GR105	-	-	-
115	-15.447	140.165	31.50	-	CAM99	GR106	-	-	-
116	-15.445	140.187	38.50	-	CAM100	GR107	-	-	-
117	-15.433	140.175	44.00	CTD58	CAM101	GR108	-	-	-

Table 4.1e. Summary details of operations undertaken at each sample station for Area E: Reef R3.

Area E: Reef R3									
Stn	**Lat.**	**Long.**	**Depth (m)**			**Operations**			
106	-15.528	140.107	41.00	-	CAM90	GR98	-	-	-
107	-15.522	140.116	19.60	-	CAM91	GR99	-	-	-
108	-15.525	140.113	27.50	-	CAM92	GR100	-	-	-
109	-15.519	140.110	30.00	-	CAM93	GR101	-	-	-
110	-15.515	140.110	28.50	-	CAM94	GR102	-	-	-
111	-15.510	140.115	43.50	-	CAM95	GR103	-	-	-

4.1.1. Water samples

A Seabird™ SBE911 CTD was deployed with a Seatech transmissometer, calibrated to measure suspended sediment concentration using surface and near-bed water samples (Fig. 4.1). The CTD was deployed from the starboard A-frame and automatically recorded salinity (‰), temperature (°C), and transmission (%). Water samples were collected using Niskin bottles fixed to the CTD rosette, which were fired remotely from the ship. Samples were collected 1 m from the bed and 1 m from the water surface.

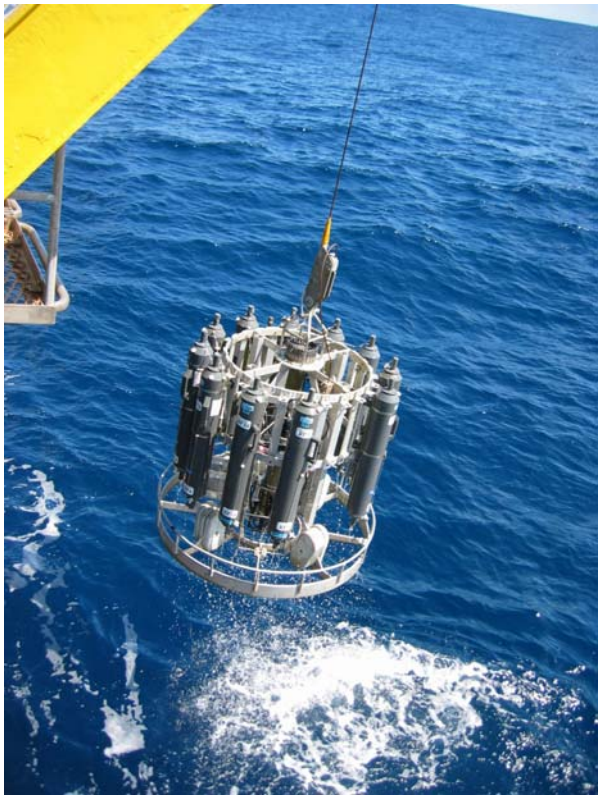

Figure 4.1. Photograph of CTD rosette deployed from starboard A-frame. Niskin bottles were attached to the rosette to collect water samples from near the bed and at the surface.

4.1.2. Digital Video Footage

Video footage of the seabed was collected to characterise the substrate, morphology and benthic biota in the study area. At each station, a video camera was lowered to the seafloor and recorded a minimum of three minutes of video. The video camera was built by

Geoscience Australia and comprises a digital video camera in a watertight titanium housing attached to a steel frame (Fig. 4.2). Four battery-powered 25W halogen lights fixed to the camera frame were used to illuminate the seabed where necessary, although at most sites only two lights were used to reduce glare and over exposure. A cm-scale bar was set up on the camera frame so that it was in the viewing area to determine the size of seabed features and objects in the water column. The underwater camera captured real-time footage that was recorded on digital videotape in the camera and was also fed to VHS tape on board the vessel. This "live" video feed enabled the winch control operator to manoeuvre the camera in order to image a representative area of the seabed and specific seabed features. Broad-scale seabed characteristics and the main types of biota were described on board the ship from the video and recorded in the shipboard database. A total of 101 camera deployments were undertaken during the survey, which totalled ~8.5 hours of footage.

Figure 4.2. Photograph of the underwater digital video camera system. The camera provides broadcast quality digital video. The camera and lights are powered from the surface and a live video feed is transmitted to the vessel.

4.1.3. Surface Sediment Sampling

Samples of the seabed were collected using a Smith-McIntyre grab deployed from the starboard A-frame (Fig. 4.3). Each grab was then sub-sampled for bulk sediment, biota and internal structures, where possible. A representative sample was obtained for bulk sediment (sub-sample A; e.g., 266/4GR4A). Another sub-sample was then collected for biota and preserved in ethanol (sub-sample B; e.g., 266/4GR4B). In samples that contained internal structures mini-cores of 0.15 m were collected from the grab by pushing a 0.09 m diameter piece of PVC core liner into the top of the sediment (sub-sample C; e.g., 266/4GR4C). The mini-core was then removed and sealed with end caps. Any living biota was also separately collected and recorded (sub-sample D; e.g., 266/4GR4D). The remainder of the grab was then sieved through a 5 mm mesh and the coarse fraction retained (sub-sample E; e.g., 266/4GR4E). Sediment sub-samples including those containing ethanol, were double bagged, labelled (including an aluminium tag), and stored in a refrigerated container. Sub-samples for biota were packed into wax boxes and frozen for transport to CSIRO laboratories. Details of the surface samples were entered into Geoscience Australia's Marine Samples database http://www.ga.gov.au/oracle/mars).

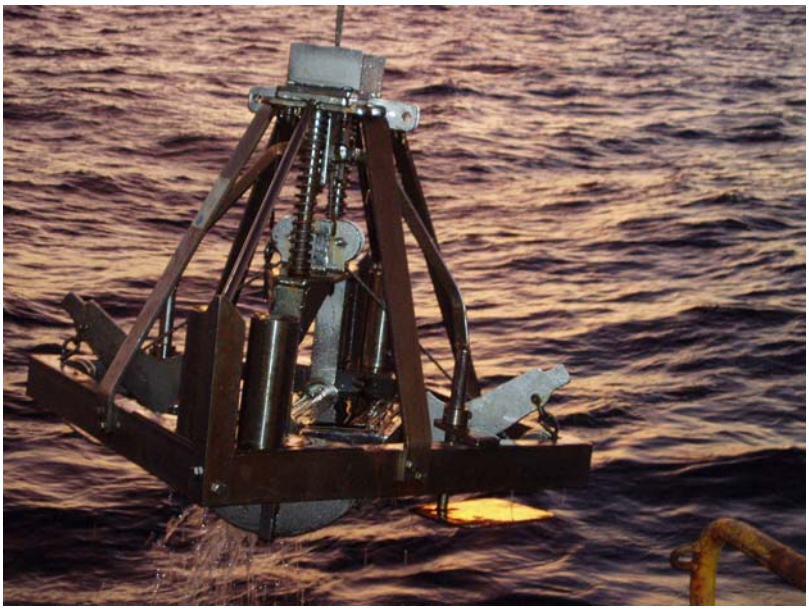

Figure 4.3. Photograph showing Smith-McIntyre grab sampler used on the survey.

4.1.4. Benthic Biota Sampling

A benthic sled constructed by CSIRO was used at select stations to collect samples of benthic biota. The benthic sled comprised a plastic net attached to a 1 m wide metal frame that was lowered to the seabed and then dragged along the surface for approximately 200 m (Fig. 4.4). Benthic biota collected in the net were then brought on board with the sled. A total of 62 benthic sled samples were collected from the study area. Each sample was sorted by hand on board the ship to pick out relevant biota and then frozen for later description and analysis.

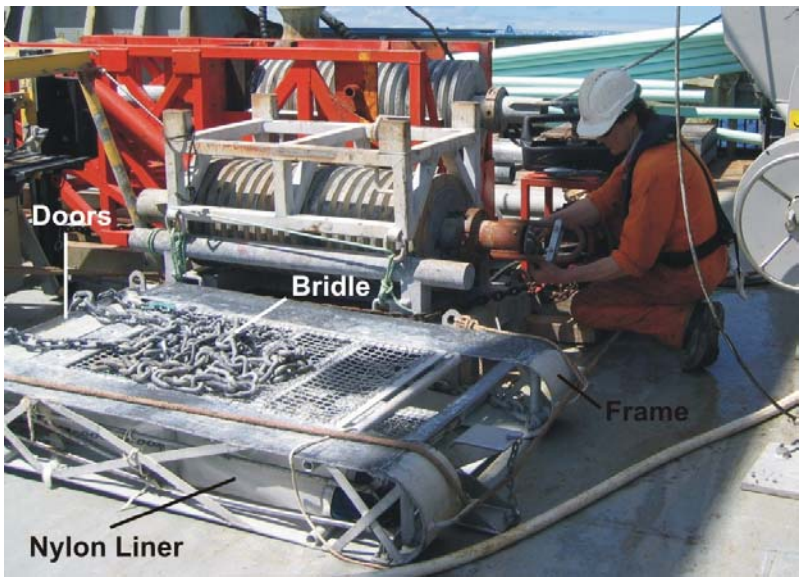

Figure 4.4. Photograph of benthic sled used on the survey, which is towed along the seabed behind the ship. Benthic biota collects in the nylon liner, and the doors close over the liner when the sled is raised off the seabed to prevent the sample from being lost on recovery.

4.1.5. Subsurface Sediment Sampling

Subsurface sediments were sampled using a 6 m-long electric-powered vibrocorer deployed using Geoscience Australia's coring cradle and the ship' coring winch (Fig. 4.5). The 415V

electric cable connected to the vibrating head unit was attached to the coring wire as a 'lazy' line and powered from an isolated control unit on the deck. The core frame was held upright on the seabed by three legs that extended outwards by hydrostatic pressure and maintained orientation into the current by a fin attached to one of the legs. The core barrels were 0.90 m diameter aluminium pipe and contained a 0.80 m diameter PVC liner fitted with a core catcher. The empty core liners were 6 m long and contained a piston that was tethered to the frame to assist with core recovery. From previous experience, each core was vibrated into the seabed for about 5 mins to achieve maximum penetration. On board, the cores were cut into 1 m sections, sealed with end caps (and packed with high-density foam biscuits where necessary), labelled, engraved and stored in a refrigerated container before being transported to Canberra for geophysical logging. Details were entered into the MARS database.

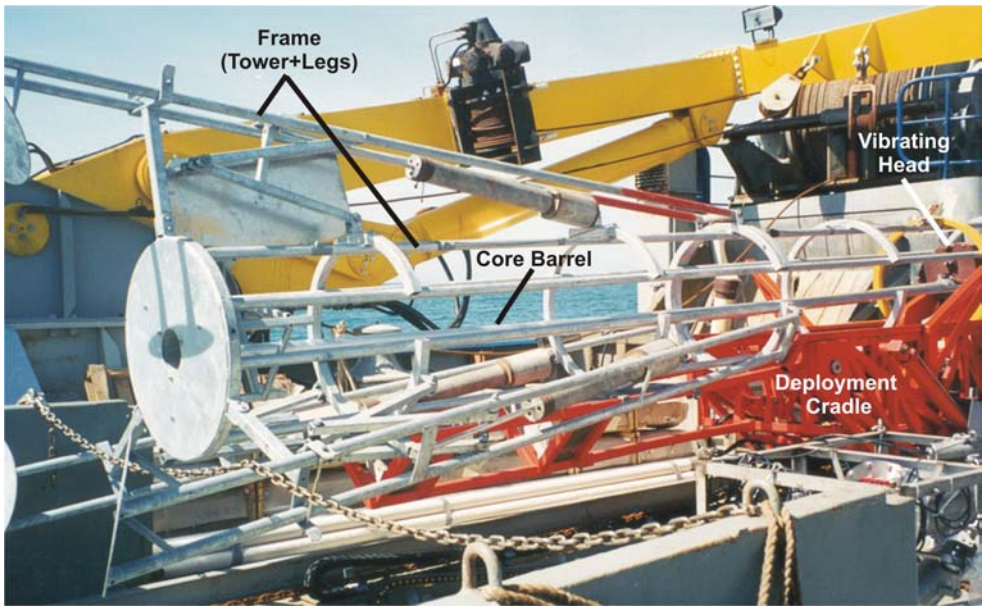

Figure 4.5. Photograph showing the vibrocorer used on the survey. The 6.5 m-long frame is deployed using a hydraulically powered deployment cradle. Power to the vibrating head unit is transmitted down an armoured cable from the vessel.

4.2. SAMPLE PROCESSING AND ANALYSIS

4.2.1. Water Samples

One litre of water was filtered through pre-weighed 0.45 µm mesh glass filter papers using a vacuum system on board the vessel (Fig. 4.6). The filter papers were then stored in a dry freezer and on return to the laboratory were oven dried at 60° C and re-weighed to ±0.0001 g to obtain the weight of suspended sediment. Suspended sediment concentrations were then calculated from these weights for the 1 litre of seawater filtered through the paper. Select filter papers were then visually inspected using a standard binocular microscope to provide an assessment of the type and nature of particles in suspension.

4.2.2. Digital Video Footage

Approximately 3-5 minutes of video was captured at each site which was edited down to 20-30 s snippets that showed the major habitats, biota and sedimentary processes that were observed at each station. The video was edited using standard video editing software. The 20-30 s video snippets for all 101 camera stations are contained in Appendix D.

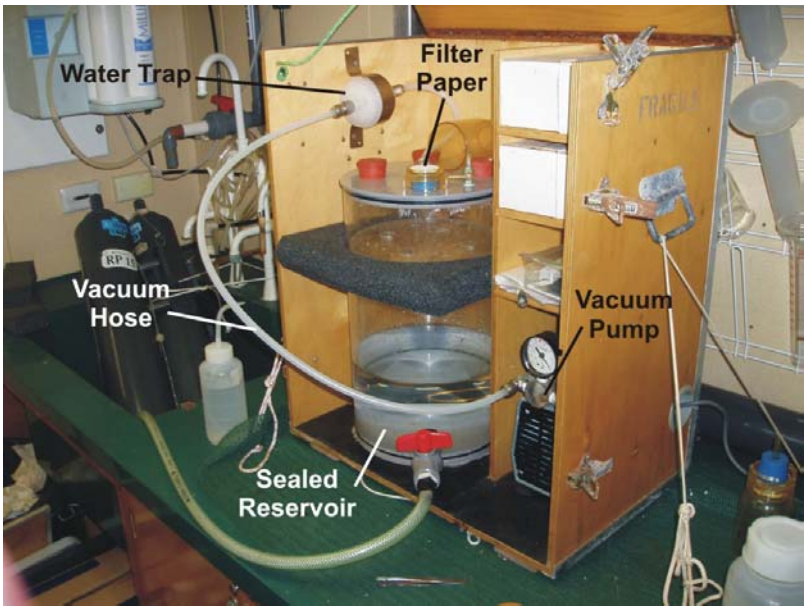

Figure 4.6. Photograph showing Geoscience Australia's purpose-built water filtering system. A total of 1 litre of seawater is filtered through 45 μm mesh filters. The filter papers are then weighed in the laboratory to determine total suspended solids (sediments).

4.2.3. Surface Sediments

Select samples were analysed for texture and composition to characterise the nature of the sedimentary environments in the southern gulf. All of the grab samples were analysed for grain size distribution, gravel-sand-mud concentrations and calcium carbonate concentrations, except for 93GR86, 107GR99, 109GR101, and 110GR102 due to insufficient sample for analysis.

4.2.3.1. Sediment texture

Initially, the bulk sample was split into two sub-samples for grain size analysis. Bulk grain size distributions were determined for the first sub-sample using a Malvern™ Mastersizer-2000 laser particle size analyser (e.g., Heap et al., 1999). The bulk sample was sieved through a 2 mm mesh to remove the gravel fraction, which was retained for visual inspection. Organic matter in the fine fraction was then removed by immersing the sample in 10-20 ml of dilute hydrogen peroxide (H_2O_2). After rinsing thoroughly with distilled water, the sample was placed in an ultrasonic bath for up to 2 mins to break up any remaining aggregates. The grain size distribution of the fine fraction was then determined using the laser particle size analyser.

Approximately 10-20 g of the second sub-sample was sieved through both 2 mm and 63 μm sieves with distilled water. Each size fraction was retained. The mud fraction was spun in a centrifuge at 3,500 rpm for 10 mins to separate out the sample. All of the fractions were dried in an oven at 40° C for at least 24 hours and then allowed to cool to room temperature. The dried material for each fraction was then weighed with an analytical balance to obtain the amount of gravel, sand and mud in the sample.

4.2.3.2. Sediment composition

Carbonate concentrations were determined on all of the bulk samples, as well as the sand and mud fractions using the "carbonate bomb" method of Muller and Gastner (1971).

Initially the 3-5 g of bulk sample was dried in an oven at 40° C for 24 hours. This sample was then ground to a fine powder and exactly 0.8 g was reacted with 10 ml of orthophosphoric acid (H_3PO_4). The flask was agitated until the entire sample had reacted with the acid (usually about 60 s). The pressure of the gas liberated was then compared to a standard curve that converted the pressure into carbonate concentrations (the curve is constructed by reacting known amounts of pure calcium carbonate between 0.1 – 0.8 g and recording the corresponding pressure). The carbonate content of the gravel fraction was estimated from a visual inspection for all samples.

Select samples were visually inspected for composition on board the vessel and in the laboratory using a standard binocular microscope. The bulk, gravel, sand and mud fractions were inspected separately, with only the coarse silt-sized grains visible in the mud fraction. An estimate of the abundance of each constituent in each fraction was made based on a visual assessment of the grains.

A preliminary study of the fossil content of the surface sediments was also performed on 20 grab samples from Areas A-E (Table 4.2). The absolute abundance of sixteen different associations in the sand fraction (63 μm-2 mm) was calculated together with the number of unrecognised organic fragments and lithic grains. The grab samples were repeatedly split with a micro-splitter to obtained 0.2 g of sediment for analysis. All the shells and fragments present in the sub-samples were then counted and expressed as number of specimens per gram of dry sediment (# g^{-1}). Fragments of organic origin too small for a straightforward identification were termed 'Other Bioclasts' and the term 'lithics' is used to denote all fragments of inorganic origin.

Table 4.2. List of select grab samples analysed for fossil content of surface sediments*.

Area	Sample
A	GR01, GR02, GR03, GR10, GR12, GR27
B	GR46, GR51, GR52, GR58, GR61
C	GR74, GR76, GR83, GR84, GR85
D	GR105, GR107
E	GR98, GR113

* See Tables 4.1a-e for grab sample locations.

4.2.4. Subsurface Sediments

To characterise the Late Quaternary history comprising the shallow sediments in the southern gulf the texture and composition, physical properties (i.e., wet bulk density, P-wave velocity, fractional porosity), and age of the sediments were determined (Table 4.3). The data for each physical property were "cleaned" by a visual inspection of the downcore profiles to remove spurious and bad data caused by logging artefacts (such as those around section breaks) and poor core condition.

4.2.4.1. Sediment texture

Grain size distributions were determined for bulk samples using a Malvern™ Mastersizer-2000 laser particle size analyser (e.g., Heap et al., 1999). The samples were prepared and analysed using the same methods as those undertaken for the surface samples (section 4.2.3.1).

Table 4.3. Summary of sediment analyses undertaken on the vibrocores.

Sample	Grain Size	G:S:M	$CaCO_3$	XRF	C-14 Ages	Bulk Density	P-wave Velocity*
22VC01	X	X	X	X		X	X
23VC02	X	X	X		X	X	X
24VC03	X	X	X	X	X	X	X
25VC04	X	X	X	X	X	X	X
26VC05	X	X	X	X	X	X	X
27VC06	X	X	X	X	X	X	X
28VC07						X	X
29VC08				X	X	X	X
30VC09	X	X	X	X		X	X
31VC10						X	X
32VC11						X	X
33VC12						X	X
34VC13						X	X
35VC14				X	X	X	X
36VC15						X	X
37VC16						X	X
38VC17				X	X	X	X
39VC18						X	X
46VC20						X	X
53VC22						X	X
56VC23				X		X	X
58VC25						X	X
60VC26						X	X
62VC27						X	X
79VC28						X	X
80VC29	X	X	X	X	X	X	X
81VC30	X	X	X	X	X	X	X
85VC31						X	X
89VC32					X	X	X
90VC33						X	X
90VC34	X	X	X	X	X	X	X
91VC35						X	X
100VC37	X	X	X	X	X	X	X
102VC38						X	X
103VC39						X	X
104VC40	X	X	X	X		X	X

* = measured but reliability of data uncertain due to effects of aluminium liner.

Core sub-samples were analysed for percent gravel, sand and mud. Between 5-10 g of bulk sediment was washed with distilled water through sieves of mesh sizes of 2 mm and 63 μm. The sub-samples were then treated and analysed using the same methods as those undertaken for the surface samples (section 4.2.3.1).

4.2.4.2. Sediment Composition

Carbonate concentrations were determined on the bulk samples, as well as the sand and mud fractions according to the bomb method of Muller and Gastner (1971). The procedure used is the same as that for the surface sediments (section 4.2.3.2).

4.2.4.3. Sediment Age

In order to obtain a chronology for the late-Holocene deposition in the southern gulf, a total of 77 samples collected from the vibrocores were submitted for Accelerator Mass Spectrometry (AMS) radiocarbon age determinations at Rafter Radiocarbon Laboratories in New Zealand. All of the samples were prepared at Geoscience Australia using the methods specified by Rafter Radiocarbon. Uncorrected ages were corrected by applying the marine reservoir correction of 450 years where applicable.

4.2.4.4. Physical Properties

After equilibration with ambient laboratory conditions (between 18° and 20°C), wet bulk density (WBD), P-wave Velocity (Vp), and Fractional Porosity (FP) were determined at 0.01 m intervals down VC1-5 using a GEOTEK™ MS2 multi-sensor core logger (e.g., Heap et al., 2001).

Wet bulk density (WBD) was determined by measuring the gamma attenuation of the sediment from a Cs-137 source. WBD of the sediment is positively correlated with gamma attenuation. The relationship between density and gamma attenuation was initially calibrated using a graduated density standard consisting of 13 water/aluminium density components (e.g., Best and Gunn, 1999). This procedure corrects for gamma attenuation (caused by the Al liner), count rate effects (e.g., Weber et al., 1997), and the different scattering properties of seawater and sediment (e.g., Gerland and Villinger, 1995). The calibration was undertaken using a water density of 1.001 g cm^{-3}, and aluminium density of 2.71 g cm^{-3}, which is approximately equal to the mineral densities of siliciclastic (2.65 g cm^{-3}) and carbonate (2.67 g cm^{-3}) grains. Using this calibration, repeat density measurements were within 0.05 g cm^{-3}.

P-wave velocity (Vp) was determined by measuring the travel time of a 500 kHz ultrasonic compressional pulse across the core. The pulse propagates through the core from the transmitter and is detected by the receiver. Vp is directly related to changes in the composition and texture of the sediments (e.g., mineral composition, grain shape and size, packing, etc.). To prevent variations in the ambient conditions masking differences between sedimentary units, the Vp was also corrected for temperature of the water and sediment and salinity of the interstitial fluid for each core.

Fractional Porosity (FP) was calculated directly from the WBD using equation 6:

$$FP = (MGD - WBD) / (MGD - WD) \quad (6)$$

where FP = fractional porosity, MGD = mineral grain density, WBD = wet bulk density, and WD = fluid density (i.e., sea water). This calculation assumes that the sediment was fully saturated with seawater, a mineral density of siliciclastic and carbonate sediment of ~2.65 g cm^{-3}, and a fluid (i.e., seawater) density of 1.024 g cm^{-3}.

The colour spectrum of the subsurface sediment was measured using the GEOTEK Geoscan digital imaging system attached to the multi-sensor core logger. The Geoscan system consists of a 3 megapixel CCD digital camera mounted vertically to the track of the

multi-sensor core logger. The whole cores were split and the archived half selected for colour imaging of the exposed surface. After calibrating the camera with black and white standards, and focussing it on the core surface, colour samples were collected at 0.01 m intervals down the core in a 0.05 m wide band located between 4.0-4.5 cm across the surface. Individual objects that skewed the measurements (e.g., large shells and voids) were avoided.

4.3. RESULTS

4.3.1. Water Samples

A total of 58 CTD casts were collected over the southeast gulf regions (Tables 4.1a-e). CTD casts and water samples were collected from representative sedimentary environments, including the gulf floor and high-standing platforms. A total of 32 CTD casts and water sample stations were occupied during the regional survey to provide the regional context, with more detailed measurements made at each of the reef study sites.

4.3.1.1. Area A: Regional Survey

Water temperature ranges from a maximum of 28.71°C at 3CTD3 to a minimum of 26.75°C at 31CTD25 with an average for the regional survey of 27.94°C (Fig. 4.7a). The maximum variation in water temperature of 0.54°C occurs at 3CTD3 and the minimum variation of 0.004°C occurs at station 22CTD21. Salinity ranges from a maximum of 34.27‰ at 37CTD30 to a minimum of 32.00‰ at 31CTD25 with an average for the regional survey of 33.54‰ (Fig. 4.7b). The maximum variation in salinity of 0.32‰ occurs at 11CTD10 and the minimum variation of 0.001‰ occurs at station 37CTD30. Transmission ranges from a maximum of 93.07% at 19CTD18 to a minimum of 49.69 at 2CTD2 with an average of 81.15% across the region (Fig. 4.7c). The maximum variation in transmission of 40.55% occurs at 2CTD2 and the minimum variation of 1.95% occurs at station 22CTD21. The average variation from the surface to near-bed waters for temperature, salinity, and transmission all stations is 0.15°C, 0.05‰, and 8.91%, respectively indicating that the SE gulf waters are well mixed and clear.

The CTD data reveal a number of interesting trends (Fig. 4.7a). Firstly, stations with relatively high water temperatures (i.e., >28.3°C) are all located in water depths of >40 m and stations with relatively low water temperatures (i.e., <27.5°C) are all located in water depths of <20 m. Stations with moderate temperatures (i.e., between 27.5 and 28.2°C) are all located in water depths of <40 m. Similar trends occur in the salinity data (Fig. 4.7b). Stations with relatively low salinities (i.e., <32.3‰) occur in water depths of <20 m while stations with elevated salinities (i.e., >33.9‰) occur in water depths of between 40 and 20 m. Those stations with moderate salinities (i.e., 32.8-33.9‰) occur in water depths of 13.5-65 m. Of these stations, those in water depths of <21 m contain higher transmission values. The maximum salinity range and the minimum temperature recorded at any station in Area A occurs at station 11CTD10. Maximum salinity and the maximum temperature range from the surface to the near-bed waters occurs at station 31CTD25. Station 2CTD2 has the maximum transmission but also displays the maximum variation in transmission from the surface to the near-bed waters. Profiles from a total of 15 stations show the existence of differences in water properties that are defined by possible thermoclines and haloclines (Fig. 4.7a-c). However, only three stations (21CTD20, 16CTD15, 20CTD19) show evidence of the different water properties from coincident changes in their temperature, salinity and transmission.

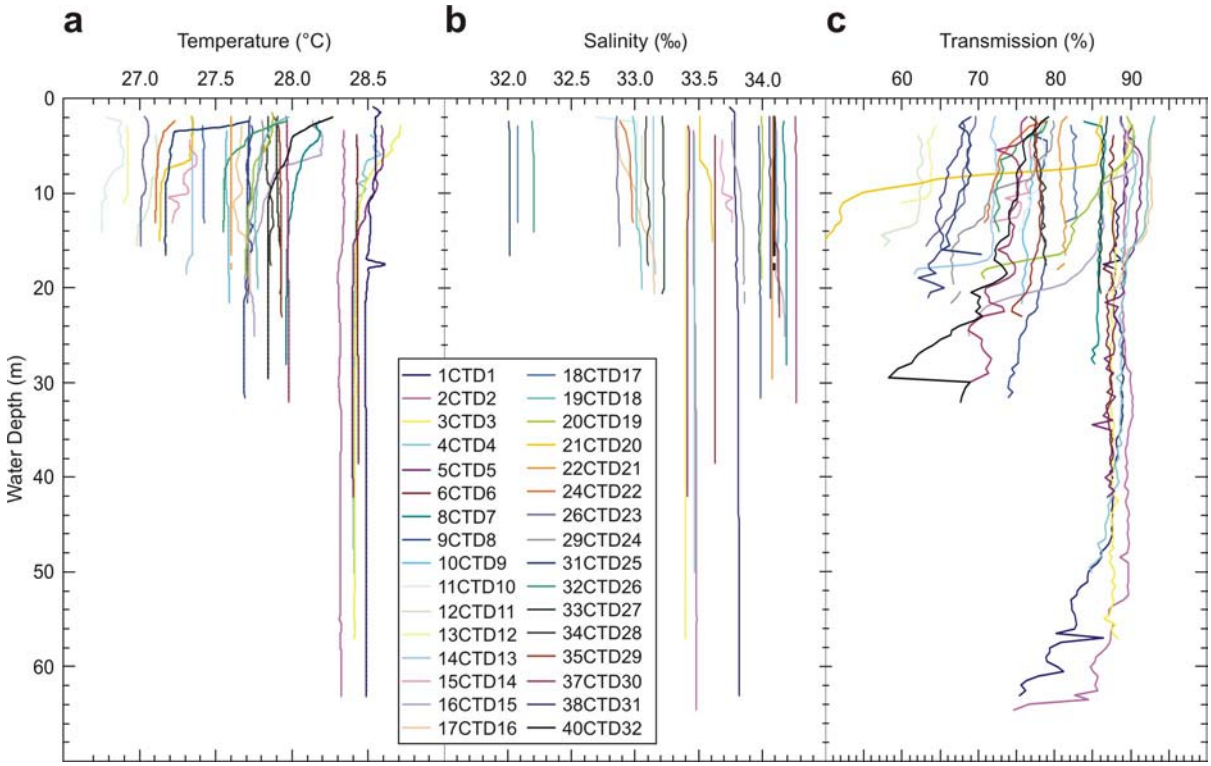

Figure 4.7. Graphs showing: a) temperature (°C), b) salinity (‰), and c) transmission (%) for the waters in Area A: Regional Survey from the CTD casts. A thermocline is evident between 2-5 m depth at some stations (e.g., 8CTD7). Transmission decreases with depth. Otherwise, the data indicate that the waters in Area A are mostly well-mixed and relatively clear.

A one-way Analysis of Variance (ANOVA) performed on the temperature, salinity and transmission profiles from Area A indicates that there are statistically significant differences between the stations (Table 4.4). A Scheffe's Test was then undertaken as a post-hoc comparison to determine the combinations of stations contributing to the effect (Appendix E). Of the total 496 station combinations, a total of 443 (89%), 475 (96%) and 335 (68%) show

Table 4.4. One-way Analysis of Variance (ANOVA) for temperature, salinity and transmission profiles from Area A.

Temperature						
Source of Variation	SS	df	MS	F-statistic	P-value	F crit
Between Groups	325.7899	31	10.5093	3399.3853	0	1.4590
Within Groups	4.5631	1476	0.0031			
Total	330.3531	1507				

Salinity						
Source of Variation	SS	df	MS	F-statistic	P-value	F crit
Between Groups	432.4048	31	13.9485	25995.9850	0	1.4590
Within Groups	0.7920	1476	0.0005			
Total	433.1967	1507				

Transmission						
Source of Variation	SS	df	MS	F-statistic	P-value	F crit
Between Groups	98777.6890	31	3186.3771	259.7120	0	1.4590
Within Groups	18145.6840	1479	12.2689			
Total	116923.3700	1510				

significant differences in their means for temperature, salinity and transmission, respectively, at the 95% confidence level. Stations with statistical differences in temperature, salinity and transmission do not occur consistently across the different gulf environments, indicating that there is significant variability in the water properties in the SE gulf.

In the southeast gulf, near-bed suspended sediment concentrations range from 11.06 mg l^{-1} to 0.43 mg l^{-1} and surface concentrations range from 13.2 mg l^{-1} to 0.45 mg l^{-1} (Fig. 4.8; Table 4.5a). The average near-bed and surface concentrations are 4.66 mg l^{-1} and 4.02 mg l^{-1}, respectively, indicating that near-bed concentrations are slightly higher than those at the surface. A z-test for the difference between the sample means indicates that this difference is not statistically significant between the near-bed and surface samples collected from the SE gulf (Table 4.5b).

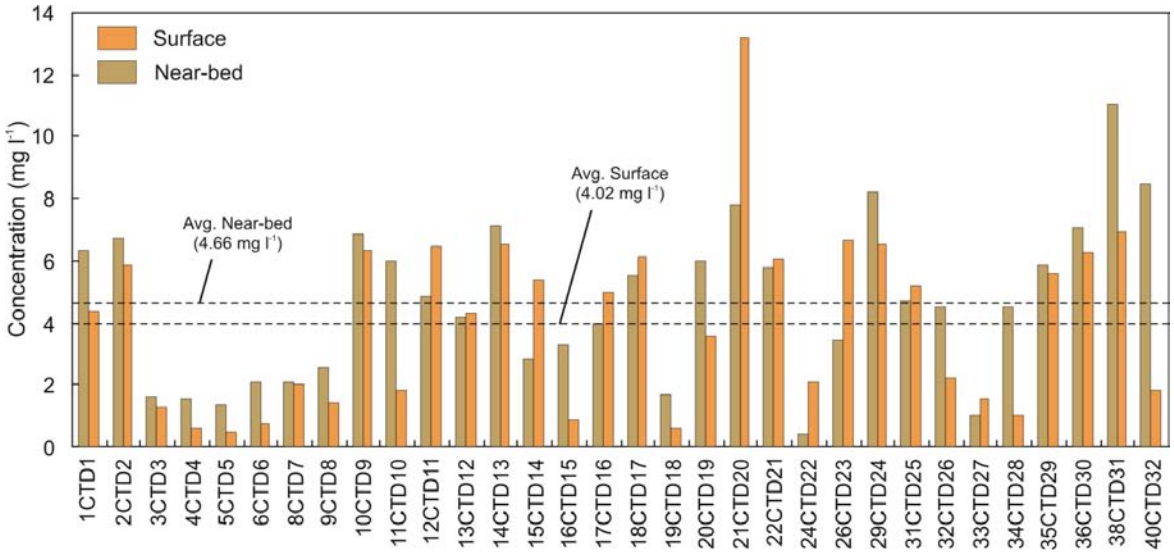

Figure 4.8. Graph showing near-bed and surface suspended sediment concentrations from Area A: Regional Survey. Near-bed concentrations are slightly higher than surface concentrations. However, this difference is not statistically significant.

Table 4.5a. Descriptive statistics of near-bed and surface suspended sediment concentrations.

	Area A		**Area B**		**Area C**	
	Near-bed	Surface	Near-bed	Surface	Near-bed	Surface
Mean (mg l^{-1})	4.66	4.02	5.17	4.54	3.31	3.09
Mode (mg l^{-1})	2.10	0.60	5.60	2.50	1.35	4.85
Std Dev. (mg l^{-1})	2.53	2.87	3.04	3.66	1.89	1.78
Variance (mg l^{-1})	6.42	8.21	9.26	13.40	3.57	3.18
Kurtosis	-0.28	1.56	0.45	1.15	-2.04	-2.64
Skewness	0.33	0.88	1.14	1.51	0.01	-0.24
Minimum (mg l^{-1})	0.43	0.45	2.00	1.45	1.35	1.15
Maximum (mg l^{-1})	11.06	13.20	12.00	13.20	5.90	4.85
Count	33	32	17	17	7	7

4.3.1.2. Area B: Bryomol Reef

A total of 17 CTD casts were completed in Area B (Table 4.1b). Water temperature ranges from a maximum of 27.67°C at 47CTD39 to a minimum of 27.01°C at 74CTD48 with an average of 27.45°C across the study area (Fig. 4.9a). The data indicate that the water temperature is relatively constant with depth. The maximum variation in water temperature

Table 4.5b. Z-test for difference between means for suspended sediment concentrations observed at Areas A, B, and C.

	Area A		**Area B**		**Area C**	
	Near-bed	Surface	Near-bed	Surface	Near-bed	Surface
Mean (mg l^{-1})	4.66	4.02	5.17	4.54	3.31	3.09
Var. (mg l^{-1})	6.42	8.21	9.26	13.40	3.57	3.18
Observations	33	32	17	17	7	7
HMD*	0		0		0	
z-statistic	0.94		0.54		0.23	
P(Z≤z) 1-tail	0.17		0.29		0.41	
z Crit. 1-tail	1.64		1.64		1.64	
P(Z≤z) 2-tail	0.35		0.59		0.82	
z Crit. 2-tail	1.96		1.96		1.96	

* = Hypothesised Mean Difference (mg l^{-1})

of 0.13°C occurs at 76CTD49 and the minimum variation of 0.006°C occurs at station 41CTD33. Salinity ranges from a maximum of 34.26‰ at 76CTD49 to a minimum of 34.10‰ at 45CTD37 with an average of 34.17‰ across the study area (Fig. 4.9b). The profiles show that there is a general increase in salinity with depth. The maximum variation in salinity of 0.04‰ occurs at 47CTD39 and the minimum variation of 0.001‰ occurs at station 41CTD33. Transmission ranges from a maximum of 84.47% at 76CTD49 to a minimum of 57.44% at 58CTD44 with an average of 71.51% across the study area (Fig. 4.9c). As expected the data reveal that there is a slight decrease in transmission with water depth. The maximum variation in transmission of 16.12% occurs at 47CTD39 and the minimum variation of 0.43%

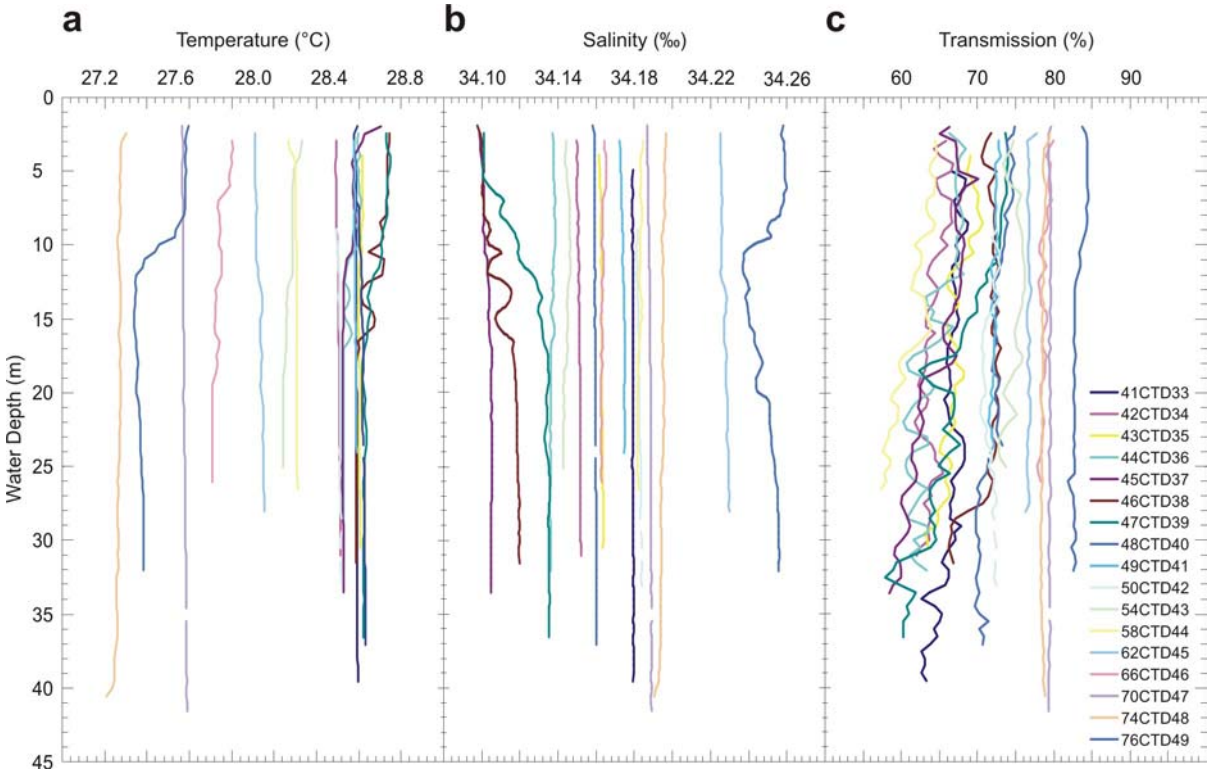

Figure 4.9. Graphs showing: a) temperature (°C), b) salinity (‰), and c) transmission (%) for the waters in Area B: Bryomol Reef from the CTD casts. A slight thermocline and halocline can been seen at around 10 m water depth at station 48CTD10. Otherwise, the data indicate that the waters in Area B are mostly well-mixed and relatively clear.

occurs at station 70CTD47. The average variation from the surface to near-bed waters for temperature, salinity, and transmission all stations is 0.04°C, 0.007‰, and 5.29%, respectively, indicating that the waters in Area B are well mixed and clear.

The maximum temperature and maximum variations in salinity and transmission recorded at any station in Area B occur at station 47CTD39. Maximum salinity, maximum transmission and the maximum variation in temperature from the surface to the near-bed waters occurs at station 76CTD49. Station 41CTD33 has the minimum variations in temperature and salinity of all stations in Area B. Profiles from a total of 6 stations show the existence of differences in water properties that are defined by possible thermoclines and haloclines. Interestingly, four of those stations (45CTD37, 46CTD38, 47CTD39, 76CTD49) show evidence of the different water properties from coincident changes in their temperature, salinity and transmission profiles (Fig. 4.9a-c). All of these stations occur in similar water depths on the hard-grounds to the east of the bryomol reef.

A one-way ANOVA performed on the temperature, salinity and transmission profiles from Area B indicates that there are statistically significant differences between the stations (Table 4.6). A Scheffe's Test was then undertaken as a post-hoc comparison to determine the combinations of stations contributing to the effect (Appendix E). Of the total 136 station combinations, a total of 123 (90%), 131 (96%) and 120 (88%) show significant differences in their means for temperature, salinity and transmission, respectively, at the 95% confidence level. Stations with statistical differences in temperature, salinity and transmission do not occur consistently across the different environments in Area B, including stations on the reef compared with those from the depressions and hard-grounds. This pattern indicates that the water properties are not specific to the different sedimentary environments in Area B.

Table 4.6. One-way Analysis of Variance (ANOVA) for temperature, salinity and transmission profiles from Area B.

Temperature						
Source of Variation	SS	df	MS	F-statistic	P-value	F crit
Between Groups	39.9819	16	2.4989	8612.0479	0	1.6538
Within Groups	0.2867	988	0.0003			
Total	40.2686	1004				
Salinity						
Source of Variation	SS	df	MS	F-statistic	P-value	F crit
Between Groups	1.3645	16	0.0853	4933.2302	0	1.6538
Within Groups	0.0171	988	0			
Total	1.3816	1004				
Transmission						
Source of Variation	SS	df	MS	F-statistic	P-value	F crit
Between Groups	40284.4060	16	2517.7754	643.2256	0	1.6538
Within Groups	3871.2387	989	3.9143			
Total	44155.6450	1005				

In Area B, near-bed suspended sediment concentrations range from 12 mg l^{-1} to 2 mg l^{-1} and surface concentrations range from 13.2 mg l^{-1} to 1.45 mg l^{-1} (Fig. 4.10; Table 4.5a). The average near-bed and surface concentrations are 5.17 mg l^{-1} and 4.54 mg l^{-1}, respectively,

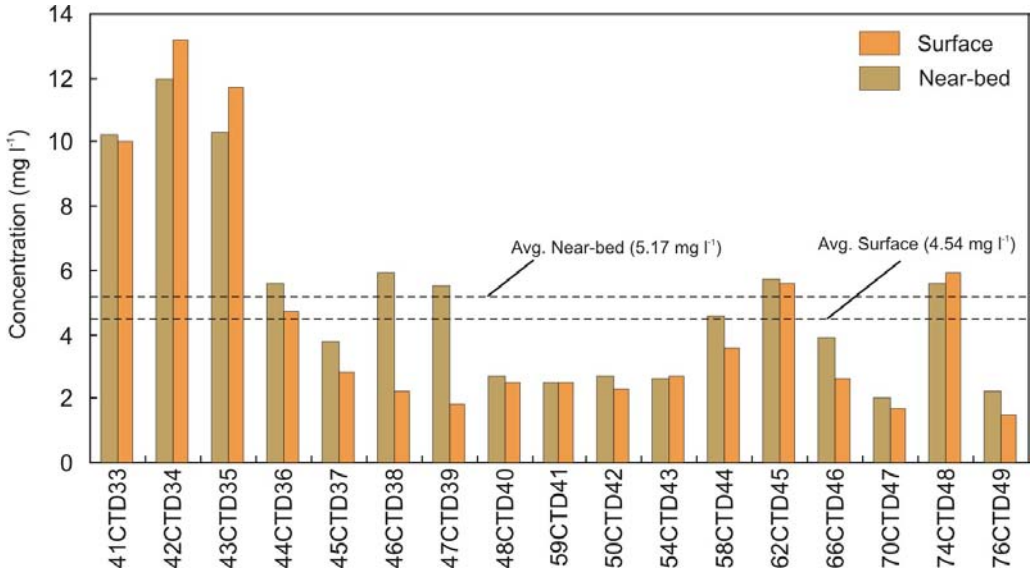

Figure 4.10. Graph showing near-bed and surface suspended sediment concentrations from Area B: Bryomol Reef. Near-bed concentrations are slightly higher than surface concentrations. However, this difference is not statistically significant.

indicating that near-bed concentrations are slightly higher than those at the surface. A z-test for the difference between the sample means indicates that this difference is not statistically significant between the near-bed and surface samples collected from Area B (Table 4.5b).

4.3.1.3. Area C: Reef R1

A total of 7 CTD casts were completed in Area C (Table 4.1c). Water temperature ranges from a maximum of 28.30°C at 79CTD52 to a minimum of 27.83°C at 100CTD56 with an average of 28.01°C (Fig. 4.11a). The data show that the water temperature is relatively constant with depth, with two stations (89CTD54, 105CTD57) showing a slight decrease with depth. The maximum variation in water temperature of 0.34°C occurs at 79CTD52 and the minimum variation of 0.008°C occurs at station 83CTD53. Salinity ranges from a maximum of 33.56‰ at 78CTD51 to a minimum of 33.49‰ at 79CTD52 with an average of 33.52‰ across the study area (Fig. 4.11b). There is no consistent trend in salinity with depth with approximately half of the stations indicating an increase with depth (e.g., 83CTD53, 100CTD56) and the other half indicating a decrease with depth (e.g., 79CTD52, 105CTD57). The maximum variation in salinity of 0.007‰ occurs at 105CTD57 and the minimum variation of 0.001‰ occurs at station 78CTD51. Transmission ranges from a maximum of 88.64% at 78CTD51 to a minimum of 83.24% at 100CTD56 with an average of 86.37% across the study area (Fig. 4.11c). As expected the data reveal that there is a slight decrease in transmission with water depth. The maximum variation in transmission of 3.65% occurs at 105CTD57 and the minimum variation of 0.52% occurs at station 94CTD35. The average variation from the surface to near-bed waters for temperature, salinity, and transmission all stations is 0.13°C, 0.004‰, and 1.64%, respectively, indicating that the waters in Area C are well mixed and clear. Transmission at Area C is the highest for all the study areas.

The maximum salinity and transmission recorded at any station in Area C occur at station 78CTD51. This station also recorded the minimum variation in salinity of all stations in Area C. The maximum temperature and temperature variation at any station in Area C occur at station 79CTD52. Minimum temperature and transmission occur at station 100CTD56. The maximum variations in salinity and transmission occur at station 105CTD57.

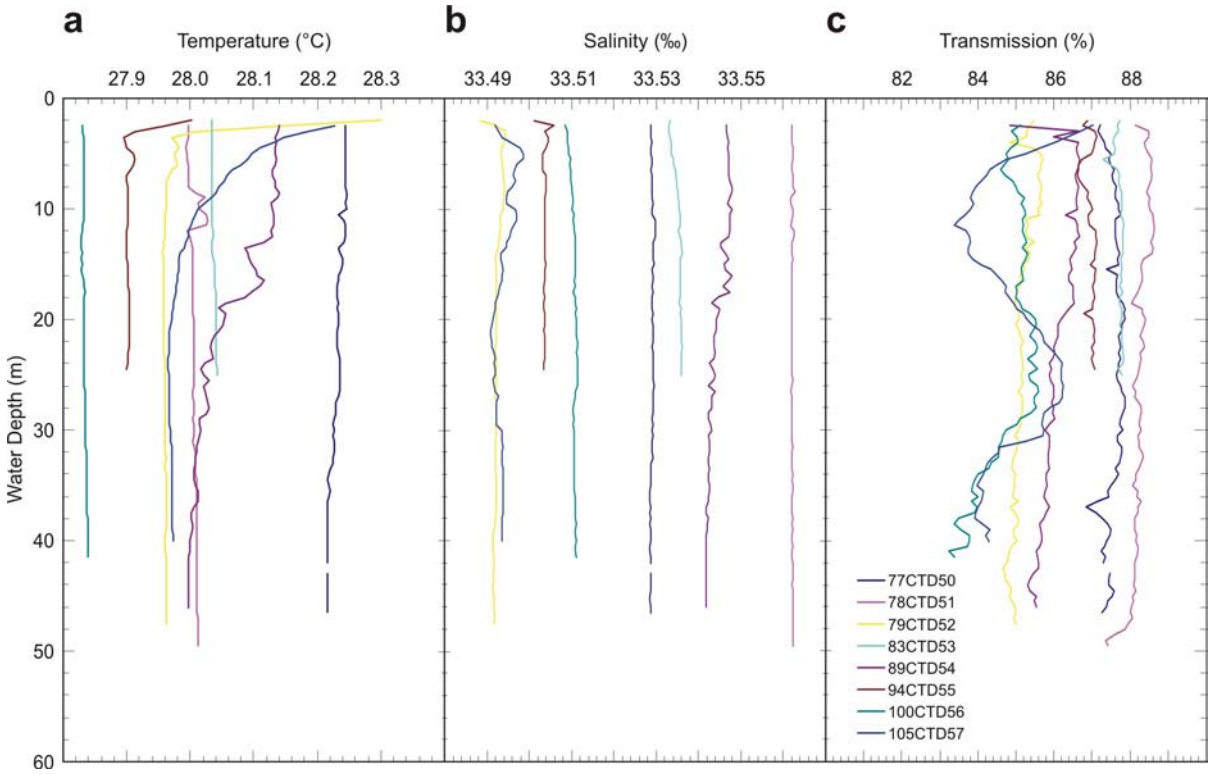

Figure 4.11. Graphs showing: a) temperature (°C), b) salinity (‰), and c) transmission (%) for the waters in Area C: Reef R1 from the CTD casts. There is a slight decrease in transmission with water depth. Otherwise, the data indicate that the waters in Area B are mostly well-mixed and relatively clear. Transmission in Area C is the highest for all study areas.

Profiles from a total of 3 stations (89CTD54, 100CTD56, 105CTD57) show the existence of differences in water properties that are defined by possible thermoclines and haloclines (Fig. 4.11a-c). Interestingly, only 1 of those stations (105CTD57) shows evidence of the different water properties from coincident changes in temperature, salinity and transmission profiles. This station occurs to the southeast of the reef, associated with the cemented ridge.

A one-way ANOVA performed on the temperature, salinity and transmission profiles from Area C indicates that there are statistically significant differences between the stations (Table 4.7). A Scheffe's Test was then undertaken as a post-hoc comparison to determine the combinations of stations contributing to the effect (Appendix E). Of the total 28 station combinations, a total of 26 (93%), 28 (100%) and 27 (96%) show significant differences in their means for temperature, salinity and transmission, respectively, at the 95% confidence level. Stations with statistical differences in temperature, salinity and transmission do not occur consistently across the different environments in Area C, including stations on the reef compared with those from the surrounding seabed. This pattern indicates that the water properties are not specific to the different sedimentary environments in Area C.

In Area C, near-bed suspended sediment concentrations range from 5.90 mg l^{-1} to 1.35 mg l^{-1} and surface concentrations range from 4.85 mg l^{-1} to 1.15 mg l^{-1} (Fig. 4.12; Table 4.5a). The average near-bed and surface concentrations are 3.31 mg l^{-1} and 3.09 mg l^{-1}, respectively, indicating that near-bed concentrations are slightly higher than those at the surface. A z-test for the difference between the sample means indicates that this difference is not statistically significant between the near-bed and surface samples collected from Area C (Table 4.5b).

4.3.1.4. Area D: Reef R2

Only one CTD cast (117CTD58) was completed in Area D (Table 4.1d). The CTD was taken in 43 m water depth to the north of the reef. Water temperature at this station

Table 4.7. One-way Analysis of Variance (ANOVA) for temperature, salinity and transmission profiles from Area C.

Temperature						
Source of Variation	SS	df	MS	F	P-value	F crit
Between Groups	7.6016	7	1.0859	1005.5931	0	2.0247
Within Groups	0.6512	603	0.0011			
Total	8.2528	610				
Salinity						
Source of Variation	SS	df	MS	F	P-value	F crit
Between Groups	0.3759	7	0.0537	37229.3653	0	2.0247
Within Groups	0.0009	603	0			
Total	0.3767	610				
Transmission						
Source of Variation	SS	df	MS	F	P-value	F crit
Between Groups	1079.954	7	154.2791	713.3135	0	2.0247
Within Groups	130.4200	603	0.2163			
Total	1210.374	610				

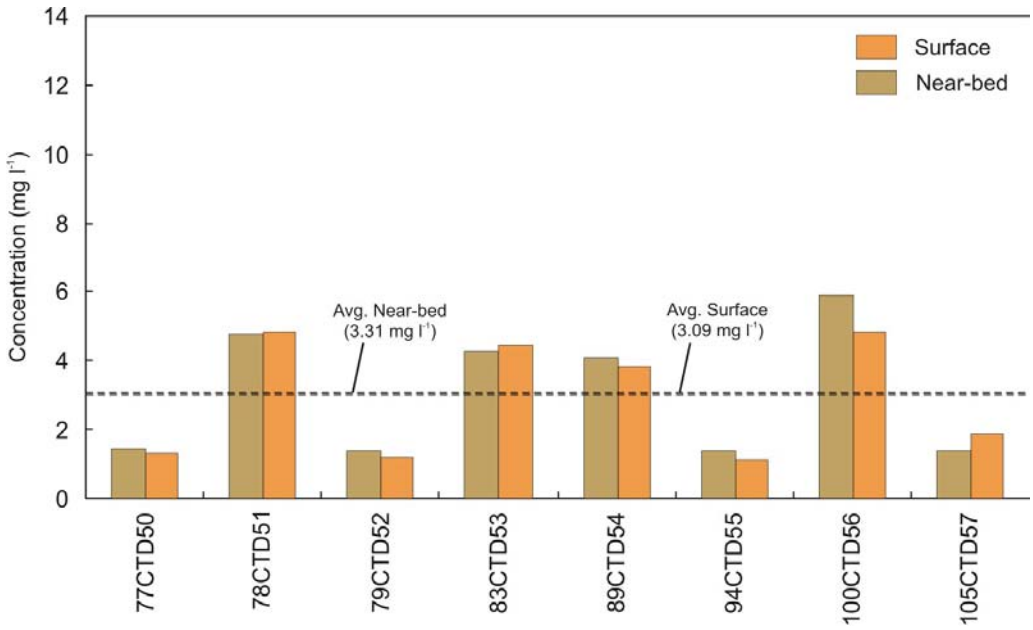

Figure 4.12. Graph showing near-bed and surface suspended sediment concentrations from Area C: Reef R1. Near-bed concentrations are slightly higher than surface concentrations. However, this difference is not statistically significant.

ranges from from a maximum of 27.97°C at 14.5 m to a minimum of 27.96°C at 32.5 m, changing by only 0.01°C with depth (Fig. 4.13a). Salinity ranges from a maximum of 33.57‰ at 40.5 m to a minimum of 33.59‰ at 8 m, with an average of 33.56‰ (Fig. 4.13b). Transmission ranges from a maximum of 87.86% at 2 m to a minimum of 86.30% at 42.5 m, changing only 0.77% with depth (Fig. 4.13c). Not surprisingly there is a general decrease in transmission with water depth at this station. A comparison of temperature, salinity and transmission profiles indicates that there is a strong inverse relationship (r^2=0.9355) between temperature and salinity (Fig. 4.13d), with temperature decreasing and salinity increasing

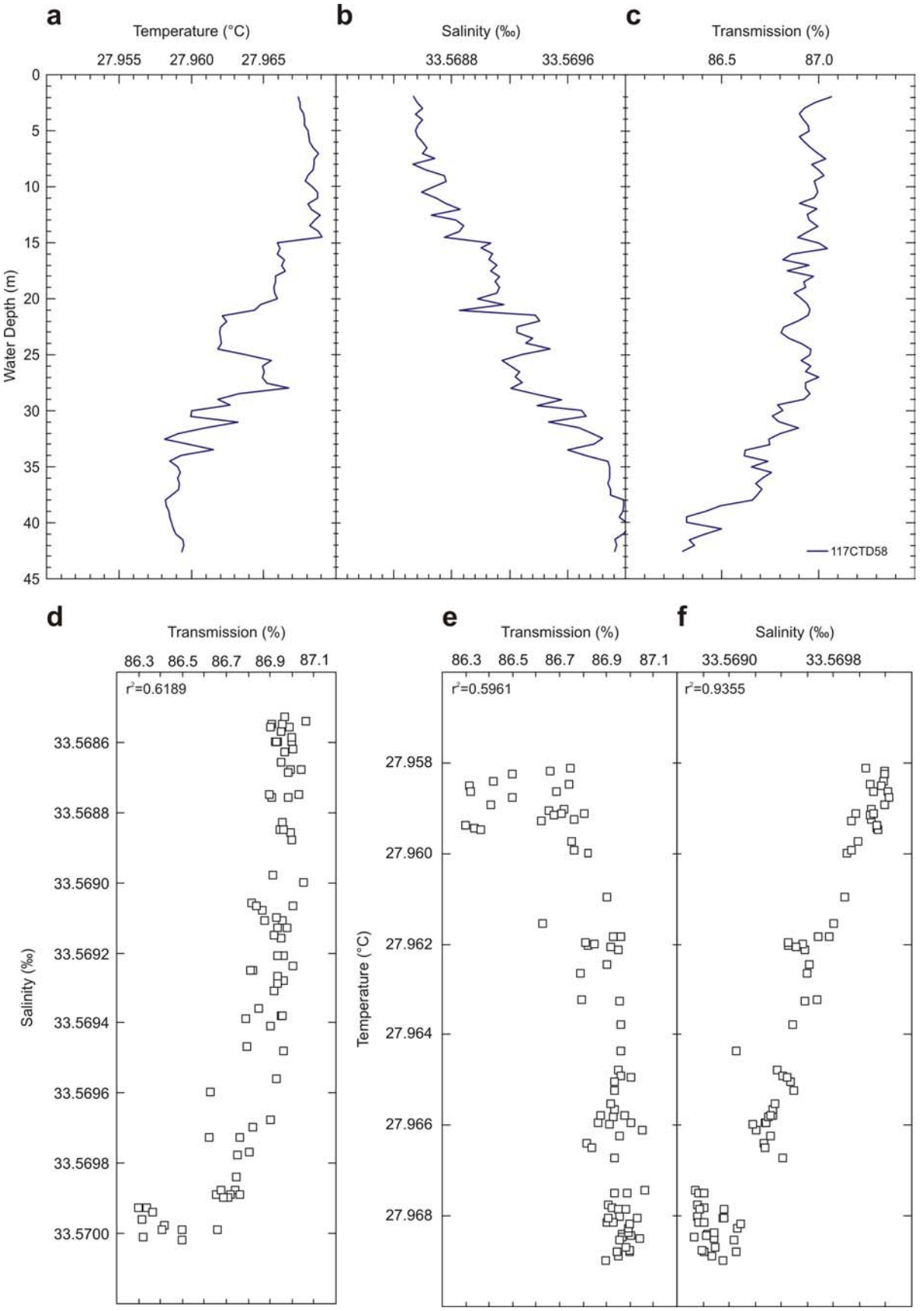

Figure 4.13. Graphs showing: a) temperature (°C), b) salinity (‰), c) transmission, d) salinity v transmission, e) temperature v transmission, and e) temperature v salinity for the CTD cast taken in Area D: Reef R2. The data indicate that the water near the reef is relatively well mixed and clear. There is a strong inverse relationship between temperature and salinity, positive relationship between temperature and transmission, and an inverse relationship between salinity and transmission.

with depth (Fig. 4.13d, e). There is a positive relationship (r^2=0.5961) between temperature and transmission (Fig. 4.13e), with both temperature and transmission decreasing slightly with depth (Fig. 4.13d, f). There is an inverse relationship (r^2=0.6189) between salinity and transmission (Fig. 4.13f), with salinity increasing and transmission decreasing with depth (Fig. 4.13e, f). Near-bed suspended sediment concentrations are 5.00 mg l^{-1} and surface concentrations are 4.45 mg l^{-1}.

4.3.1.5. Area E: Reef R3

No CTD casts were undertaken in this study area.

4.3.1.6. Regional Trends

A comparison of the CTD data observed at stations occupied along a N-S transect from the relatively deep (>60 m) central gulf regions to the relatively shallow (<30 m) inner shelf regions shows that the water properties vary considerably with latitude and water depth (Fig. 4.14a-c). From the central gulf to the inner-shelf, water temperatures decrease by between 1°C and 1.5°C and transmissions decrease by >10%. Salinity shows a more variable distribution, with little variation through the water column, although the inner-shelf regions are slightly more saline on average than the cental gulf waters. A one-way ANOVA performed on the data indicates that the differences observed in the temperature, salinity, and transmission data along the N-S transect are statistically significant (Table 4.8).

The Scheffe's test (Table 4.9) indicates that water properties observed in the central gulf (1CTD1-8CTD7) are significantly different from those observed on the inner-shelf (9CTD8, 10CTD9, 24CTD22). The Scheffe's test also reveals that the temperature profiles observed at stations located in the vicinity of the platform reefs (3CTD3-6CTD6) in the central gulf are not statistically different from each other but are different from all other locations. All the stations show significant differences in salinity, due to the very small variations observed in the water column throughout the SE gulf. Transmission shows significant variability across the SE gulf, particularly in the northern and deepest regions of the central gulf (1CTD1, 2CTD2) where transmissions decrease by up to 12% below 52 m probably because of bottom re-suspension by waves. The Scheffe's test reveals that the transmission observed at these two northern and deepest stations is significantly different to those recorded in other parts of the central gulf, in particular those stations occupied in the vicinity of the reefs where transmission near the bed is up to 10% higher. Interestingly, transmissions observed at the shallow inner-shelf station (24CTD22) are not significantly different to those observed at the stations occupied in the central gulf (1CTD1-8CTD7).

Differences in transmission observed in the CTD data is not reflected in the suspended sediment data collected during the survey. A one-way ANOVA performed on all the suspended sediment data collected from Areas A, B and C indicates that there is no significant difference in the concentrations between any of the study areas either near the bed or at the surface (Table 4.10). These results demonstrate that suspended sediment concentrations were similar throughout the southeast gulf during the time of the survey. Interestingly, this result also indicates that there is no significant difference in the suspended sediment concentrations between the reefal and off-reef sites. Because no significant difference was observed from the ANOVA, there was no requirement to perform a post-hoc comparison test (e.g., Scheffe's Test) to determine which station combinations were contributing to the differences.

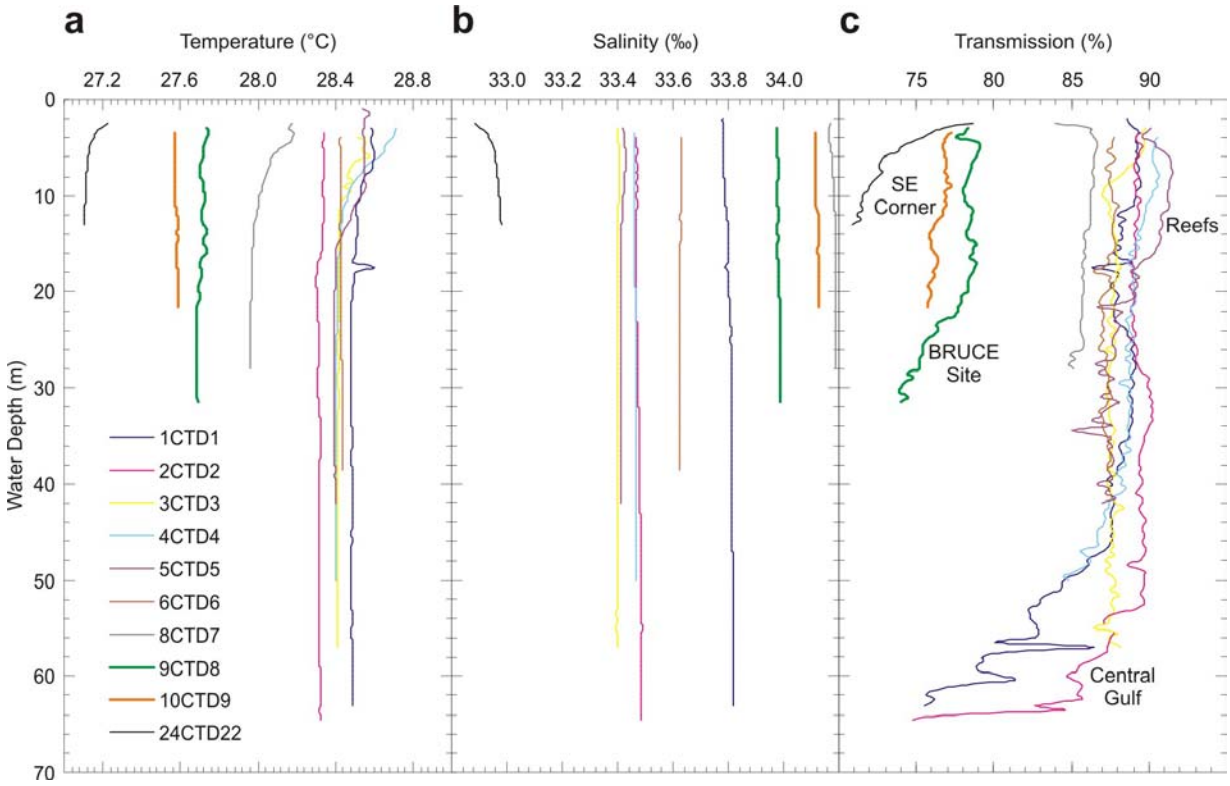

Figure 4.14. Graphs showing: a) temperature, b) salinity, and c) transmission for CTD casts collected from a north-south transect in the southern Gulf of Carpentaria. There are clear differences in the water properties between the relatively deep central Gulf regions and the shallow SE regions. See text for full details and analysis.

Table 4.8. One-way Analysis of Variance (ANOVA) for temperature, salinity and transmission from regional N-S transect.

Temperature						
Source of Variation	SS	df	MS	F	P-value	F crit
Between Groups	84.5919	9	9.3991	5151.1597	0	1.8922
Within Groups	1.3831	758	0.0018			
Total	85.9750	767				
Salinity						
Source of Variation	SS	df	MS	F	P-value	F crit
Between Groups	60.8720	9	6.7636	57771.9330	0	1.8922
Within Groups	0.0953	758	0.0001			
Total	60.9674	767				
Transmission						
Source of Variation	SS	df	MS	F	P-value	F crit
Between Groups	13976.7901	9	1552.9767	442.0455	0	1.8923
Within Groups	2652.4362	755	3.5132			
Total	16629.2262	764				

Table 4.9. Scheffe's post-hoc comparison test of data recorded on a regional N-S transect from the central gulf to inner shelf*.

Temperature									
	1CTD1	2CTD2	3CTD3	4CTD4	5CTD5	6CTD6	8CTD7	9CTD8	10CTD9
1CTD1									
2CTD2	*0*								
3CTD3	*0*	*0*							
4CTD4	*0*	*0*	0.3323						
5CTD5	*0*	*0*	1	0.4527					
6CTD6	*0*	*0*	0.9921	0.9865	0.9948				
8CTD7	*0*	*0*	*0*	*0*	*0*	*0*			
9CTD8	*0*	*0*	*0*	*0*	*0*	*0*	*0*		
10CTD9	*0*	*0*	*0*	*0*	*0*	*0*	*0*	*0*	
24CTD22	*0*	*0*	*0*	*0*	*0*	*0*	*0*	*0*	*0*

Salinity									
	1CTD1	2CTD2	3CTD3	4CTD4	5CTD5	6CTD6	8CTD7	9CTD8	10CTD9
1CTD1									
2CTD2	*0*								
3CTD3	*0*	*0*							
4CTD4	*0*	*0.0022*	*0*						
5CTD5	*0*	*0*	*0*	*0*					
6CTD6	*0*	*0*	*0*	*0*	*0*				
8CTD7	*0*	*0*	*0*	*0*	*0*	*0*			
9CTD8	*0*	*0*	*0*	*0*	*0*	*0*	*0*		
10CTD9	*0*	*0*	*0*	*0*	*0*	*0*	*0*	*0*	
24CTD22	*0*	*0*	*0*	*0*	*0*	*0*	*0*	*0*	*0*

Transmission									
	1CTD1	2CTD2	3CTD3	4CTD4	5CTD5	6CTD6	8CTD7	9CTD8	10CTD9
1CTD1									
2CTD2	*0*								
3CTD3	*0.0188*	0.1937							
4CTD4	*0*	1	0.3837						
5CTD5	*0*	1	0.1248	0.9999					
6CTD6	0.7367	*0.0140*	0.9899	*0.0453*	*0.0088*				
8CTD7	0.8146	*0*	*0.0002*	*0*	*0*	0.0589			
9CTD8	*0*	*0*	*0*	*0*	*0*	*0*	*0*		
10CTD9	*0*	*0*	*0*	*0*	*0*	*0*	*0*	0.7917	
24CTD22	*0*	*0*	*0*	*0*	*0*	*0*	*0*	*0*	*0*

* Italicised probabilities are significant at 95% confidence level ($p<0.05$).

4.3.2. Digital Video Footage

Video footage of the seabed was recorded at a total of 101 camera stations (Tables 4.1a-e). A representative selection of sedimentary environments was selected for study, including the

Table 4.10. One-way Analysis of Variance (ANOVA) of suspended sediment concentrations at Areas A, B, and C.

	SS Effect	df Effect	MS Effect	SS Error	df Error	MS Error	F-statistic	p
All Data	27.2788	2	13.6394	873.2086	110	7.9383	1.7182	0.1842
Near-bed	17.1771	2	8.5885	375.1136	54	6.9465	1.2364	0.2985
Surface	10.6236	2	5.3118	488.0666	53	9.2088	0.5768	0.5652

hard-grounds, depressions and reefal environments in Area B, and off-reef and reefal environments in Areas C, D and E. Where they could be determined genus and species names are given for the biota (mostly megafauna) observed in the video. Only a cursory description of the seabed and biota observed in the video footage is presented. A full analysis of the video for biota will be conducted by CSIRO – Marine and Atmospheric Research. The 20-30 s video snippets for all 101 camera stations are contained in Appendix D.

4.3.2.1. Area A: Regional Survey

A total of 30 camera stations were occupied during the regional survey in water depths ranging from 64 m to 14 m (Fig. 4.15; Table 4.1a). The video revealed that the seabed across the southeast gulf mostly comprises calcareous muddy sand with a high level of suspended material (e.g., 02CAM02). The seabed is pock-marked by numerous burrows surrounded by mounds and mollusc shells (e.g., 13CAM13).

On the seabed, the biota is generally sparse with extensive tracts of smooth (bioturbated?) muddy sand. Soft corals are most abundant and include: gorgonians, sea whips, sea pens and anemones. Less abundant biota include: sponges (*Pelaroides leptolepis*), crustaceans (19CAM19), echinoderms (crinoids, heart urchins and star fish), hydroids, ascidians, and bryozoans. Seagrass was also observed at one location (17CAM17). Fishes in the southeast gulf include: flounder, leather jacket, bream (*Nemipterus* sp.), grinner (*Trachinocephalus myops*), and a longtail seamoth (*Pegasus volitans*) at station 34CAM29.

4.3.2.2. Area B: Bryomol Reef

A total of 33 camera stations were occupied from Area B: Bryomol Reef (Fig. 4.16; Table 4.1b). On the hard-grounds, depressions, and reef a total of 25, 4, and 4 camera stations were occupied in water depths ranging from 44.5-25 m, 43-27.5 m, and 35-26 m, respectively. On the hard-grounds the video revealed that the seabed mostly comprises calcareous muddy and gravelly sands. Pebbles and mollusc shells were observed on the seabed at several stations. In the depressions, the seabed comprises calcareous coarse sands with abundant coralline rubble and mollusc shells on the surface. Bedload transport was also observed in all the stations from the depressions (e.g., 41CAM31). On the reef top, the seabed is rugose with large areas of rocky reef interspersed with calcareous coarse sand.

Biota observed from the hard-grounds is generally sparse but relatively more abundant on the cemented ridges (60CAM48). Biota on the hard-grounds include: soft corals (gorgonians, sea whips), sponges (*Lanthella* sp., *Ircinia* sp.), hydroids, holothurians, echinoderms. Fishes on the hard-grounds include angel fish and trevally (71CAM59). Biota in the depressions include: sponges, soft corals (gorgonians, sea whips), hydroids, echinoderms (basket star) and fish. Biota on the reef top include: sponges (*Lanthella* sp.), soft corals (gorgonians), hydroids, echinoderms (star fish), and ascidians (*Hypodistoma deeratum*). Surface sediments in a local depression on the reef top comprise well sorted calcareous sand with little biota (50CAM40).

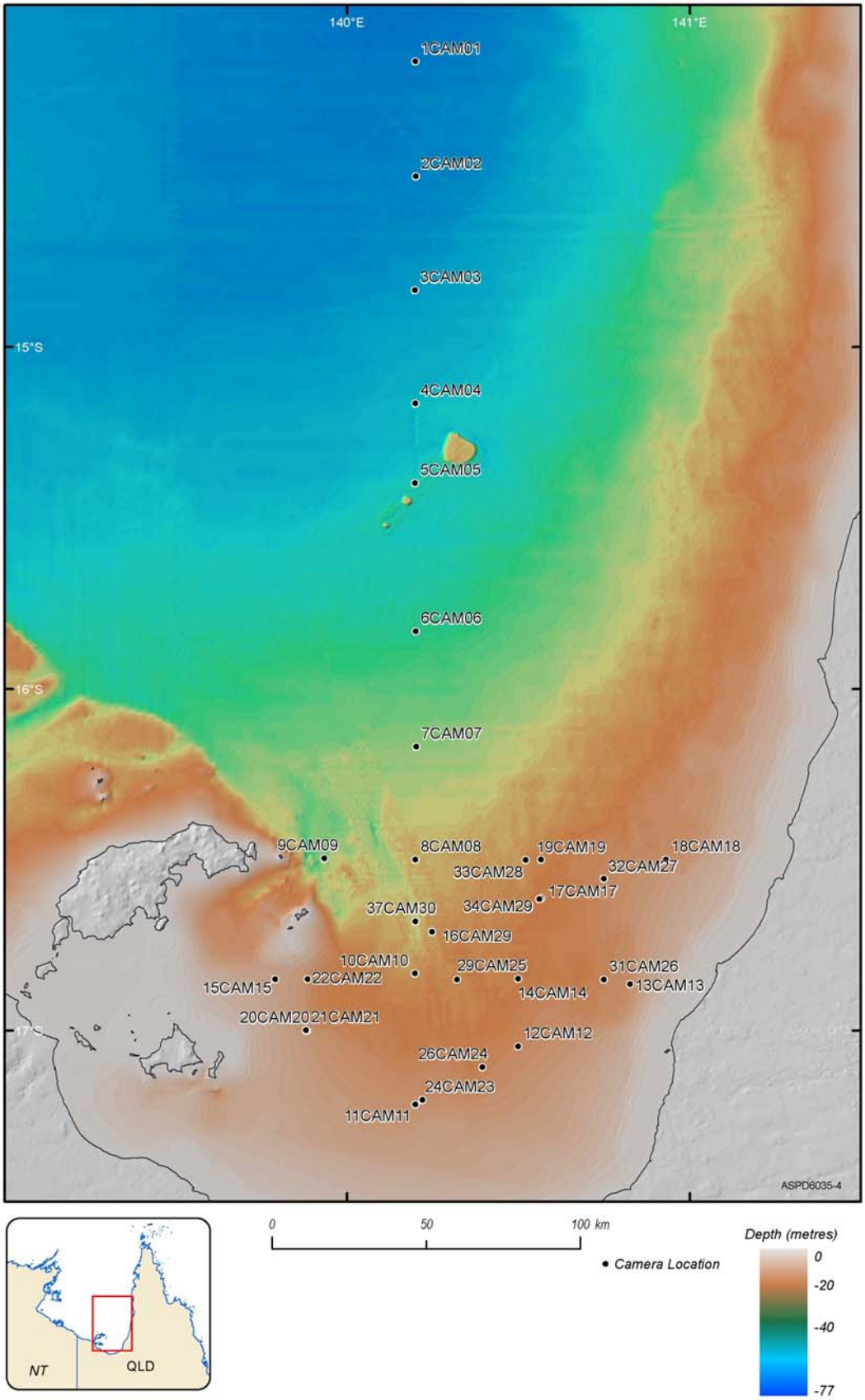

Figure 4.15. Bathymetry map showing location of camera stations occupied in Area A: Regional Survey.

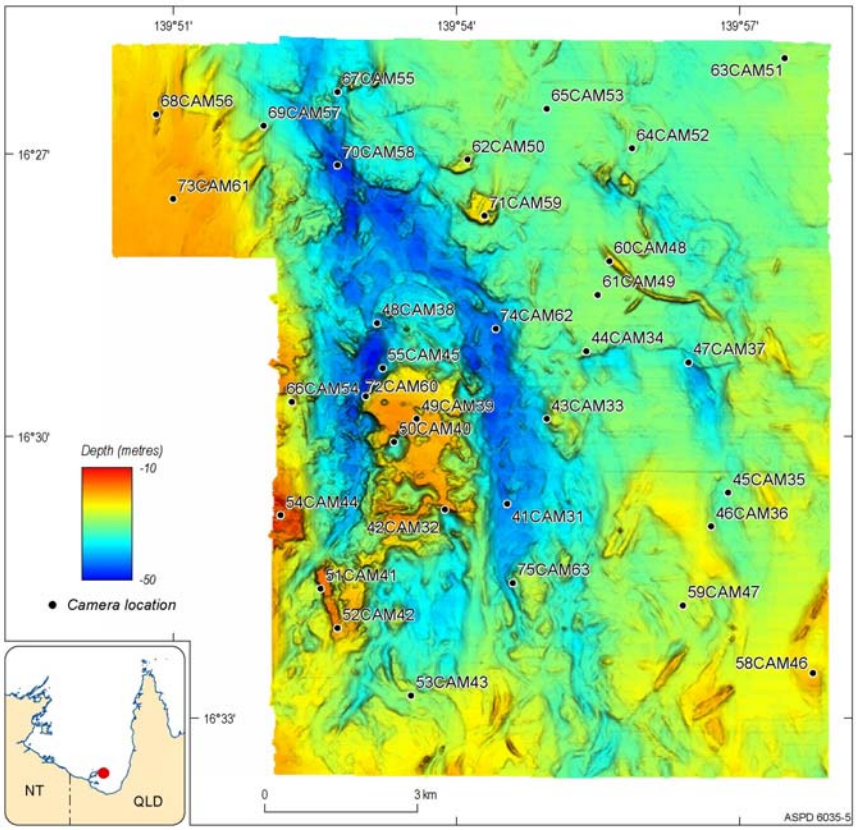

Figure 4.16. Bathymetry map showing location of camera stations occupied in Area B: Bryomol Reef.

4.3.2.3. Area C: Reef R1

A total of 26 camera stations were occupied from Area C: Reef R1 in water depths ranging from 49.5 m on the surrounding seabed to 20 m on the reef (Fig. 4.17; Table 4.1c). Around the reef, the seabed is composed of smooth muddy sand with numerous burrows (<0.2 m in diameter) and mounds (e.g., 85CAM70). Mollusc shells are also common. The reef platform is very rugose with numerous rocky (limestone?) outcrops interspersed by relatively flat-lying regions of calcareous coarse to medium sand (e.g., 88CAM73).

Biota on the seabed surrounding the reef is relatively sparse with soft corals (gorgonians, sea whips, anemones) most abundant. Other biota include: hydroids, sponges (*Lanthella* sp.), echinoderms (crinoids), and squid. Fishes observed on the seabed include fusiliers (*Caesio* sp.) and grinner (*Saurida* sp.). On the reef, biota is much more abundant, with most cover occurring on the rocky outcrops. Living colonial hard corals were observed on the reef crests (e.g., 87CAM72, 95CAM80), including staghorn (*Acropora* sp.) and plate (*Turbinaria* sp.) corals. Other biota include: sponges (*Lanthella* sp., *Xestospongia* sp.), soft corals (gorgonians, sea whips and anemones), bryozoans, holothurians, echinoderms (star fish [*Linkia* sp.]), and ascidians. The rocky outcrops also support sea snakes (*Aipesurus laevis*) (92CAM77) and octopus (94CAM79).

4.3.2.4. Area D: Reef R2

A total of 6 camera stations were occupied from Area D: Reef R2 in water depths of 44 m on the surrounding seabed to 19.5 m on the reef (Fig. 4.18; Table 4.1d). Around the reef,

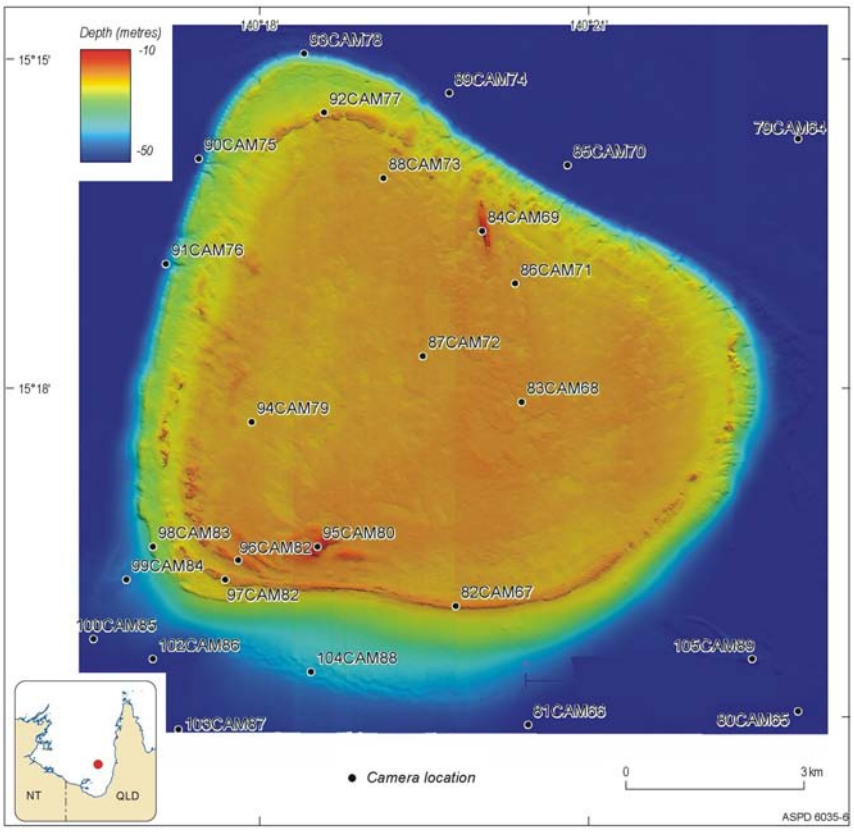

Figure 4.17. Bathymetry map showing location of camera stations occupied on Reef R1.

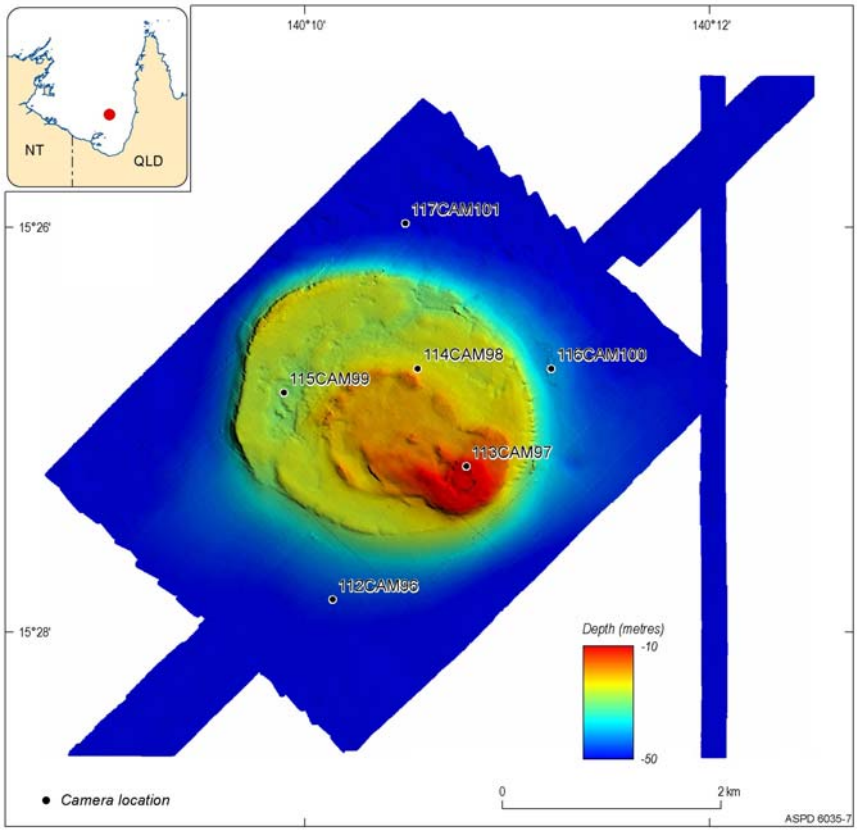

Figure 4.18. Bathymetry map showing location of camera stations occupied on Reef R2.

the seabed is composed of smooth muddy sand with numerous burrows and sparse coralline rubble (112CAM96; 117CAM101). On the reef, the seabed comprises rocky (limestone?) outcrops interspersed with patches of calcareous sand and gravel (e.g., 113CAM97).

The seabed surrounding the reef contains relatively sparse and less abundant biota comprising of soft corals (gorgonians, sea whips, anemones), hydroids, sponges, echinoderms (crinoids, holothurians, sea urchins, starfish) and ascidians. Fishes observed on the seabed include: grinner (*Saurida* sp.) and goatfish (116CAM100). On the reef, the biota is much more abundant, with most cover occurring on the rocky outcrops. Living hard corals were observed on the reef crests (e.g., 113CAM97, 114CAM98), including: plate (*Turbinaria* sp.) and fire (*Millepora* sp.) corals. Other biota include: soft corals (gorgonians, sea whip), hydroids, echinoderms (sea urchins, holothurians, crinoids), and sponges. The rocky outcrops also support sea snakes (*Aipesurus laevis*) and butterfly fish (*Chaetodon* sp.) (113CAM97).

4.3.2.5. Area E: Reef R3

A total of 6 camera stations were occupied from Area E: Reef R3 in water depths of 43.5 m on the surrounding seabed to 20 m on the reef (Fig. 4.19; Table 4.1e). Around the reef, the seabed is composed of smooth muddy sand with numerous burrows (106CAM90). On the reef, the seabed comprises rocky (limestone?) outcrops interspersed with patches of calcareous sand and gravel (107CAM91).

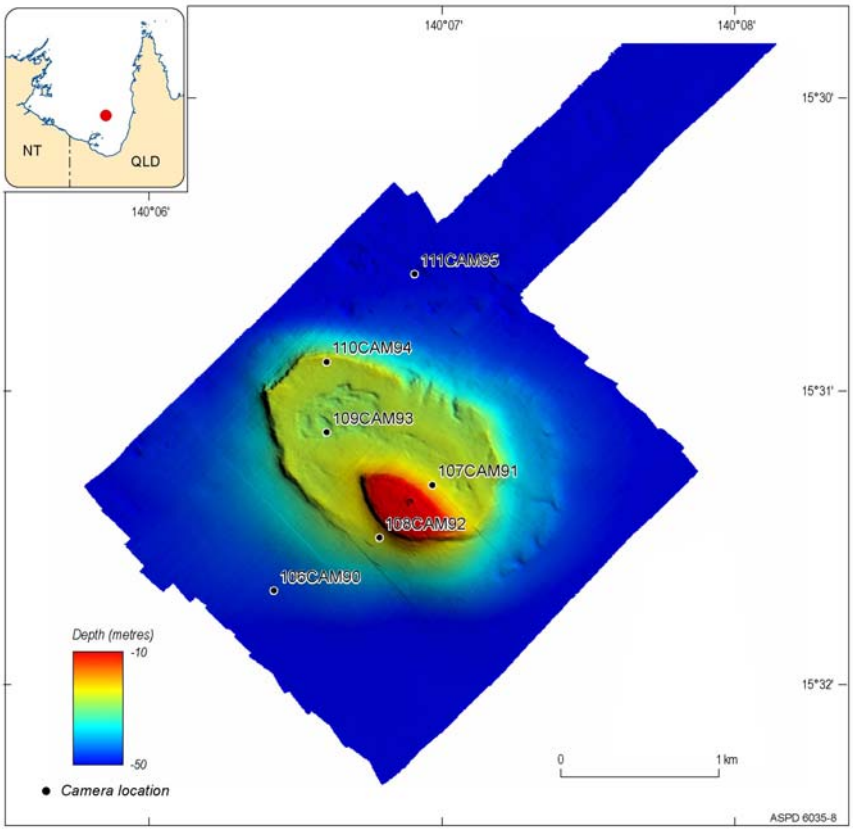

Figure 4.19. Bathymetry map showing location of camera stations occupied on Reef R3.

Biota is relatively sparse on the seabed surrounding the reef. The most abundant biota is soft corals (gorgonians, sea whips), followed by hydroids and ascidians. By comparison, biota is relatively abundant on the reef, particularly on the rocky outcrops, where living hard

corals including staghorn (*Acropora* sp.), plate (*Turbinaria* sp.) and encrusting corals occur (e.g., 108CAM92). Other biota include: sponges (*Lanthella basta*, *L. flabelliformis*), holothurians, soft corals (gorgonians, sea whips), and echinoderms (crinoids). Fishes associated with the reef include: barramundi (*Lates calcarifer*), snapper (*Lutjanus* sp.) and fusilier (*Caesio* sp.).

4.3.3. Surface Sediments

This section presents descriptions of the sedimentology of grab samples and core tops from the five study areas. A total of 108 grabs (GR1-GR108) were collected that broadly characterise the texture and composition of the seabed sediments and associated benthic habitats (Tables 4.1a-e). Some core top samples from the vibrocores (VC1-VC5, VC29, VC30, VC40, VC34, and VC47) are used to supplement the surface sediment information provided by the grabs. Generally, the seabed sediment samples contain mud, sand and gravel, with high carbonate concentrations.

4.3.3.1. Area A: Regional Survey

Folk Classification:— Sediment distributions in over the southeast region of the Gulf of Carpentaria show changes in texture and composition over a extensive region, from the basin in the north and seabed surrounding the platform reefs to the shallow inner-shelf environments in the south and east. The seabed of the central gulf is generally comprised of well sorted, olive-grey muddy shelly sand, with molluscs and small amounts of beach rock. Gravel concentrations are generally low. Mean grain size (Fig. 4.20a) generally increases onshore from 276.698 μm in the central gulf (4GR04) to 487.223 μm in the south (5GR05). Sediments characterising the inner-shelf environments are generally moderately-sorted calcareous medium sands containing abundant shell hash and relatively high proportions of terrigenous sand-sized grains of mudstone and siltstone. Mean grain size in these environments ranges from 204.414 μm (13GR13A) to 590.899 μm (32GR31A). Further to the west, sediments generally comprise green-grey calcareous well sorted, fine to medium muddy sand, with small quantities of terrigenous sand grains. The sediments also contain a small amount of carbonate gravel comprised of mollusc fragments, bryozoans, sponge, heart urchins, tube worms, and solitary corals. Mean grain size in these deep-water environments ranges from 133.354 μm (15GR15A) to 395.39 μm (22GR22A). At moderate water depths, sediments comprise muddy olive grey slightly gravely muddy sand, with small quantities of mollusc and bryozoan fragments and echinoids.

Gravel:— Gravel concentrations range from 0.11% to 15.58%, and 33 of the 37 samples contain <10% gravel (Fig. 4.20b). Generally, the distribution of gravel is variable across the southern gulf. Low gravel concentrations occur on the shallow inner shelf (e.g., 28GR28A), with the lowest concentration of 0.11% occurring in a sample collected from the shallow waters of the eastern shore (e.g. 18GR18A). Highest gravel concentrations generally occur in the west near Mornington Island, with the highest overall gravel concentration of 15.58% (20GR20) (Fig. 4.17b). The gravel component is principally composed of mollusc fragments and foraminifer tests, with smaller amounts of bryozoan and siltstone and mudstone clasts. The carbonate clasts are typically encrusted with red coralline algae.

Sand:— Sand is the dominant component of the sediments on the bed of the gulf, with concentrations ranging from 50.70% to 97.59% and all but two samples containing >70% (Fig. 4.20c). Lowest concentrations occur in the north and the highest concentrations occur in the

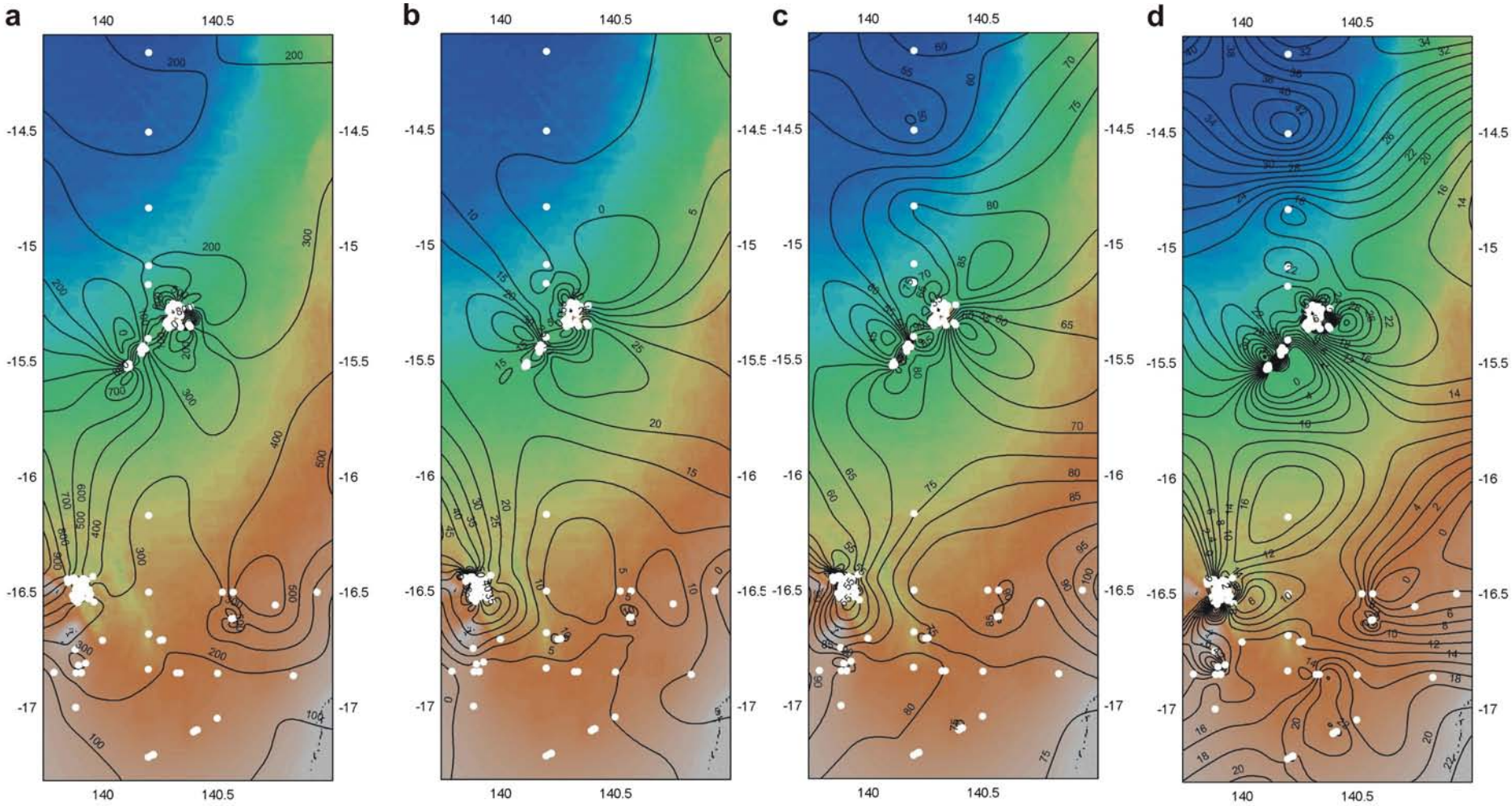

Figure 4.20. Maps showing: a) grain size (μm), b) %Gravel, c) %Sand, and d) %Mud from the surface sediments in Area A: Regional survey. Gravel and Sand are the dominant size fractions, with very little mud present. See text for full details. Textural and compositional data for the samples are reported in Appendix G.

west and inner shelf environments to the east. The sand fraction is principally comprised of bryozoan and mollusc fragments, with smaller amounts of quartz and rare mudstone and siltstone grains.

Mud:— Mud concentrations are highly variable across the southern gulf ranging from 0.61% to 42.5% (Fig. 4.20d). Low mud concentrations of <2.3% occur in the south. Throughout the study area low mud concentrations coincide with high sand concentrations. Highest mud concentrations of up to 42% occur in the deep-water gulf floor in the north (e.g., 1GR1, 2GR2, 6GR6A). High concentrations of >20% also occur in the relatively shallow inner-shelf regions in the south (e.g., 24GR24A, 27GR27, 28GR28A, 26GR26A). A microscopic inspection of the mud fraction indicates that the silt-sized grains are composed of calcareous (mollusc and foraminifer?) and a small quantity of terrigenous grains.

Carbonate (Bulk):— Bulk carbonate concentrations range from 11.1% to 62.8% with samples containing concentrations of >50% recovered from the gulf floor in the north and inner-shelf environments to the south and east (Fig. 4.21a). Highest bulk carbonate concentrations of 59.8% to 62.8% correspond to the highest carbonate sand concentrations. The bulk carbonate fraction consists principally of molluscs, bryozoans, foraminifers and worm tubes. The grains generally have a fresh to intermediate preservation with many of the gravel clasts encrusted by worm tubes and with red coralline algae.

Carbonate (Sand):— Carbonate sand concentrations range from 10.1% to 90.2% (Fig. 4.21b). Concentrations are highly variable but generally increase from <40% in the inner-shelf environments to >80% on the deeper gulf floor. Carbonate sand concentrations are also predictably higher near the offshore platform reefs, where concentrations of >70% occur. The carbonate sand fraction is mostly comprised of mollusc and bryozoan fragments and foraminifers.

Carbonate (Mud):— Carbonate mud concentrations range from 13.1% to 35.4% (Fig. 4.21c). Concentrations generally increase with water depth, with the highest concentrations of >25% occurring mainly in the basin environments in the north (e.g., 1GR1, 2GR2, 5GR5A , 6GR6A). Samples on the shallow-water inner-shelf environments in the south and east contain carbonate mud concentrations of <20% (e.g., 20GR20A, 23GR23A, 38GR37A, 11GR11A, 24GR24A), with lowest concentrations contained in samples collected in the west near Mornington Island. A total of 7 samples from Area A contained insufficient mud to be analysed.

4.3.3.2. Area B: Bryomol Reef

Folk Classification:— Seabed sediments in Area B differ in texture and composition between the hard-grounds, reef platforms, and channel-like depressions. Muddy sand and sandy mud occurs in the depressions. Mean grain size of sediments recovered from the depressions ranges from 418.664 μm (41GR39A) to 793.142 μm (48GR46). Poorly-sorted, calcareous muddy gravelly coarse sand occurs on the hard-grounds. Mean grain size (Fig. 4.22a) of sediments recovered from the hard-grounds ranges from 367.547 μm (58GR55A) to 707.857 μm (62GR59A). Interestingly, the gravel fraction of samples collected from the hard-grounds contains approximately equal quantities of carbonate and siliciclastic clasts. The siliciclastic clasts are composed of rounded-angular sandstone, shale or iron-stained siltstone pebbles. Siliciclastic clasts were recovered in sediments from throughout Area B which suggests that these components have probably been weathered from the underlying substrate. Moderately-sorted mollusc-rich sand occurs on the bryomol reef platform. Mean grain size for the reef platform sediments ranges from 604.84 μm (54GR53A) to

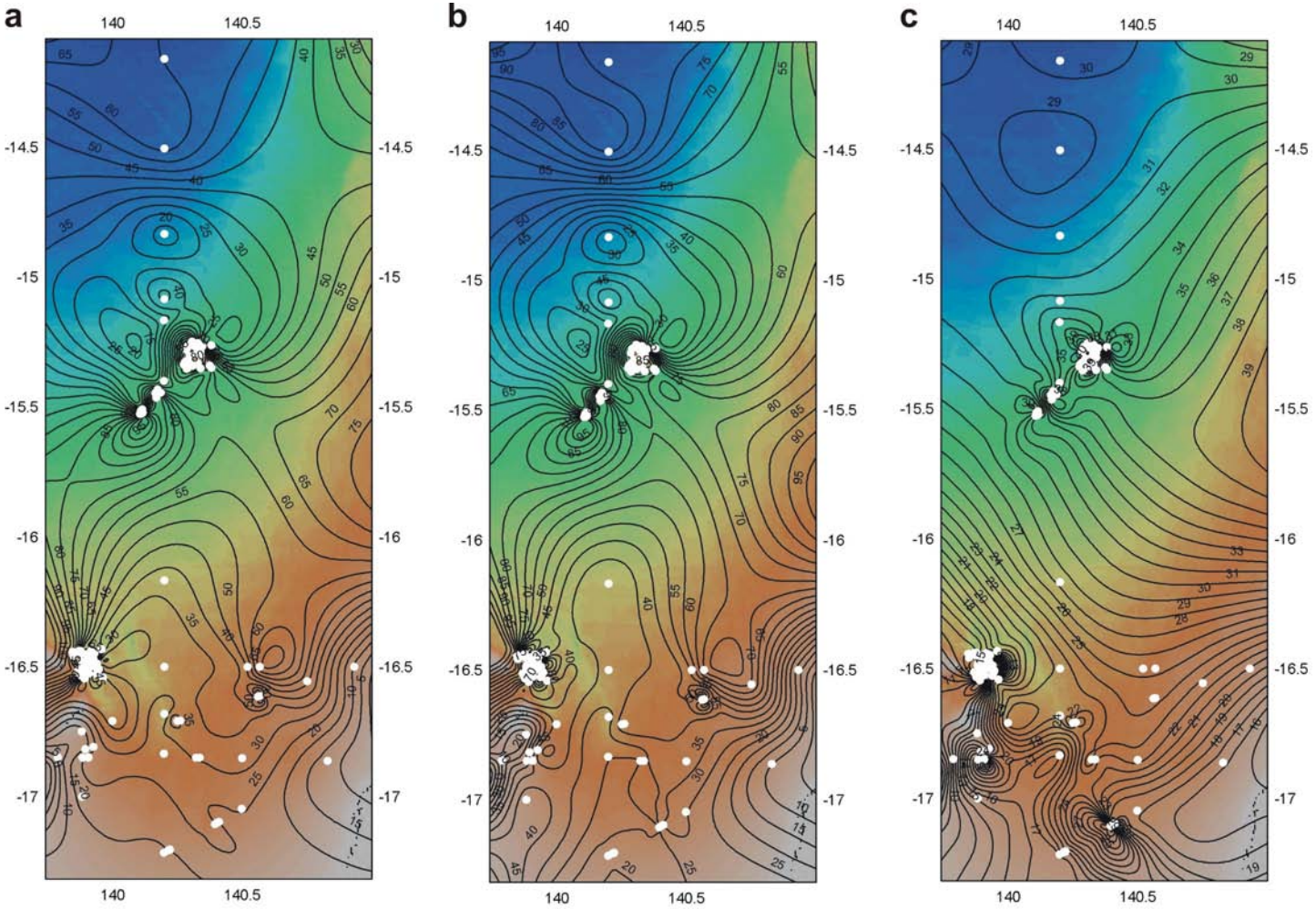

Figure 4.21. Maps showing: a) %$CaCo_3$(Bulk), b) %$CaCO_3$(Sand), and, c) %$CaCO_3$(Mud) from the surface sediments in Area A: Regional survey. Carbonate concentration generally decrease with decreasing water depth and proximity to the coast. See text for full details. Textural and compositional data for the samples are reported in Appendix G.

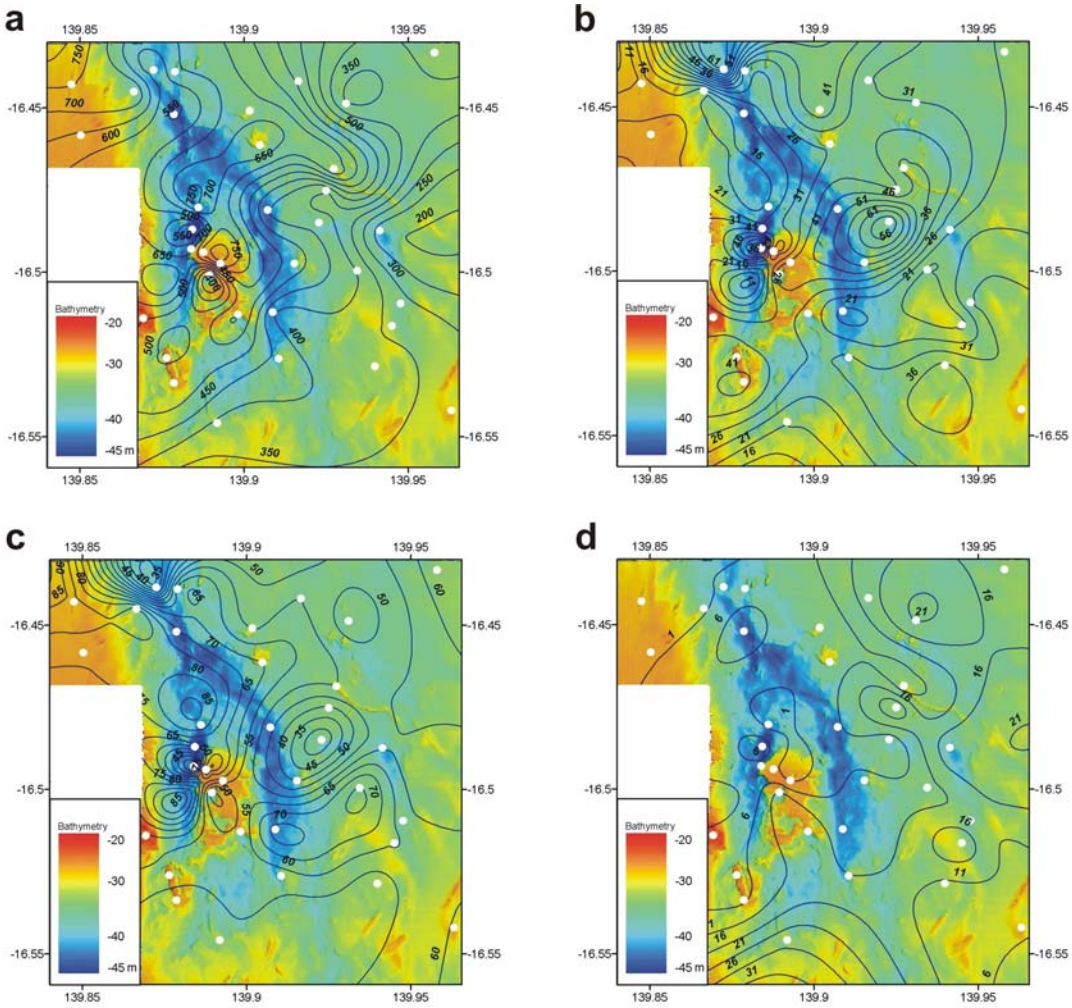

Figure 4.22. Maps showing: a) mean grain size (μm), b) %Gravel, c) %Sand, and d) %Mud from the surface sediments in Area B: Bryomol Reef. Sand and gravel and are the dominant size fractions, with very little mud present. See text for full details. Textural and compositional data for the samples are reported in Appendix G.

784.441 μm (66GR63A). On the reefs, the gravel fraction is generally dominated by mollusc and bryozoan fragments, benthic foraminifer tests as well as cemented cobble-sized reef fragments.

Gravel:— Gravel concentrations range from 17.2% to 70.14% (Fig. 4.22b). Low gravel concentrations of <20% occur throughout Area B although concentrations of <20% occur in samples collected from the depression north of the Bryomol Reef (e.g., 48GR46) and the western reef platform (e.g., 69GR67A). Sample 67GR65A which contains the highest gravel concentration of 70.14% was recovered from a small depression in the north of the survey area. The gravel fraction in samples from this depression is composed mostly of reefal fragments, including abundant sponges and hard corals. Gravel concentrations are more variable on the hard-grounds, ranging from 19.85% in the south (46GR44A) to 64.25% in central areas (44GR42). Samples collected on the Bryomol Reef contain gravel concentrations of 56.96% (72GR70A) and 29.47% (42GR40A). In these samples, the gravel fraction comprises mollusc fragments, worm tubes, encrusted carbonate clasts and sandstone pebbles.

Sand:— Sand is the dominant size fraction of all the seabed sediments sampled in Area B. Sand concentrations range from 27.94% to 82.71%, with most samples containing between 50-80% sand (Fig. 4.22c). Concentrations of <50% occur in all of the seabed environments sampled. The lowest concentration of 27.94% found in a sample collected from the

depression north of the reef. Other low sand content environments, include parts of the hard-grounds to the east, with values of 31.88% and 47.78% (e.g., 44GR42A, 64GR61), and a depression in Bryomol reef, with a value of 48.85% (50GR49A). Sand concentrations are generally higher on the reef platform than the surrounding hard-grounds and depression, with samples in the south of the reef platform containing up to 64.54% sand (e.g., 54GR53A) and the north up to 82.21% (e.g., 68GR66A). The sand fraction mostly consists of mollusc and bryozoan fragments encrusted with coralline algae, with minor quantities of foraminifer tests, sponge spicules and coral fragments. The carbonate fraction has an intermediate preservation containing numerous weathered grains and grains encrusted with red coralline algae.

Mud:— Mud is the least abundant size fraction in samples collected from Area B with concentrations ranging from 0.09% to 24.34% (Fig. 4.22d). Lowest mud concentrations of <2% occur on the reef platforms and corresponds to relatively high concentrations of sand. Highest mud concentrations of >10% occur on the hard-grounds in the east. Samples containing the highest mud concentrations of 21.09% (64GR61) and 24.34% (53GR52) were recovered in the northern and southern parts of the hard grounds, respectively. Silt-sized grains in the mud fraction are composed of mollusc and bryozoan fragments with minor amounts of hard coral and terrigenous siltstones grains.

Carbonate (Bulk):— Bulk carbonate concentrations are between 20.2% and 79.6% (Fig. 4.23a). Samples containing >70% bulk carbonate occur mainly on the reefal platforms (e.g., 49GR48A, 68GR66A, 71GR69A). The highest bulk carbonate concentration of 79.6% was observed in a sample collected from the northern region of the hard-grounds (62GR59A). However, generally the hard-grounds and depressions are regions of lowest bulk carbonate concentrations of <50%. The carbonate fraction is composed of reefal fragments, including mollusc and bryozoan fragments, worm tubes, echinoid spines and foraminifer tests.

Carbonate (Sand):— Carbonate sand is the dominant carbonate component with concentrations ranging from 14.1% to 87.2% (Fig. 4.23b). The highest carbonate sand concentration of 87.2% occurs in sample recovered from the depression north of Bryomol reef (48GR46). Generally, carbonate sand concentrations of >80% occur on the reefal platforms (e.g. 49GR48A, 69GR67A, 68GR66A) and at one location on the hard-grounds (60GR57A), and carbonate sand concentrations of <50% occur on the hard-grounds (e.g. 9GR9A, 61GR58). The carbonate sand fraction is dominated by mollusc and bryozoan fragments, with minor quantities of echinoid spines, foraminifer tests and coral fragments.

Carbonate (Mud):— Carbonate mud is the least dominant fraction with concentrations ranging from 7% to 20.2% (Fig. 4.23c). A total of 16 samples contained insufficient carbonate mud for analysis. These samples are mostly from the reefal environments. Generally, lowest carbonate mud concentrations of 9%-18% occur on the hard-grounds (e.g., 47GR45A). Silt-sized grains are composed of mollusc and bryozon fragments, foraminifer tests and coral fragments.

4.3.3.3. Area C: Reef R1

Folk Classification:— Seabed sediments on Reef R1 differ in texture and composition between the reef platform, reef crest (marginal ridges), reef flat, talus slopes and surrounding gulf floor. On the reef environments, sediments are composed of calcareous sand and gravel clasts of primarily reefal origin, including fresh coral and relict coral rubble, molluscs, echinoderms and bryozoans. Sediments recovered from the reef platform have a mean grain size that ranges from 560.732 μm (94GR88A) to 637.168 μm (82GR77) (Fig. 4.24a). Adjacent to

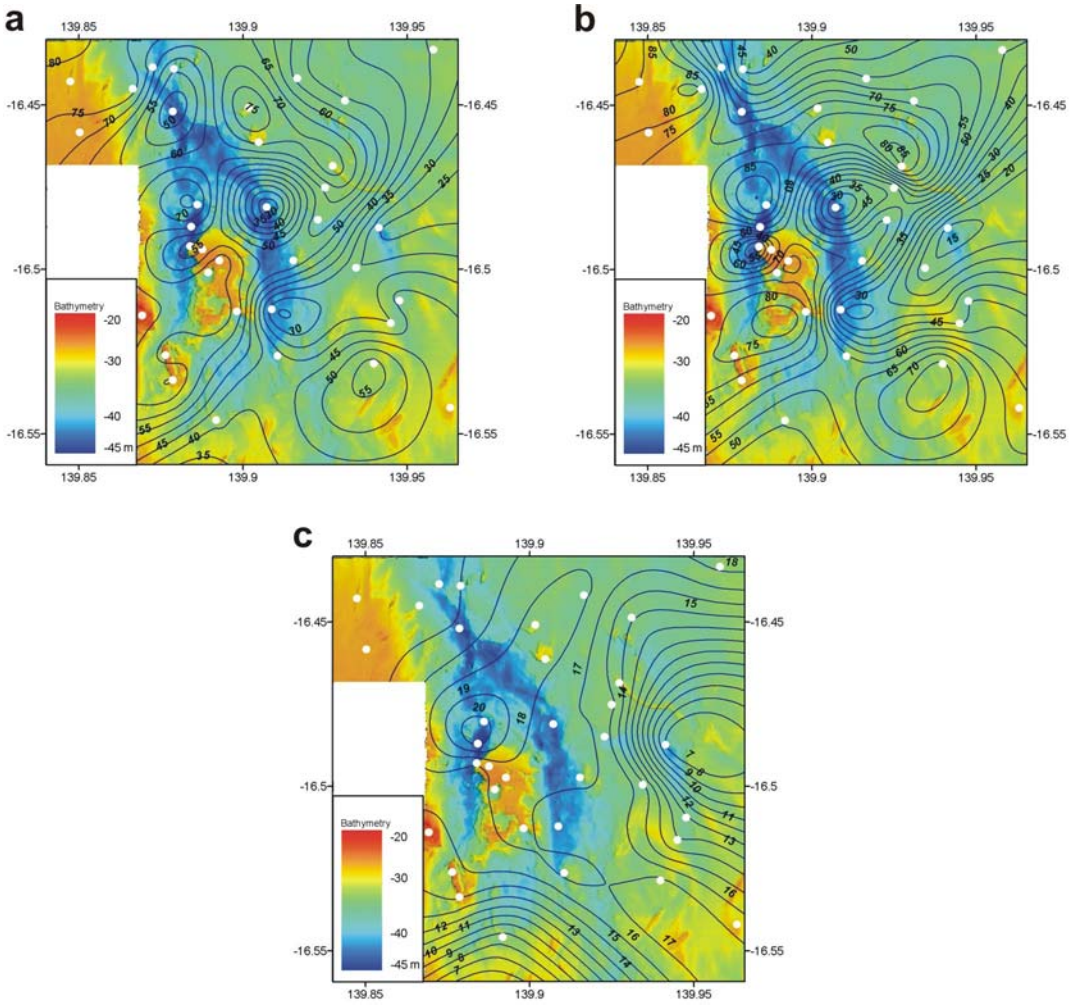

Figure 4.23. Maps showing: a) %$CaCO_3$(Bulk), b) %$CaCO_3$(Sand), and c) %$CaCO_3$(Mud) from the surface sediments in Area B: Bryomol Reef. Carbonate concentrations are greatest on the shallow reef platforms and decrease on the gulf floor. See text for full details. Textural and compositional data for the samples are reported in Appendix G.

the reef, the seabed comprises moderately sorted, olive grey, calcareous muddy fine sand, with a minor amount of gravel. Mean grain size for sediments recovered from the surrounding seabed ranges from 202.033 μm (81VC30) to 914.377 μm (105GR97A). Sediments on the north margin of the reef platform are dominated by bioclastic gravel. On the south margin, sediments making up the talus slope contain small quantities of bioclastic gravel.

Gravel:— Gravel concentrations range from 0.33% to 91.35% (Fig. 4.24b). Low gravel concentrations occur generally adjacent to the reef with the lowest concentrations occurring on the talus slope (104GR96A). Regions with a gravel content of <10% correspond to regions of high sand concentrations (e.g., 79GR74, 102GR94A) including the reef platform (e.g. 94GR88A). The highest gravel concentration of 91.35% occurs on the windward side of the reef platform (88GR82A). Gravel concentrations of >20% occur along the margin reef ridges (e.g. 96GR89A) and adjacent gulf floor (e.g. 105GR97A). The gravel fraction is composed entirely of carbonate clasts and includes abundant mollusc and sponge fragments with minor amounts of living and relict coral rubble (88GR82A), bryozoan fragments (102GR94A), echinoid spines (e.g. 87GR81, 96GR89), pebble to cobble -sized limestone clasts (e.g. 82GR77), tube worms (e.g. 94GR88). One sample from the reef platform (86GR80) also contained siliciclastic clasts.

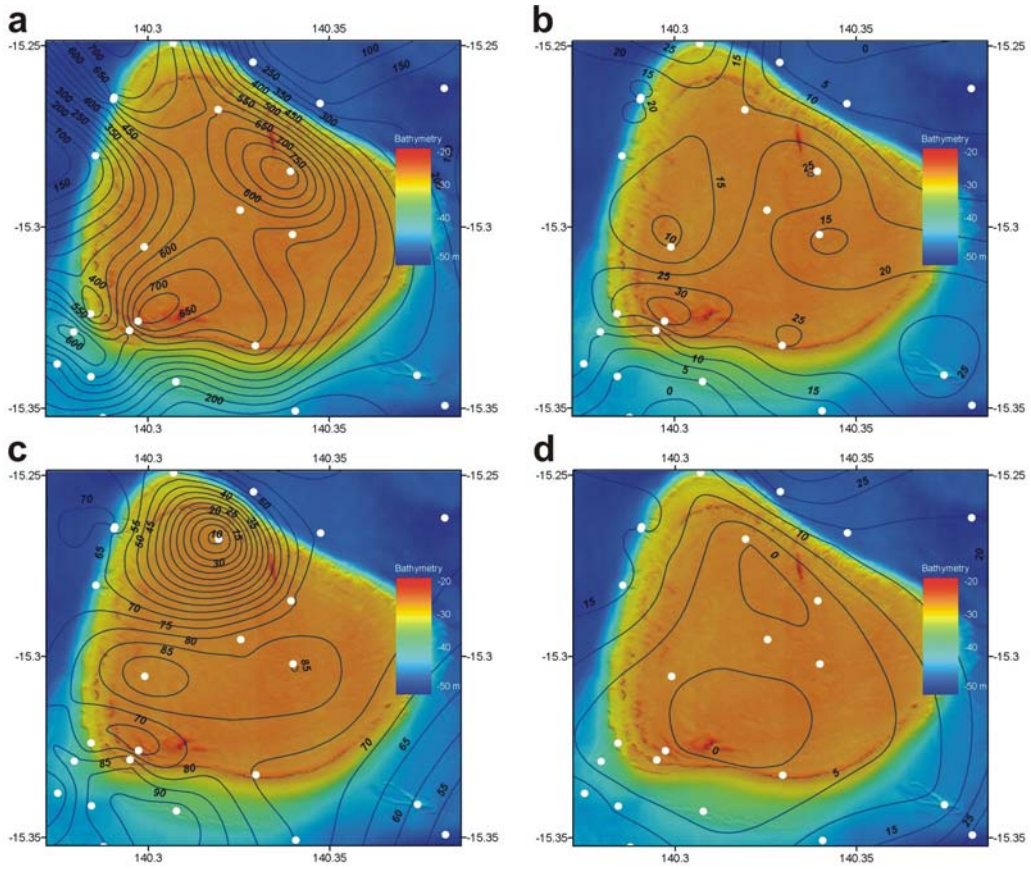

Figure 4.24. Maps showing: a) mean grain size (μm), b) %Gravel, c) %Sand, and d) %Mud from the surface sediments in Area C: Reef R1. Sand and gravel and are the dominant size fractions, with very little mud present. See text for full details. Textural and compositional data for the samples are reported in Appendix G.

Sand:— Sand is the dominant size fraction of all the seabed sediments sampled in Area C. Sand concentrations range from 55.1% to 93.66% (Fig. 4.24c). A single sample (88GR82A) from the windward margin contains 7.88% sand contains the highest gravel concentrations. Generally, sand concentrations are higher on the reef platform, reef crests and reef flat environments with concentrations great >70% (e.g. 86GR80A, 87GR81A, 83GR78A, 94GR88A). On the reef platform, the samples contain medium to coarse sand and a small amount of fine sand. The highest sand concentration of 93.66% occurs on the talus slope (104GR96A). This sample comprises well-sorted fine to medium calcareous sand. Generally, lowest sand concentrations occur on the seabed adjacent to the reef. Sand concentrations are <70% on the fore-reef slope (e.g., 93GR87A) and marginal ridges (68GR25).

Mud:— Generally, mud comprises a small amount of the total sediment from Area C. Mud concentrations range from 0.39% to 25.60% (Fig. 4.24d). High mud concentrations occur on the seabed adjacent to the reef with the highest concentration of 25.6% occurring on the fore-reef slope (89GR83). Sediments containing >20% mud also occur on the seabed adjacent to the leeward margin (e.g., 80GR75A, 81GR76). Low mud concentrations occur on the reef platform and on the leeward margin, with the lowest concentration of 0.39% (96GR89A) occurring on the marginal ridge. Regions of low mud concentrations correspond to regions of high gravel content. Analysis of the silt-sized grains indicates that they are composed of benthic foraminifers and mollusic fragments (e.g. 79GR74, 89GR83).

Carbonate (Bulk):— Bulk carbonate concentrations are >30% for all samples collected in Area C (Fig. 4.25a). Sediments on the reef platform contain bulk carbonate concentrations of

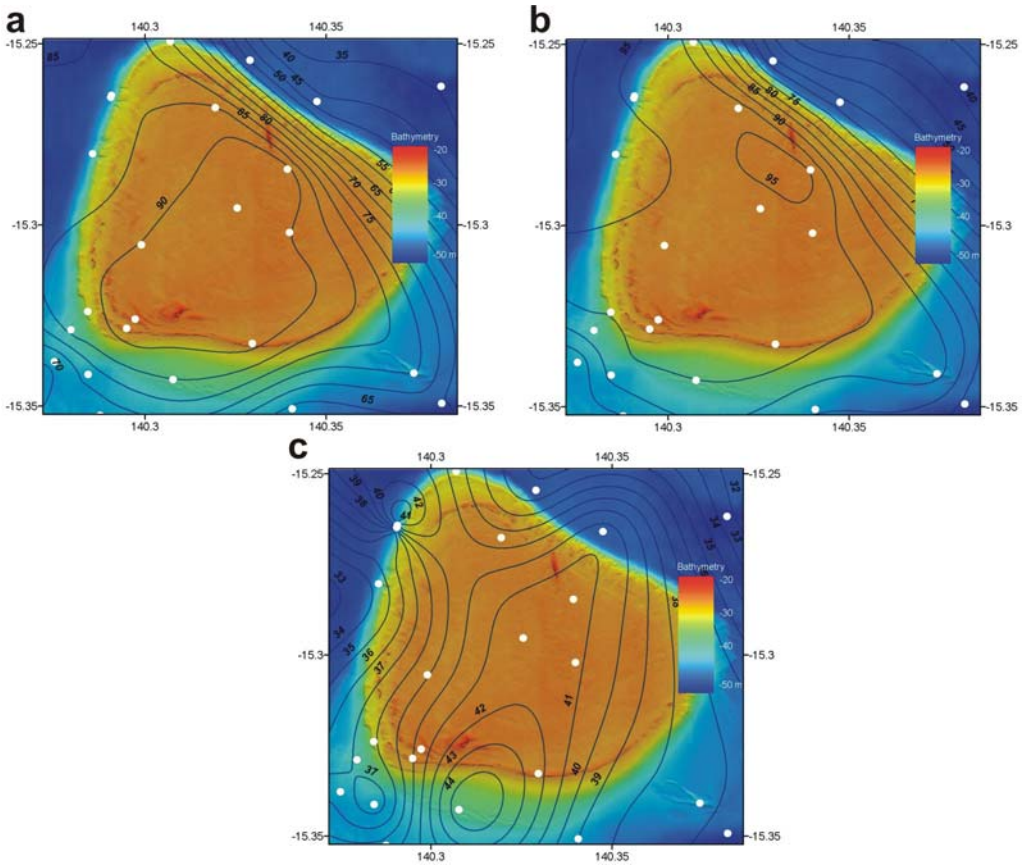

Figure 4.25. Maps showing: a) %$CaCO_3$(Bulk), b) %$CaCO_3$(Sand), and c) %$CaCO_3$(Mud) from the surface sediments in Area C: Reef R1. Carbonate concentrations are greatest on the shallow reef platform and decrease on the gulf floor. See text for full details. Textural and compositional data for the samples are reported in Appendix G.

>90%, with the highest concentrations recorded on the marginal ridges (e.g. 96GR89A, 97GR90A). On the adjacent seabed regions bulk carbonate concentrations are <75% and increase closer to the reef platform. The low bulk carbonate concentrations of the adjacent seabed correspond to the generally low gravel contents recorded in these regions (e.g., 79GR74, 85GR79A). The carbonate fraction comprises mollusc and echinoid fragments and coral rubble with intermediate preservation. Carbonate grains are both fresh and relict, with many encrusted with worm tubes and coralline algae

Carbonate (Sand):— Carbonate sand concentrations range from 38.5% to 98.3% (Fig. 4.25b). Highest carbonate sand concentrations of 94.3% and 98.3% occur on the western margin (e.g., 90GR84, 91GR85). Sand concentrations of >90% also occur on the marginal ridges (e.g., 96GR89A) and windward margin (e.g., 86GR80A). On the reef platform, high carbonate sand concentrations correspond to high sand concentrations in these areas and reflect the dominant sediment type on the reef. Lowest carbonate concentrations <40% occur on the seabed adjacent to the windward margin (e.g., 85GR79A, 89GR83). The carbonate sand is composed of reefal fragments, including hard coral, mollusc and bryozoan fragments and foraminifer tests.

Carbonate (Mud):— Carbonate mud concentrations range from 32.4% to 44.6% (Fig. 4.25c). Carbonate mud is a dominant component of the seabed sediments surrounding the reef with concentrations attaining 44.6%. Generally, highest concentrations occur on the leeward margin. Interestingly, concentrations of >40% also occur on the windward margin although the lowest concentrations of <35% also occur here. Carbonate mud is absent from the reef platform. A total of 12 samples contained insufficient carbonate mud for analysis.

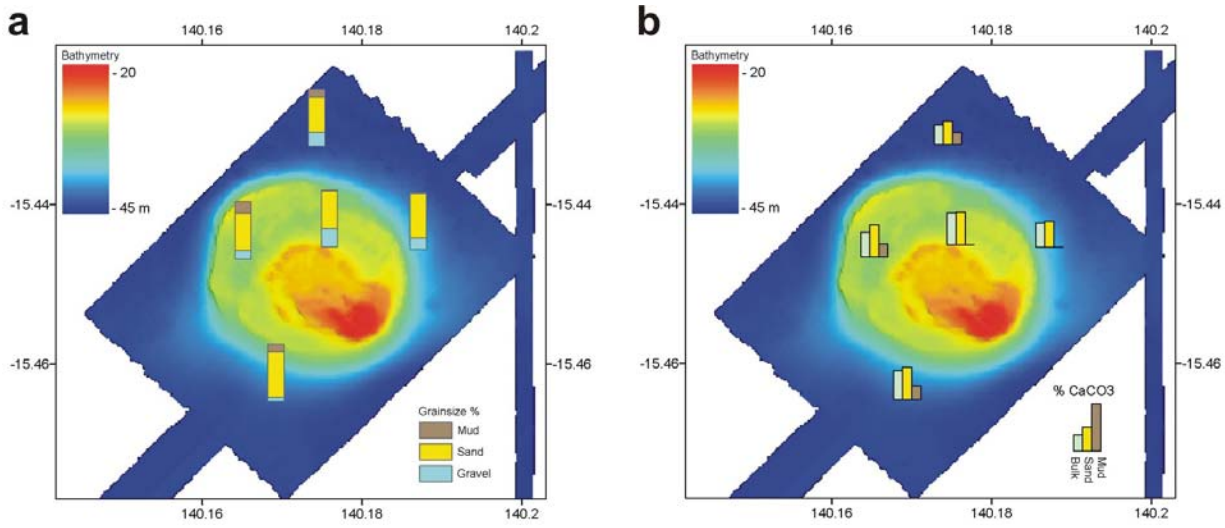

Figure 4.26. Maps showing: a) %Gravel, %Sand and %Mud, and b) %$CaCO_3$(Bulk), %$CaCO_3$(Sand) and %$CaCO_3$(Mud) from samples collected in Area D: Reef R2. Due to the relatively low number of samples the data could not be contoured and are instead shown as bar charts. Sand and gravel and are the dominant size fractions, with very little mud present. Carbonate concentrations are greatest on the shallow reef platform and decrease on the gulf floor. See text for full details. Textural and compositional data for the samples are reported in Appendix G.

4.3.3.4. Area D: Reef R2

Folk Classification:— Seabed sediments in Area D differ in texture and composition between the reef platform and adjacent seabed. Sediments on the reef platform are poorly-sorted calcareous sand with abundant gravel including encrusted coral pebbles and cobbles. Other major components include mollusc fragments, sponge spicules and benthic foraminifers. Mean grain size for sediments on the reef platform range from 391.901 µm (117GR108A) to 647.937 µm (112GR104A). Adjacent to the reef, the seabed is composed of poorly-sorted calcareous muddy sand containing a mixture of calcareous and siliciclastic grains. The siliciclastic component comprises well-rounded sandstone and siltstone grains. Mean grain size for sediments surrounding the reef range from 607.844 µm (115GR106A) to 858.457 µm (114GR105).

Gravel:— Gravel concentrations in Area D are generally low and range from 7.68% to 32.51% (Fig. 4.26a). On the reef platform, gravel concentrations are variable and range from 14.08% (115GR106A) in the west to 32.51% (e.g. 114GR105) in the centre. The gravel fraction is dominated by pebble- to cobble-sized coral rubble with small amounts of sandstone clasts. The coral rubble has a relict appearance with clasts heavily encrusted with red coralline algae. The seabed adjacent to the reef contains lower concentrations of gravel with the lowest concentration of 7.68% occurring on the leeward (south) margin (112GR104A). Gravel concentrations are higher on the windward (north) margin ranging from 19.65% (116GR107) to 24.27% (117GR108A) on the fore reef slope.

Sand:— Sand is the dominant size fraction of all the seabed sediments sampled in Area D. Sand concentrations range from 61.78% to 79.36% (Fig. 4.26a). Generally, highest sand concentrations occur on the leeward margin with concentrations attaining 79.36% (112GR104A). On the reef platform, sand concentrations are similar and range from 65.97% to 66.24% (114GR105, 115GR106A). Sand concentrations are lowest on the surrounding seabed sediments with a concentration of 61.78% (117GR108A). The sand fraction is generally composed of coral, mollusc and bryozoan fragments, foraminifers, sponge spicules and echinoid spines.

Mud:— Generally, mud comprises a small amount of the total sediment from Area D. Mud concentrations range from 1.25% to 19.96% (Fig. 4.26a). The lowest and highest mud concentrations were obtained from samples collected from the reef platform, with a concentration of 1.25% (114GR105) in the centre and 19.96% (115GR106A) in the western regions. On the surrounding seabed, mud concentrations are also variable and range from 2.35% to 13.96%. A microscopic inspection revealed that the silt-sized grains comprise mollusc fragments, abundant benthic foraminifers and coral fragments. The mud fraction has an intermediate preservation with large amount of weathered and relict carbonate grains.

Carbonate (Bulk):— Bulk carbonate values range from 55.7% to 91.2% (Fig. 4.26b). The highest bulk carbonate concentration of 91.2% (114GR105) occurs on the reef crest. Generally, sediments of the adjacent seabed contain less carbonate with concentrations of <80% and values increasing for samples closer to the reef. The lowest bulk carbonate concentration of 55.7% occurs on the windward margin of the reef (117GR108A). The bulk carbonate fraction is composed of coral rubble, mollusc and bryozoan fragments, foraminifers and echinoid spines. The carbonate fraction has an overall relict preservation with clasts heavily encrusted with worm tubes and red coralline algae.

Carbonate (Sand):— Concentrations of carbonate sand range from 65.9% to 94.3% (Fig. 4.26b). Highest concentrations of carbonate sand of >90% occur on the reef crest (112GR104A) and also on the adjacent seabed of the leeward margin (114GR105). Lowest concentrations of 65.9% (117GR108A) occur on the seabed of the windward margin. Carbonate sand concentrations display a similar distribution to bulk carbonate. The carbonate sand fraction is composed of coral and mollusc fragments, with minor amounts of bryozoan fragments and benthic foraminifers.

Carbonate (Mud):— Carbonate mud concentrations range from 34.4% to 38.5% (Fig. 4.26b). Lowest concentrations occur on the windward margin (117GR108A) which also corresponds to low bulk and carbonate sand concentrations. Generally, higher carbonate mud concentrations of >35% occur on the leeward margin and reef crest (112GR104A, 115GR106A). A microscopic inspection of the carbonate mud fraction revealed that the silt-sized grains are composed of mollusc fragments and benthic foraminifers with minor amounts of coral. Two samples contained insufficient amounts of carbonate mud for analysis.

4.3.3.5. Area E: Reef R3

Folk Classification:— Seabed sediments in Area E differ in texture and composition between the reef platform and adjacent seabed. Sediments on the reef platform are poorly-sorted calcareous gravelly sand with abundant carbonate gravel clasts in the form of coral rubble and encrusted mollusc shells. Mean grain size of the sample recovered from the reef crest is 749.151 μm (108GR100A). On the surrounding seabed the sediment is composed of poorly-sorted calcareous muddy gravelly sand consisting of molluscs and bryozoans fragments, echinoid spines and encrusted limestone and coral fragments. Mean grain size for these sediments ranges from 323.754 μm (111GR103A) to 622.068 μm (106GR98).

Gravel:— Gravel concentrations in Area E range from 12.40% to 17.85% (Fig. 4.27a). Gravel concentrations are 12.40% (111GR103) on the windward (north) margin, which is slightly lower than that contained in the sample collected from the leeward (south) margin of 17.85% (106GR98). At the single location where sediments were sampled on the reef platform, the gravel content is 14.61% (108GR100A). The gravel fraction is composed of coral,

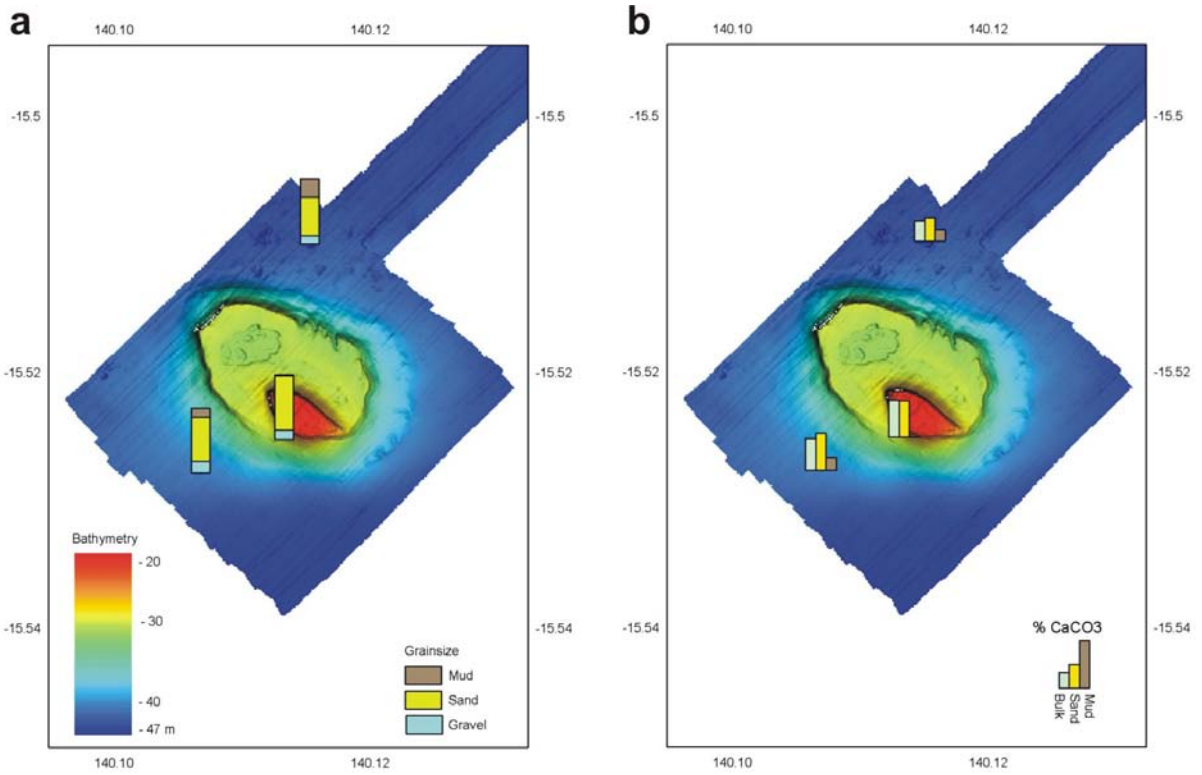

Figure 4.27. Maps showing: a) %Gravel, %Sand and %Mud, and b) %$CaCO_3$(Bulk), %$CaCO_3$(Sand) and %$CaCO_3$(Mud) from samples collected in Area E: Reef R3. Due to the relatively low number of samples the data could not be contoured and are instead shown as bar charts. Sand and gravel and are the dominant size fractions, with very little mud present. Carbonate concentrations are greatest on the shallow reef platform and decrease on the gulf floor. See text for full details. Textural and compositional data for the samples are reported in Appendix G.

mollusc and bryozoan fragments that are typically encrusted with worm tubes and coralline algae.

Sand:— Sand concentrations range from 59.91% to 83.92% (Fig. 4.27a). The highest concentration of 83.92% occurs on the reef crest (108GR100A) and is significantly higher here than the surround seabed. The sand concentration of the sample collected on the windward margin is 59.91% (111GR103), which is higher than the sand concentration of the sample collected on the leeward margin of 68.04% (106GR98). The sand fraction is composed of coral, mollusc and bryozoan fragments with a small amount of sponge spicules. The sand fraction has an intermediate preservation with many grains showing weathering and encrusted with coralline algae.

Mud:— Mud concentrations range from 1.47% to 27.68% (Fig. 4.27a). The highest concentration of 27.68% occurs in the sample collected from the windward margin (111GR103), with the sample collected from the leeward margin containing 14.11% mud (106GR98). The sample collected from the reef crest has a mud concentration of 1.47% (108GR100A) which may be typical of the reef platform. A microscopic inspection of the mud fraction revealed that the silt-sized grains are composed of coral and mollusc fragments and benthic foraminifers, with a small amount of bryozoan fragments and sponge spicules.

Carbonate (Bulk):— Bulk carbonate concentrations range from 50.7% to 92.3% (Fig. 4.27b). Highest bulk carbonate concentration of 92.3% occurs on the reef platform (e.g. 108GR100A). The bulk carbonate concentration of 50.7% in the sample collected from the windward margin (111GR103) is significantly lower than the concentration of 81.1% in the sample collected from the leeward margin (106GR98). The carbonate fraction is composed of coral, mollusc and bryozoan fragments with smaller amounts of benthic foraminifers and

echinoid spines. Overall, the carbonate fraction has an intermediate preservation with nearly equal amounts of fresh and relict grains. Relict material is heavily encrusted with worm tubes and red coralline algae.

Carbonate (Sand):— Carbonate sand concentrations range from 59.8% to 94.3% (Fig. 4.27b). The highest carbonate sand concentration of 94.3% occurs in the sample collected from the leeward margin (106GR98A) and the lowest sand concentration of 59.8% occurs in the sample collected from the windward margin (111GR103). The sample collected from the reef crest contains a carbonate sand concentration of 91.2% (108GR100A). The carbonate sand fraction is composed of coral and mollusc fragments, with minor amounts of bryozoan fragments and benthic foraminifers.

Carbonate (Mud):— Carbonate mud concentrations range from 29.3% to 32.4% (Fig. 4.27b). The highest carbonate mud concentration of 32.4% occurs in the sample collected from the leeward margin (106GR98A) and the lowest sand concentration of 29.3% occurs in the sample collected from the windward margin (111GR103). A microscopic inspection of the carbonate mud fraction revealed that the silt-sized grains are composed of mollusc fragments and benthic foraminifers with minor amounts of coral. Sample 108GR100A from the reef platform contained insufficient carbonate mud for analysis.

4.3.4. Benthic Biota

Overall, a very diverse living benthic fauna was collected with a total of 569 taxa (species groups) identified within 64 major taxonomic groups (family level or higher). The most number of species occur in the crustacean group (139 species), followed by bivalves (64), sponges (60), soft corals (56), gastropods (39), tunicates (32), starfish (28), bryozoans (26), sea cucumbers (24), hydroids (19), fish (15), hard corals (12), worms (12), and algae (5) (Fig. 4.28).

The benthic sleds and occasional rock dredges contained numerous species (Table 4.11). Fauna collected from regions of very rough seabed (e.g., stations 54, 90) are indicative of a living coral reef. A live specimen of *Turbinaria* sp. (plate coral) was obtained from Station 82 located on Area C in 20 m of water. Also, abundant hard corals (*Leptoseris* sp.) were observed in underwater video footage collected on the reef. Biota associated with the reefs comprise three species of hard corals, seven species of gorgonians (sea ferns), four species of sponge, one species of soft coral, and one species of starfish (*Linkia* sp.).

The fossil content of the sediment shows different patterns between the five study areas. Areas C, D, and E contain higher abundances and diversity of biota and organic fragments compared to Areas A and B (Fig. 4.29). Bioclastic material comprises more than half of the total sediment in Areas C, D, and E. Benthic foraminifera tests are a very abundant constituent of the surface sediments throughout the southeast gulf (Table 4.12); in samples collected on the regional survey (Area A) they comprise as much as 50% of the total fossil assemblage (Fig. 4.30). The most abundant forms observed are *Ammonia* sp. and *Elphidium* sp. Other benthic foraminifera associations are variable and a dominant biota could not be identified. Planktonic foraminifera tests are present at all sites, although in relatively low abundances. The most abundant form is *Gallitellia vivans*, a small (<150 μm) tropical species observed in the Gulf of Carpentaria by Chivas *et al*. (2001). A more extensive and systematic study of *G. vivans*, typical of nutrient-rich waters, would provide valuable information about the productivity of the southern gulf waters.

Bryozoans are generally well represented, particularly in Area B, the most proximal site to the land (Mornington Island), where they make up <16% of the total fossil assemblage

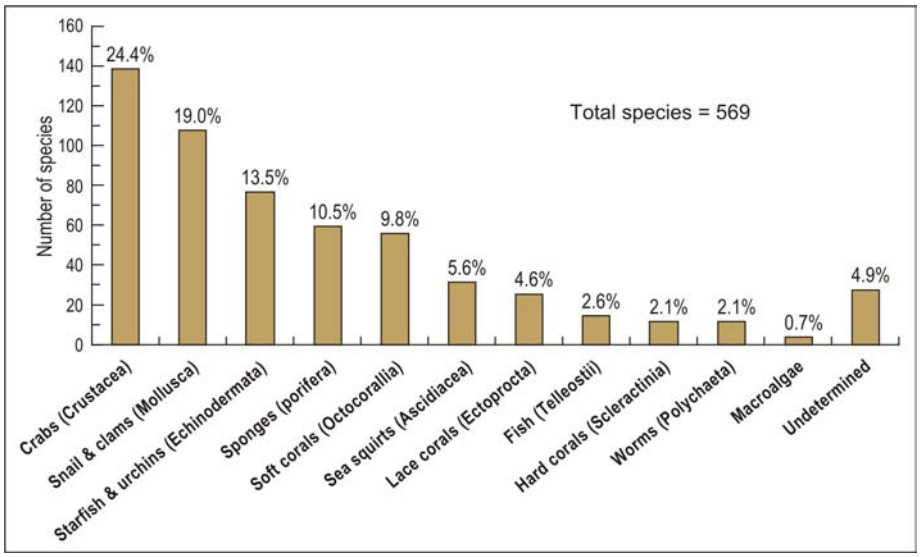

Figure 4.28. Graph showing the composition of benthic biota recovered from the samples collected in the southern Gulf of Carpentaria. The seabed is relative diverse with 569 species identified. Biota were collected from the muddy seabed of the central gulf and reefal habits (i.e., marginal ridges, terraces, plateaus). Many of the samples are first obtained from these regions of the gulf.

(Table 4.12; Fig. 4.30). Arthropods, mostly crabs, are also more abundant in Area B, comprising up to 20% of the total fossil assemblage. Interestingly, both of these groups are absent in the fossil content of samples analysed from the regional survey (Area A), from where some of the deepest samples have been collected. Soft corals are also relatively more abundant in Area B compared with the other sites. Surprisingly, other "coral-type" groups including *Halimeda* and hard corals occur in only very low abundances. Pteropods occur in each of the study regions except for Area B, confirming their preference for open-sea environments. Other groups including ostracods and bivalves do not show any distinct pattern in their abundance in the southeast gulf and are present in similarly low abundances in each of the study regions.

Table 4.11. Number of benthic biota species collected by each sampling device in each study area.

Area	Operation	No.	No. of species	Avg. no. species
Area B: Bryomol Reef	Dredge	5	78	16
	Grab	35	83	2
	Benthic Sled	18	553	31
Area C: Reef R1	Dredge	6	79	13
	Grab	25	20	<1
	Benthic Sled	12	347	29
Area D: Reef R2	Grab	5	8	2
Area E: Reef R3	Grab	6	2	<1
Area A: Central-East	Grab	9	4	<1
	Benthic Sled	8	237	34
Area A: Southeast	Grab	28	35	1
	Benthic Sled	23	589	26

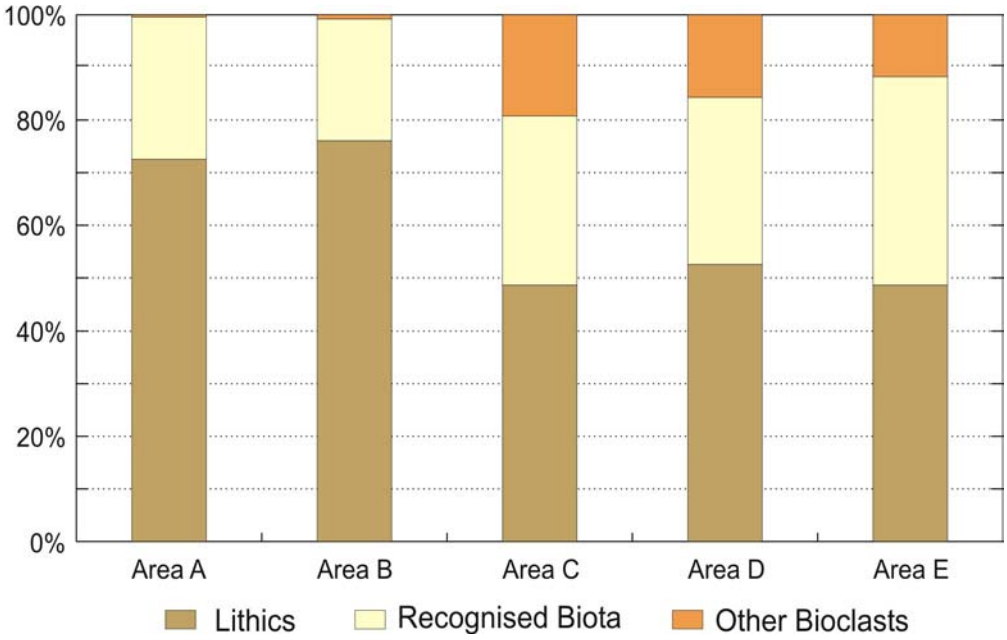

Figure 4.29. Graph showing the overall composition of the surface sediment from the southern Gulf of Carpentaria. Lithic fragments are the dominant sediment type found on the regional survey, consistent with this region being a zone of terrigenous dominated sedimentation. This pattern is also seen at Area B: Bryomol Reef and probably reflects the proximity to Mornington Island. Bioclastic grains dominate the sediment of the patch reefs, with lithic material <50% of the total composition.

4.3.5. Subsurface Sediments

In order to fully characterise the late Quaternary sediments and evolution of the regions, cores were collected from a variety of sedimentary environments in the southeastern gulf, including: infilled channels, floodplain deposits, talus slopes, sediment drapes and reef flats. A total of 40 vibrocores ranging in length from 0.31 m to 4.76 m representing a total length of 71.60 m were recovered (Tables 4.1a-e). Cores VC1-VC18 were collected from Area A (regional survey), cores VC19-VC27 were recovered from Area B (Bryomol Reef), cores VC28-VC40 were recovered from Area C (Reef R1). No cores were collected from Areas D (Reef R2) and E (Reef R3). Core logs and photos are presented in Appendix H. Texture and composition information for the sub-surface samples collected from the cores are contained in Appendix I.

4.3.5.1. Sediment Facies

Sediment contained in all the cores from the southern gulf is very similar in texture and composition (see Appendices H and I). However, regional differences are observed in the sedimentary sequence from the cores collected from Area A (Regional Survey), Area B (Bryomol Reef), and Area C (Reef R1).

Area A: Regional Survey:— A total of five distinct sub-surface facies occur across the southeast Gulf of Carpentaria. At the base of the sequence is Facies 1 which comprises stiff and de-watered grey to greenish grey silty clay at the bottom of VC1, 2, 7, 9-12, 15 and 18. Although the base of this facies was not sampled, it is at least 0.26 m thick (VC11) and contains calcrete (pedogenic) clasts (VC2). These factors and its colour indicate that it has been oxidised and subaerially exposed in the past. This unit is interpreted to be the weathered horizon of the old land surface or lake bed that was exposed during the last glacial maximum and before the latest marine transgression.

Table 4.12. Abundance and occurrence of the 16 major sources of bioclastic material in the surface sediments.

Group	Abundance	Occurrence
Benthic Foraminifera	Very high	Whole/fragments
Bivalves	Medium-low	Whole
Brachiopods	Very low	Whole
Bryozoans	Medium-high	Fragments
Corals	Very low	Fragments
Echinoderms	Medium-high	Fragments
Gastropods	Low	Whole/fragments
Coralline Algae (*Halimeda*)	Very low	Fragments
Ostracods	Low	Whole
Other Arthropods	High	Fragments
Planktonic Foraminifera	Low	Whole
Porifera	Medium-low	Fragments
Pteropods	Medium-low	Whole/fragments
Radiolaria	Low	Whole/fragments
Serpulids	Very low	Fragments
Soft corals	Medium-low	Fragments

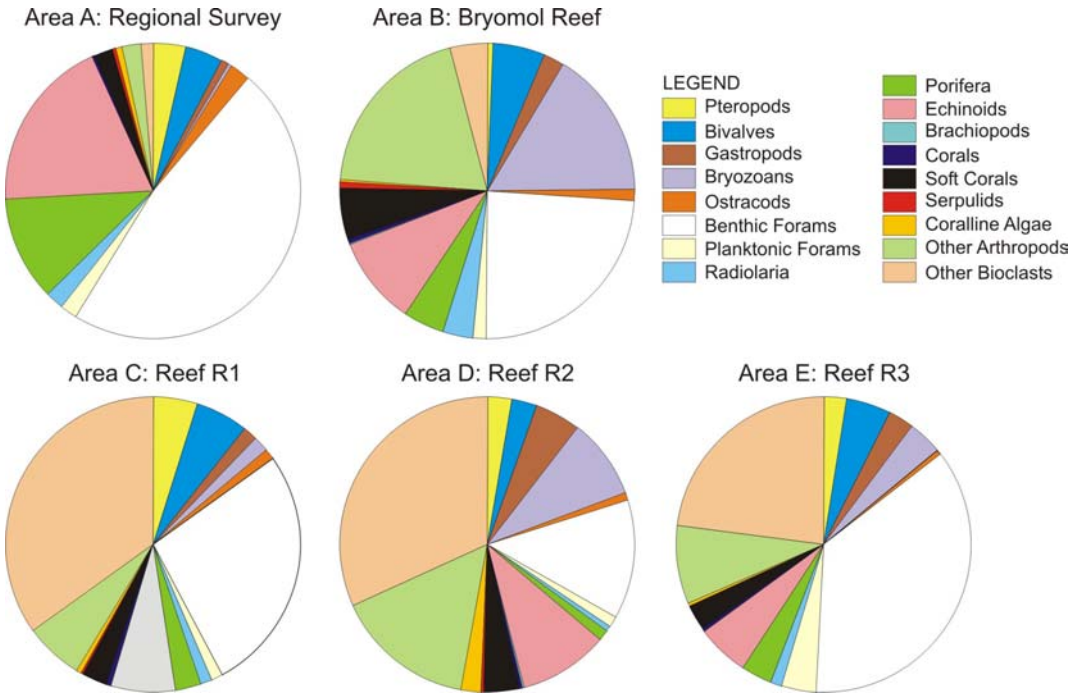

Figure 4.30. Graphs showing the composition of fossil biota in the surface sediments of the southern Gulf of Carpentaria. Benthic foraminifers and "other bioclasts" make up the largest contributions.

Facies 2 comprises moderately- to well-sorted quartz sand that forms beds up to 0.25 m thick at the base of VC5, 8 and 16, which were taken to sample material in depressions eroded into the old land surface, as seen in shallow seismic profiles. Grains are sub-angular to sub-rounded and minor amounts of feldspar are also present. This facies is interpreted to be river sand that was deposited at lowstand or early transgression in depressions and channels eroded into the old land surface/lake bed.

Facies 3 occurs unconformably above Facies 1 and Facies 2, attains 3.25 m thick (VC9), and occurs only in cores that sampled material from subsurface depressions in the old land surface, as seen in the shallow seismic profiles. This facies can be divided into two discrete sub-facies: Facies 3A which is composed of alternating poorly-sorted mud and numerous medium and coarse sand beds up to 0.05 m thick (VC8, 14, 16); and Facies 3B which is composed of alternating poorly-sorted mud and fine sand laminations and clay beds (VC4, 6-7, 9, 13). A total of 13 radiocarbon ages were recovered from peat samples contained in Facies 3. The ages indicate that Facies 3 was deposited between 8,500-10,200 years BP (Table 4.13). This rapid accumulation is consistent with the preservation of the laminations and bedding and peat deposits. Carbonate concentrations throughout the facies are <5% by weight (Appendix I). Facies 3A and 3B are thus interpreted to represent shallow fluvial-deltaic deposits—with the laminations and sand beds representing varying river influence (e.g., floods)—that have filled depression/channels in the old land surface.

Facies 4 comprises poorly-sorted sandy silt and mud and occurs in VC1-3, 4-6, 8-9, 13-14, 16-18. This facies ranges in thickness from 0.19 m (VC13) to 4.37 m (VC14) and occurs in association with Facies 3. Extensive mud-filled burrows are characteristic of this facies in VC4, 9, and 17-18. Radiocarbon ages from material contained in this unit put its age at 7,300-9,900 years BP (Table 4.13) indicating that this unit was deposited during mid to late transgression. Carbonate concentrations throughout the facies are <5% by weight (Appendix I). This facies is interpreted to be shallow fluvial-deltaic sediments, deposited in quiescent environments away from the river influence.

Facies 5 occurs at the top of the sequence and comprises fossil-rich poorly-sorted calcareous muddy gravelly sand, muddy sand and sandy mud. The facies is contained in all the cores recovered from Area A and occurs unconformably above Facies 1, 2, 3A and 3B. It ranges in thickness from 0.24 m (VC1) to 1.8 m (VC5) and is composed principally of mollusc fragments and foraminifer tests, with minor amounts of bryozoan, coral and siliciclastic grains, including sponge spicules (cf. section 4.3.5; Table 4.11). Radiocarbon ages derived from shell material recovered from Facies 5 put the age of this unit at <4,700 years BP (Table 4.13), with the age of surface material up to 2,600 years BP (VC2). The large age range of surface material indicates that Facies 5 is a mixture of modern and much older carbonate grains. This is quite typical of modern shelf sediments in northern Australia and is a product of very low modern sedimentation rates and extensive sediment re-working by cyclones and bioturbation. This facies is interpreted to represent modern shallow tropical shelf facies that was deposited since the sea level highstand commenced ~6,000 years BP.

In VC11 and VC12, the base of Facies 5 comprises poorly-sorted carbonate coarse sand and gravel bed occurring unconformably above Facies 1. This carbonate unit might represent a wave ravinement surface that formed during shoreline transgression over the old land surface or it could also be a lag deposit of Facies 5 (see below) formed from reworking of the modern shelf sediment (e.g., by cyclones).

Area B: Bryomol Reef:— A total of two distinct sub-surface facies occur in Area B. At the base of the sequence is Facies 1 which comprises stiff and de-watered grey to greenish grey silty clay at the bottom of VC20, 24, and 27. Although the base of this facies was not sampled, it is at least 0.62 m thick (VC27). These factors and its colour indicate that it has been oxidised and subaerially exposed in the past. This unit is interpreted to be the weathered horizon of the old land surface or lake bed that was exposed during the last glacial and before the latest marine transgression. This facies corresponds to Facies 1 of Area A.

Table 4.13. AMS radiocarbon and calibrated age determinations for samples collected from the vibrocores.

Lab Code	Sample ID	Sample Description	Radiocarbon Age (yr BP)	Corrected*/Calibrated† Age
NZA 19731	238/23VC2/0-2	Foraminifers	2,975±40	2,605±82 BP*
NZA 19730	238/23VC2/47	Shell	2,562±35	2,192±80 BP*
NZA 19774	238/23VC2/155	Shell	7,759±50	7,389±88 BP*
NZA 19598	238/23VC2/160	Peat	8,331±40	7,516-7,302 BC; 9,465-9,251 BP†
NZA 19533	238/23VC2/204	Peat	8,759±45	7,964-7,607 BC; 9,913-9,556 BP†
NZA 19534	238/23VC2/211.5-212.5	Peat	8,731±45	7,952-7,599 BC; 9,901-9,548 BP†
NZA 19535	238/23VC2/221	Peat	8,823±50	8,213-7,727 BC; 10,162-9,676 BP†
NZA 19536	238/23VC2/251-256	Peat	8,856±45	8,225-7,754 BC; 10,174-9,703 BP†
NZA 19595	238/24VC3/52	Shell	3,091±35	2,721±80 BP*
NZA 19323	238/24VC3/224-225	Peat	8,038±45	7,076-6,818 BC; 9,025-8,767 BP†
NZA 19324	238/24VC3/256-257	Peat	8,044±45	7,078-6821 BC; 9,027-8770 BP†
NZA 19517	238/25VC4/7	Shell	8,004±45	7,634±85 BP*
NZA 19518	238/25VC4/65-72	Shell	7,840±40	7,470±82 BP*
NZA 19319	238/25VC4/141	Peat	8,047±45	7,079-6,823 BC; 9,028-8,772 BP†
NZA 19728	238/26VC5/68	Shell	2,179±35	1,809±80 BP*
NZA 19729	238/26VC5/142	Shell	3,544±40	3,174±82 BP*
NZA 19525	238/26VC5/265	Bulk sediment	8,298±45	7,494-7,180 BC; 9,443-9,129 BP†
NZA 19526	238/26VC5/326	Peat	7,968±40	7,050-6,687 BC; 8,999-8,636 BP†
NZA 19726	238/27VC6/25-27	Shell	401±35	Modern*
NZA 19727	238/27VC6/76	Shell	3,876±35	3,506±80 BP*
NZA 19523	238/27VC6/128	Peat	8,028±40	7,069-6,818 BC; 9,018-8,767 BP†
NZA 19524	238/27VC6/345	Peat	8,044±40	7,075-6,825 BC; 9,024-8,774 BP†
NZA 19722	238/29VC8/0-2	Foraminifers	2,332±35	1,962±80 BP*
NZA 19592	238/29VC8/69-72	Shell	5,113±35	4,743±80 BP*
NZA 19593	238/29VC8/103-106	Shell	8,132±45	7,762±85 BP*
NZA 19320	238/29VC8/138	Peat	8,415±45	7,574-7,446 BC; 9,523-9,395 BP†
NZA 19321	238/29VC8/173	Peat	8,485±45	7,589-7,488 BC; 9,538-9,437 BP†
NZA 19322	238/29VC8/270	Peat	8,578±50	7,649-7539 BC; 9,598-9,488 BP†
NZA 19594	238/29VC8/318	Shell	421±35	Modern*
NZA 19965	238/29VC8/318_2	Shell	358±35	Modern*
NZA 19596	238/35VC14/15-17	Shell	2,095±35	1,725±80 BP*
NZA 19597	238/35VC14/34-38	Shell	4,603±40	4,233±82 BP*
NZA 19723	238/35VC14/125-127	Foraminifers	8,883±45	8,513±85 BP*
NZA 19724	238/35VC14/170-172	Foraminifers	9,264±50	8,894±88 BP*
NZA 19725	238/35VC14/230-232	Foraminifers	8,857±45	8,487±85 BP*
NZA 19519	238/35VC14/312	Peat	8,826±45	8,208-7,737 BC; 10,157-9,686 BP†
NZA 19520	238/35VC14/328	Peat	9,002±50	8,291-8,196 BC; 10,240-10,145 BP†
NZA 19521	238/35VC14/387	Peat	8,267±40	7,470-7,173 BC; 9,419-9,122 BP†
NZA 19522	238/35VC14/400	Peat	9,020±50	8,296-8,205 BC; 10,245-10,154 BP†
NZA 19636	238/35VC14/450-453	Shell	8,884±40	8,514±82 BP*
NZA 19775	238/38VC17/45	Shell	5,111±35	4,741±80 BP*
NZA 19537	238/38VC17/279-283	Peat	8,217±45	7,360-7,073 BC; 9,309-9,022 BP†

NZA 19538	238/38VC17/313-314	Peat	8,372±45	7,537-7,332 BC; 9,486-9,281 BP†
NZA 19539	238/38VC17/379-381	Peat	8,556±50	7,606-7,529 BC; 9,555-9,478 BP†
NZA 19311	238/80VC29/0-2	Foraminifers	2,427±35	2,057±80 BP*
NZA 19312	238/80VC29/30-31	Shell	2,830±40	2,460±82 BP*
NZA 19313	238/80VC29/38-39	Shell	7,396±55	7,026±91 BP*
NZA 19314	238/80VC29/72-73	Shell	6,893±40	6,523±82 BP*
NZA 19315	238/80VC29/120-123	Shell	5,674±35	5,304±80 BP*
NZA 19498	238/80VC29/156-162	Shell	5,947±35	5,577±80 BP*
NZA 19499	238/80VC29/188-192A	Shell	5,732±40	5,362±82 BP*
NZA 19500	238/80VC29/188-192B	Shell	6,221±35	5,851±80 BP*
NZA 19501	238/80VC29/210-212	Foraminifers	7,482±40	7,112±82 BP*
NZA 19316	238/80VC29/335	Bulk sediment	6,773±40	5,730-5,622 BC; 7,679-7,571 BP†
NZA 19317	238/80VC29/338	Bulk sediment	7,407±45	6,396-6,213 BC; 8,345-8,162 BP†
NZA 19502	238/80VC29/419	Bulk sediment	7,529±40	6,456-6,354 BC; 8,405-8,303 BP†
NZA 19318	238/80VC29/457-458	Bulk sediment	8,075±50	7,172-7,020 BC; 9,121-8,969 BP†
NZA 19591	238/81VC30/25-27	Shell	531±35	161±80 BP*
NZA 19514	238/81VC30/106	Shell	1,310±40	940±82 BP*
NZA 19515	238/81VC30/132-135	Shell	4,567±35	4,197±80 BP*
NZA 19516	238/81VC30/208-211	Shell	7,310±40	6,940±82 BP*
NZA 19508	238/89VC32/27-28	Shell	701±35	331±80 BP*
NZA 19509	238/89VC32/67-70	Shell	5,683±35	5,313±80 BP*
NZA 19504	238/90VC34/28	Shell	536±35	166±80 BP*
NZA 19505	238/90VC34/56-57	Shell	1,401±40	1,031±82 BP*
NZA 19506	238/90VC34/90-92	Shell	6,271±45	5,901±85 BP*
NZA 19507	238/90VC34/181-185	Shell	9,324±50	8,954±88 BP*
NZA 19510	238/100VC37/0-2	Foraminifers	2,007±35	1,637±80 BP*
NZA 19511	238/100VC37/50	Shell	6,040±35	5,670±80 BP*
NZA 19512	238/100VC37/103-104	Shell	7,998±40	7,628±82 BP*
NZA 19513	238/100VC37/122-125	Shell	7,424±40	7,054±82 BP*
NZA 20422	238/104VC40/30-32	Foraminifers	1,546±35	1,176±80 BP*
NZA 20423	238/104VC40/90-92	Foraminifers	2,760±35	2,390±80 BP*
NZA 20424	238/104VC40/140-142	Foraminifers	3,510±40	3,140±82 BP*
NZA 20425	238/104VC40/210-212	Foraminifers	4,395±40	4,025±82 BP*
NZA 20426	238/104VC40/250-252	Foraminifers	4,696±35	4,326±80 BP*
NZA 20427	238/104VC40/380-382	Foraminifers	5,970±40	5,600±82 BP*

* Corrected age is corrected for marine reservoir effect for northeast Australia of -370±72 years (Stuiver et al., 1986).
† Calibrated age at 2σ confidence interval.

Facies 2 is comprised of fossil-rich poorly-sorted calcareous coarse sand and gravel. It occurs in all cores recovered from Area B except for VC20 and occurs unconformably above Facies 1 in VC25 and 27. The base of this facies was not sampled, although it ranges in thickness from 0.11 m (VC27) to at least 1.21 m (VC23). Facies 2 is composed principally of mollusc fragments and foraminifer tests, with lesser amounts of bryozoan, arthropod and coral fragments, and siliciclastic grains (cf. section 4.3.5; Table 4.11). Significantly, siltstone and mudstone grains are common throughout this facies, suggesting a source of material from the nearby Mornington Island. VC23 was recovered from the base of a depression on

the reef and consists almost entirely of reefal material. Distinctively, Facies 2 contains relict material, with weakly cemented and encrusted carbonate fragments are common (VC22, 23, 26-27). Limestone cobbles and pebbles comprising bryomol reef fragments are also present (VC22, 27). Interestingly, the reefal fragments occur in the cores on the gulf floor that sampled environments furthest away from the bryomol reef. This facies is interpreted to be the modern shallow tropical shelf facies and is equivalent to Facies 5 of Area A.

Area C: Reef R1:— A total of four distinct sub-surface facies occur in Area C. At the base of the sequence is Facies 1 which comprises stiff and de-watered grey to greenish grey silty clay at the bottom of VC30-32 and 39. Although the base of this facies was not sampled, it is at least 0.30 m thick (VC32). These factors and its colour indicate that it has been oxidised and subaerially exposed in the past. This unit is interpreted to be the weathered horizon of the old land surface or lake bed that was exposed during the last glacial and before the latest marine transgression. This facies is equivalent to Facies 1 of Area A and Area B.

Facies 2 comprises moderately-sorted quartz sand that forms beds up to 0.10 m thick at the base of VC29, which was taken to sample material in a depression eroded into the old land surface south of the reef, as seen in shallow seismic profiles. Grains are sub-angular to sub-rounded and minor amounts of feldspar are also present. This facies is interpreted to be river sand that was deposited at lowstand or early transgression in depressions and channels eroded into the old land surface, and is equivalent to Facies 2 of Area A.

Facies 3 comprises poorly-sorted calcareous clay and silt with numerous horizontal silt and clay laminations. It occurs in cores recovered from the gulf floor on the southern and eastern margins of the reef (VC28-30, 39), including VC29 which was collected to sample material in a depression in the old land surface to the south of the reef. This facies ranges in thickness from 0.10 m (VC39) to 2.95 m (VC29). In VC29, where the silt and clay laminations are most well-preserved, the typical section consists of darker organic-rich silt beds unconformably overlying lighter clay beds, indicating that the bed are associated with different concentrations of organic material. In VC28 and VC30, the facies is heavily burrowed throughout, and hence the laminations are very poorly preserved. A total of 6 radiocarbon ages were recovered from samples contained in Facies 3. The ages indicate that Facies 3 was deposited between 6,900-9,100 years BP (Table 4.13). Carbonate concentrations throughout these facies are negligible (<2% by weight). Facies 3 is thus interpreted to represent shallow fluvial-deltaic deposits—with the laminations representing varying river influence (e.g., floods)—that have filled a depression/channel in the old land surface.

Facies 4 is at the top of the sequence in Area C and comprises two distinct sub-facies: Facies 4A which is composed of fossil-rich poorly-sorted coarse sand and gravel (VC33-35, 37); and Facies 4B which is composed of fossil-rich poorly-sorted muddy fine to medium sand (VC28-32, 38-40). Facies 4A ranges in thickness from 0.44 m (VC35) to 2.16 m (VC34) and Facies 4B ranges in thickness from 0.45 m (VC31) to 3.88 m (VC40). Interestingly, the distribution of facies shows that Facies 4A occurs on the western and northern margins of the reef and Facies 4B occurs on the eastern and southern margins. Both Facies 4A and 4B are composed principally of mollusc fragments and foraminifer tests, with minor amounts of coral and bryozoan fragments, and siliciclastic grains, including sponge spicules (cf. section 4.3.5; Table 4.12). Facies 4A and 4B contain relict carbonate (much of it reefal) material, with weakly cemented and encrusted cobble- and pebble-sized limestone fragments common (VC33-35, 37-38). Coral fragments are relatively rare and occur only in VC33-35 from the western margin of the reef. Radiocarbon ages derived from shell material recovered from

Facies 4 put the age of this unit at <5,900 years BP (Table 4.13), with the age of surface material up to 2,000 years BP (VC29). The large age range of surface material indicates that Facies 4 is a mixture of modern and much older carbonate grains. The age of the sediment in each of the cores generally increases with depth. Reversals occur at 0.38 m and 0.72 m in VC29 and may be caused by bioturbation and/or sediment re-working by cyclones. Evidence for the latter is shown by a relative lack of sediment aged between 2-5,000 years BP in all the cores except VC40. VC40 was recovered from the talus slope to the south of the reef, and shows a relatively consistent increase in age with depth, and provides the most continuous sedimentary record for Area C. Ages derived from articulated bivalves in the cores are all modern, despite being located in older surrounding material, thus providing evidence of significant downcore bioturbation (0.72 m in VC32). Facies 4A and 4B are thus interpreted to be the modern shallow tropical shelf facies and is equivalent to Facies 5 of Area A and Facies 2 of Area B. This unit was deposited since the last sea level highstand commenced approximately 6,000 years BP.

4.3.5.2. Physical Properties

Reliable data were obtained for bulk density, fractional porosity, and colour for the cores (Appendix H). Values for magnetic susceptibility were not obtained because of the influence from the aluminium liner. P-wave velocities were mostly above 3.0 km s^{-1}, much higher than would be expected from unconsolidated marine sediments. These high velocities are a record of the acoustic pulse travelling through the liner rather than the sediment, and thus they are not shown in the core logs and are not described in this report.

Even though the textural and compositional analyses of the sediments indicate that there are distinct facies changes between Areas A, B and C and with depth, the colour spectrum of the sediment shows very little change between the cores and facies, with red and green phases having very similar pixel intensities of between 60-120 and blue having generally lower pixel intensities of <80 (Appendix H). Consequently, the ratios of the three phases are relatively constant throughout the cores, with red and green comprising approximately >70% of the colour spectrum and comprising the remaining <30%. Major deviations are only associated where large shells or reefal fragments are present in the sediment and could not be avoided in the scanning process. These results are surprising given the textural and compositional differences between the facies in each of the three areas. Further analysis of these data is required to explore the subtle differences observed in the data.

Greatest variability in the physical properties of the cores occurs in the bulk densities and fractional porosity. Trends in fractional porosity are generally inversely related to those displayed by the bulk density.

Area A: Regional Survey:— Bulk densities range from a minimum of 1.4232 g cm^{-3} (VC1) to a maximum of 2.2975 g cm^{-3} (VC12), with an average of 1.7878 g cm^{-3} over the entire area (Table 4.14a). These values are comparable to bulk densities recorded elsewhere for other Quaternary sediments in northern tropical Australia (e.g, Heap et al., 2001). Significant differences in the densities occur between all the facies (Appendix H). Facies 1 and 2 have the highest bulk densities in Area A. These higher densities probably reflect the de-watered and semi-lithified nature of Facies 1, and the coarse-grained sediments comprising Facies 2. The lacustrine facies of Facies 3A, 3B and 4 have similar densities, and the modern shallow sediments of Facies 5 have slightly higher bulk densities. Generally, the sandier sediments

have relatively higher densities (VC1, 4, 6, 8-9, 14), and finer-grained sediments have relatively lower densities; there is a distinct correlation between low densities and clay beds in VC3-4, and VC6. Bulk densities increase slightly with depth in VC1, 5, 9, 15 and 17, otherwise the variability in density shown downcore coincides with facies changes, especially where these changes coincide with sharp grain size changes.

Table 4.14. Statistics of: a) bulk density and b) fractional porosity for facies in Area A: Regional Survey.

a) Bulk density (g cm^{-3})

Facies	Interpretation	Mean	Minimum	Maximum	Std Dev.	*N*
1	Old land surface	1.9074	1.4232 (VC1)	2.1641 (VC15)	0.1670	202
2	River sand	1.9556	1.6830 (VC5)	2.1365 (VC8)	0.1193	32
3A	Lacustrine	1.7975	1.3173 (VC8)	2.1959 (VC14)	0.1904	512
3B	Lacustrine	1.7301	1.2606 (VC6)	2.1491 (VC4)	0.1482	491
4	Lacustrine	1.7145	1.0256 (VC16)	2.1793 (VC3)	0.1992	1,572
5	Shallow shelf	1.8877	1.0436 (VC18)	2.2975 (VC12)	0.1272	1,169

b) Fractional porosity

Facies	Interpretation	Mean	Minimum	Maximum	Std Dev.	*N*
1	Old land surface	0.4735	0.3201 (VC15)	0.7627 (VC01)	0.0998	202
2	River sand	0.4395	0.3366 (VC8)	0.5780 (VC16)	0.0658	31
3A	Lacustrine	0.5385	0.3012 (VC14)	0.7461 (VC14)	0.1131	511
3B	Lacustrine	0.5791	0.3291 (VC4)	0.8599 (VC6)	0.0884	490
4	Lacustrine	0.5887	0.3110 (VC3)	0.9237 (VC16)	0.1190	1,571
5	Shallow shelf	0.4853	0.2405 (VC12)	0.9072 (VC18)	0.0756	1,171

Fractional porosity values range from 0.2405 (VC12) to 0.9237 (VC16), with an average of 0.5439 over the entire area (Table 4.14b). These values are comparable to porosities recorded for other Quaternary sediments in northern tropical Australia (e.g, Heap et al., 2001). Significant differences in the porosities occur between all the facies (Appendix H). Across all the cores, there is a slight decrease in porosity with depth (VC1, 4, 5-7, 9, 15, 17-18), probably associated with slight increase in sediment compaction down core. This trend is most apparent where facies are thickest at the base of each core (e.g., Facies 4 in VC3 and 17; Facies 4 and 3b in VC9). Interestingly, there is a slight increase in porosity depth in VC8 and VC14. In most cases, the variability in downcore porosity is associated with facies changes, particularly where distinct grain size changes occur. The lacustrine facies (Facies 3A, 3B and 4) have the highest porosities of over 50% on average, although Facies 3A and 4 have the highest variability over the entire area. Lowest porosities occur in Facies 2, which also has the least variability. This result is surprising given the relatively coarse-grained nature of the sediment in this facies. Facies 1 contains the lowest porosity due to the sediment being relatively de-watered and compacted. Highest porosities of >90% occur in Facies 4 and 5. The relatively high porosity of Facies 5 probably reflects the generally coarse-grained sediments and regular and frequent reworking of the material by tides and waves, especially cyclones, and bioturbation in the uppermost sections.

Area B: Bryomol Reef:— Bulk densities range from a minimum of 1.0894 g cm^{-3} (VC20) to a maximum of 2.1627 g cm^{-3} (VC26), with an average of 1.8446 g cm^{-3} over the entire area (Table 4.15a). These values are comparable to bulk densities recorded elsewhere for other

Quaternary sediments in northern tropical Australia (e.g., Heap et al., 2001). Significant differences in the densities occur between all the facies (Appendix H). Facies 2 which represents the modern shallow shelf sediments has the highest bulk densities in Area B. Bulk densities gradually increase with depth in all cores, except VC25, probably due to increased compaction of the sediments downcore. This trend is particularly apparent in Facies 2 (e.g., VC22-23) and also occurs in Facies 1 (VC27). Bulk densities show greater variability in Facies 1 compared with Facies 2, and are slightly higher where the sediments are sandier. Large changes in bulk density are associated with the major facies changes (e.g., VC25, 27). Variations in bulk density also correspond to the presence of reefal (limestone) fragments with slightly higher densities recorded (e.g., VC22, 27).

Table 4.15. Statistics of: a) bulk density and b) fractional porosity for facies in Area B: Bryomol Reef.

a) Bulk density (g cm^{-3})

Facies	Interpretation	Mean	Minimum	Maximum	Std Dev.	*N*
1	Old land surface	1.7575	1.0894 *(VC20)*	2.1010 *(VC27)*	0.2232	144
2	Shallow shelf	1.8953	1.2859 *(VC27)*	2.1627 *(VC26)*	0.1480	269

b) Fractional porosity

Facies	Interpretation	Mean	Minimum	Maximum	Std Dev.	*N*
1	Old land surface	0.5599	0.3578 *(VC27)*	0.9609 *(VC20)*	0.1299	142
2	Shallow shelf	0.4883	0.3210 *(VC26)*	0.8979 *(VC27)*	0.0904	268

Fractional porosity ranges from a minimum of 0.3210 (VC26) to a maximum of 0.9609 (VC20), with an average of 0.5151 over the entire area (Table 4.15b). These values are comparable to porosities recorded for other Quaternary sediments in northern tropical Australia (e.g, Heap et al., 2001). Significant differences in the porosities occur between the facies (Appendix H). Across all the cores, there is a slight decrease in porosity with depth, probably associated with slight increase in sediment compaction down core. This trend is most apparent where facies are thickest at the base of each core (e.g., Facies 1 in VC27; Facies 2 in VC22 and VC23). Otherwise major changes coincide with facies changes, particularly where these correspond to distinct grain size changes. Facies 1 has the highest porosity and highest variability with >50% of the facies pore space by volume. This is surprising given the relatively de-watered and compact material comprising this facies. These data might be influenced by sedimentary structures contained in this facies from this area including burrows (e.g., VC20). Facies 2 has the lowest porosity and variability in Area B, with <50% of the facies pore space by volume. These values are comparable to the poorly-sorted shallow shelf sediment sampled in Areas A and B.

Area C: Reef R1:— Bulk densities range from a minimum of 1.0894 g cm^{-3} (VC20) to a maximum of 2.1627 g cm^{-3} (VC26), with an average of 1.7002 g cm^{-3} over the entire area (Table 4.16a). These values are comparable to bulk densities recorded elsewhere for other Quaternary sediments in northern tropical Australia (e.g, Heap et al., 2001). Significant differences in the densities occur between all the facies (Appendix H). Bulk densities show significant variability over the area but generally increase with depth, probably due to increased sediment compaction downcore (e.g., VC31, 37-39). Bulk densities are positively correlated to grain size, with relatively higher values associated with sands and gravels (e.g, VC29, 33, 35, 38) as well as the presence of reefal (limestone) fragments (VC34, 38), and

relatively lower values associated with clay beds (VC29). Large changes in bulk density correspond to the major facies changes, particularly where they are associated with significant changes in grain size (e.g., VC30-33).

Table 4.16. Statistics of: a) bulk density and b) fractional porosity for facies in Area C: Reef R1.

a) Bulk density (g cm^{-3})

Facies	Interpretation	Mean	Minimum	Maximum	Std Dev.	*N*
1	Old land surface	1.8861	1.8051 *(VC32)*	2.0427 *(VC32)*	0.0535	80
2	River sand	1.3498	1.2830 *(VC29)*	1.4201 *(VC29)*	0.0479	8
3	Lacustrine	1.4720	1.2147 *(VC29)*	2.1307 *(VC39)*	0.2316	373
4A	Shallow shelf	1.7294	1.1602 *(VC33)*	2.1637 *(VC38)*	0.1448	551
4B	Shallow shelf	1.7462	1.3251 *(VC30)*	1.9840 *(VC39)*	0.1109	1,237

b) Fractional porosity

Facies	Interpretation	Mean	Minimum	Maximum	Std Dev.	*N*
1	Old land surface	0.4862	0.3927 *(VC32)*	0.5346 *(VC32)*	0.0320	80
2	River sand	0.8066	0.7676 *(VC29)*	0.8465 *(VC29)*	0.0286	8
3	Lacustrine	0.7335	0.3401 *(VC31)*	0.8873 *(VC29)*	0.1383	373
4A	Shallow shelf	0.5797	0.3204 *(VC38)*	0.9198 *(VC33)*	0.0863	551
4B	Shallow shelf	0.5698	0.4277 *(VC39)*	0.8213 *(VC30)*	0.0662	1,238

Fractional porosity ranges from a minimum of 0.3204 (VC38) to a maximum of 0.9198 (VC33), with an average of 0.5973 over the entire area (Table 4.16b). These values are comparable to porosities recorded elsewhere for other Quaternary sediments in northern tropical Australia (e.g, Heap et al., 2001). Significant differences in the porosities occur between all the facies (Appendix H). Overall, there is a slight decrease in porosity with depth, although this trend is not obvious or distinct in all the cores. Porosity is lowest for Facies 1 which is expected since this facies comprises partially compacted and de-watered clay. Facies 2 has the highest porosity with >80% comprising pore space by volume. These relatively high values are associated with the relatively coarse grained nature of this facies. Facies 3 has the second highest porosity and also has the highest variability of all the facies in Area C. Porosities are very similar in the shallow shelf facies (Facies 4A and 4B) with over half comprising pore space by volume. These relatively high values are most likely due to the coarse grained and relatively unconsolidated nature of these facies, which are produced as a result of regular and significant reworking by tides and waves (especially cyclone-generated waves) and bioturbation.

5. Discussion

The present survey has revealed the physical character of the shallow shelf environments in the southern Gulf of Carpentaria. A range of sedimentary and depositional environments were revealed, namely: shallow shelf (open marine), reefal platforms and their associated deposits, transgressive fluvial-deltas, river beds, as well as the old exposed land surface. The data contained in this report improves our understanding of the sedimentary and oceanographic processes operating in the southern Gulf, as well as providing a framework for documenting the late Quaternary evolution of the region. As such, changes to the sources and sinks of terrigenous sediment in the southern Gulf of Carpentaria are revealed through time.

5.1. SOURCES AND SINKS OF TERRIGENOUS SEDIMENT

Terrigenous sediment is partitioned into three major depocentres in the southern Gulf. The first depocentre is the network of broad depressions and shallow (<5 m deep) channels cut into the old land surface of the Gulf. Shallow seismic data reveal that terrigenous sediment in the depressions is well-bedded and the cores indicate that the material comprises silt and sand beds that are indicative of fluvial-delta deposits. These deposits represent back-filling of estuarine and deltaic channels, and have been preserved because of their relatively low elevation.

The second depocentre is terrigenous sediment incorporated into the modern shallow shelf sediment on the bed of the Gulf. Samples collected on the regional survey contained between 11->60% carbonate material, with an average of 31%. Notwithstanding, biogenic sources, this means that about two thirds of the modern shelf sediment in the southern Gulf is composed of terrigenous grains on average. As expected, sites nearer to coastal influences (Areas A and B) contain a higher percentage of siliciclastic grains than the more distal sites (Areas C, D and E).

The third major depocentre is the coastal plain of the southern Gulf. The coastal plain is composed of terrigenous deposits fashioned by the influence of waves, tides and rivers into a suite of coastal environments that can be distinguished based on their geomorphology. The 164 coastal waterways in the Gulf of Carpentaria can be classified from their geomorphology as tidal creeks (n=80/48%), tide-dominated deltas (n=24/14%), strandplains (n=21/13%), tide-dominated estuaries (n=17/10%), wave-dominated deltas (n=14/9%), wave-dominated estuaries (n=7/4%), and lagoons (n=1/<1%) (Harris and Heap, 2003). Apart from the tide- and wave-dominated deltas, the other systems tend to trap terrigenous sediment delivered to the coast on millennial time-scales (e.g., Boyd et al., 1992; Dalrymple et al. 1992).

In the area covered by the regional survey, the modern shelf sequence (Facies 5 in Area A) ranges in thickness from 0.22 m to 1.8 m with an average thickness of 0.66 m. Shallow seismic profiles reveal that this sequence is very patchy, and forms a thin veneer (<2 m thick) over the old land surface and fluvial-deltaic deposits. Given that bioclastic grains comprise 31% of the total sediment on average, and assuming an average thickness of this sequence of 0.66 m, and an average dry bulk density of 1.39 g cm^{-3} (from the physical property data obtained from the cores), equates to a total terrigenous sediment mass of 6.33 x 10^{10} T for the terrigenous-dominated region of the southern Gulf (100,000 km^2).

A relatively recent estimate of pre-European terrigenous sediment yield from local rivers is 86 T km^{-2} yr^{-1} (Wasson et al., 1996), which equates to 0.00387 x 10^{10} T yr^{-1} when

summed over the area of the local river catchments (450,000 km^2). Over the last 6,000 years, during the prolonged Holocene highstand, this amounts to 23.22 x 10^{10} T of terrigenous sediment delivered to the southern Gulf of Carpentaria.

These relatively crude estimates of terrigenous sediment flux from rivers in the southern Gulf of Carpentaria indicate that during the Holocene sea level highstand approximately 3.6 times more terrigenous sediment was delivered by local rivers than that contained on the floor of the southern gulf. It is likely that a significant proportion of the river-derived sediment was trapped in the coastal zone, and now forms the well developed salt flats, strandplains, beach ridges, and tidal flats lining the southern and eastern margins. In a relatively large and shallow shelf embayment on the central Great Barrier Reef, Carter et al. (1993) estimated that >42% of the terrigenous sediment mass from local rivers is trapped in the coastal zone. If this estimate is comparable to the southern gulf region, then this means that 13.5 x 10^{10} T of terrigenous sediment has been deposited in the gulf, or 2.6 times that estimated to occur on the southern gulf floor.

Despite our relatively crude estimates, it is possible that some of the terrigenous sediment in the southern Gulf did not come from local rivers. A likely source of any additional terrigenous material are the older deposits in the gulf (as sampled in our cores), which would have been eroded by shoreline reworking during transgression; small rises in sea level would result in significant landward transgression of the shoreline due to the very flat bed. This explanation is supported by the regional unconformity shown in all cores collected in the southern Gulf. This unconformity is located at the base of the modern calcareous muddy sands and gravels comprising the modern shallow shelf deposits and truncates the underlying terrigenous silt and clay beds comprising the fluvial-deltaic deposits and previously exposed land surface. The sources and sinks of terrigenous dominated sedimentation is understandable on timescales of sea level change, with a large amount of the terrigenous sediment on the seabed of the southern Gulf of Carpentaria having been reworked from older deposits.

5.2. LATE QUATERNARY EVOLUTION

The late Quaternary evolution of the southern Gulf of Carpentaria was dominated by back-filling of channels and shore-line reworking of terrigenous sediments across the gulf floor, followed by reef development and contemporaneous carbonate-dominated deposition in a shallow tropical shelf environment. Generally, the modern shallow marine shelf sequence is thin (<2 m thick), and overlies older transgressive deposits of fluvial, deltaic and river origins, which in turn occur unconformably over the old land surface that was exposed during the last glacial (Fig. 5.1). The high-resolution late-Quaternary evolution of the southern Gulf of Carpentaria revealed by our cores provides a palaeo-environmental reconstruction currently missing from existing models for this region (e.g., Chivas et al., 2001).

5.2.1. Deposition of Shelf Sequences

The oldest sequence sampled was an older land surface of the Gulf. The unit representing this time is stiff-dewatered, contains calcareous nodules, and appears oxidised and weathered indicating that has been subaerially exposed during periods of lower sea level. A -53 m deep sill on the northwest margin of the Gulf indicates that sea level must have been close or below this level when this unit was exposed. While we do not have any ages from

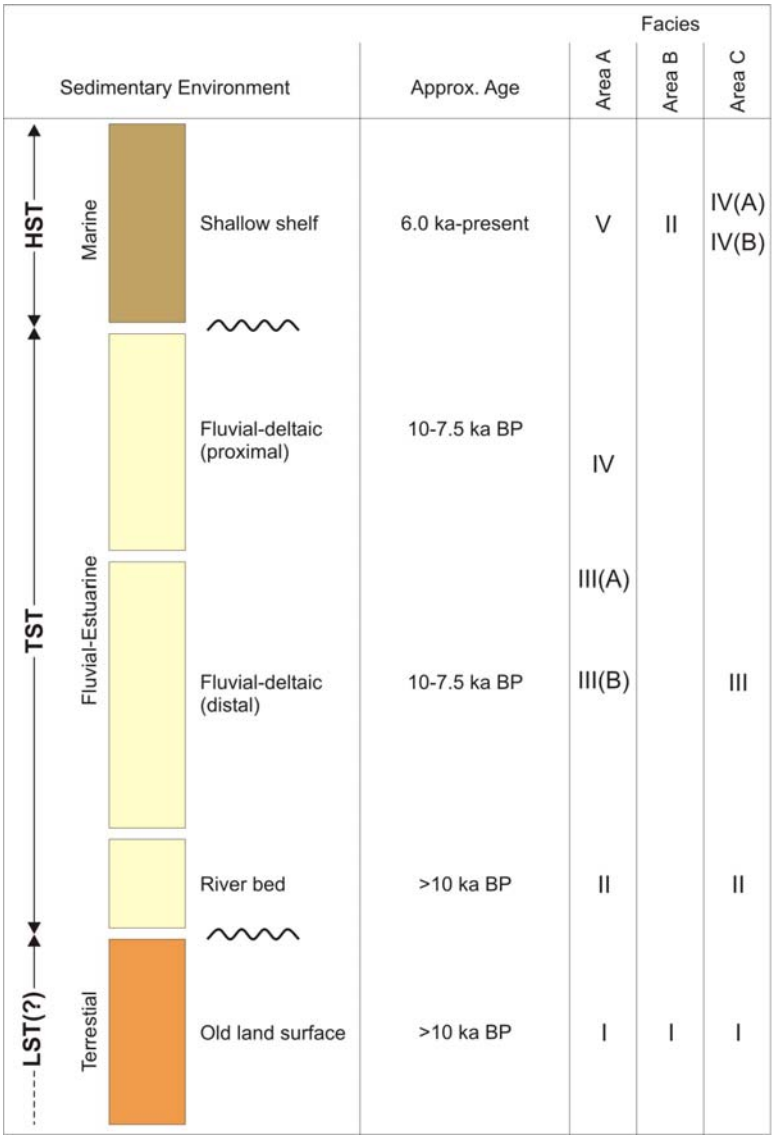

Figure 5.1. Generalized facies diagram for the southern Gulf of Carpentaria. The Holocene sequence is characterised by shallow open marine shelf deposits unconformably overlying transgressive deposits of fluvial, deltaic and river origins, which in turn occur unconformably over the old land surface that was exposed during the last glacial. This high-resolution Holocene history is currently missing from existing Late Quaternary models for the Gulf of Carpentaria.

this unit, comparison with the regional sea level curve (Fig. 5.2) indicates that it would have been exposed or been part of the Lake Carpentaria bed for up to 20% of the last 125,000 years.

Whilst over most of the southern Gulf of Carpentaria, the old land surface crops out close to the surface or is covered only by a very patchy and thin veneer of modern shelf sediment, cores collected from the broad depressions and channels incised into the old land surface reveal a more complex history. Quartz sand at the base on the channels indicates that rivers were actively depositing material in these channels during lowstand or transgression. Shallow seismic profiles indicate that the palaeo-channels of the modern local rivers once coalesced into a broad channel in the southern Gulf; this broad channel could not be traced far across the low-gradient gulf and it lost surface expression beyond Mornington Island. Smaller channels were also observed in the southern Gulf. These smaller and shallower channels could not be traced between the regional seismic lines and are inferred to have formed at the mouths of estuaries and were incised by tidal currents during the transgression.

All of the channels contained well-bedded sediments, as shown by the shallow seismic

profiles. Where sampled, these sediments are terrigenous, and comprised of fine-sand and silt laminations. Radiocarbon ages from peat contained in these sequences correspond to the relevant depths at which the deposits are found when compared with the late-Quaternary sea level curve for the region (Fig. 5.3). Fluvial-deltaic environments of the palaeo-rivers occupied southern Gulf of Carpentaria between 10-7.5 ka BP, probably as part of a low-gradient coastal plan, as seen today. Ages of the material indicate that these deposits were accumulating in the channels and depressions of the coastal plain during the latest post-glacial marine transgression.

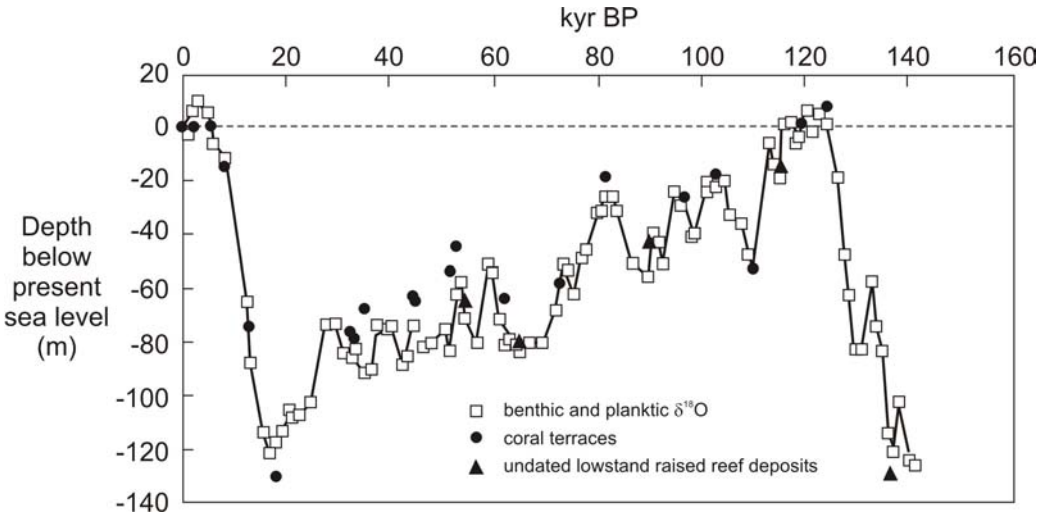

Figure 5.2. Late Quaternary eustatic sea level curve for northeast Australia and PNG derived from coral terraces at Huon Peninsula and benthic and planktic deep sea core $\delta^{18}O$ data. (Redrawn from Chappell et al., 1996).

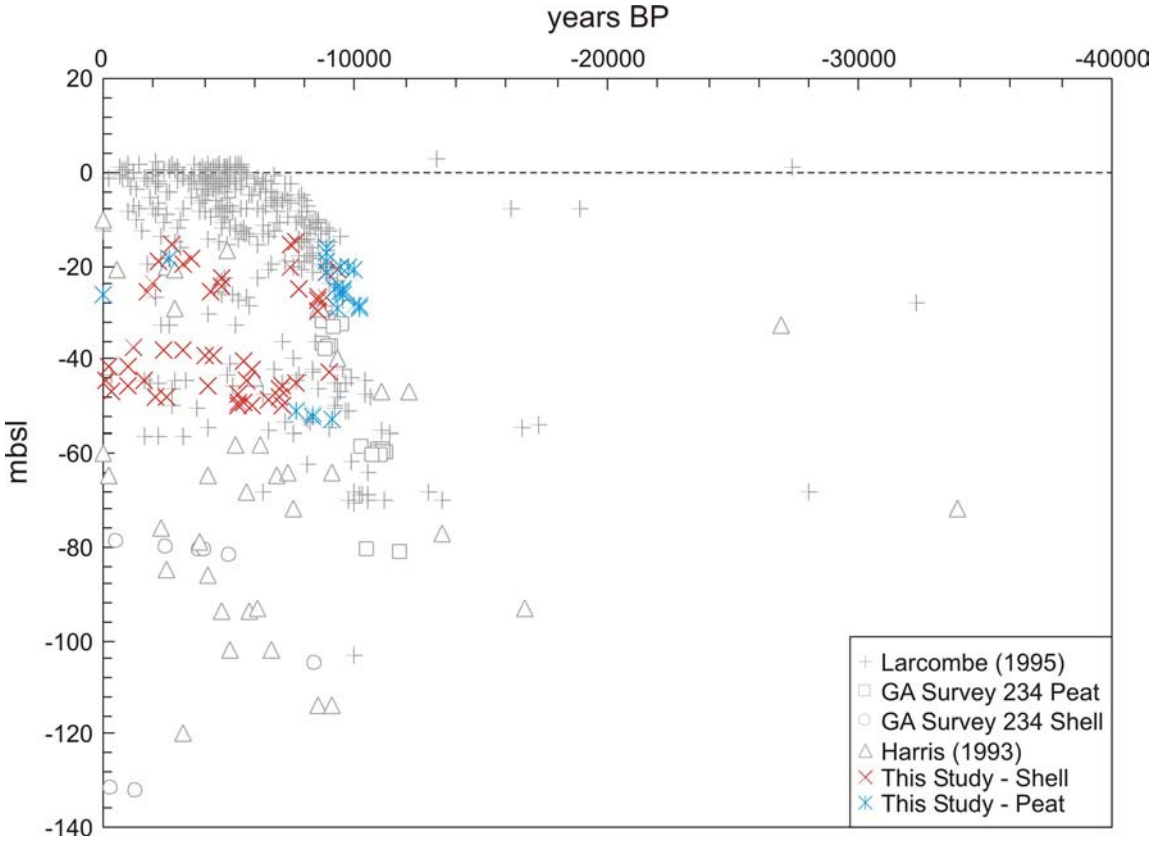

Figure 5.3. Graph of radiocarbon ages <40 kyr BP for samples collected from northeast Australia. Except for two cases, ages from peat samples from this study help to constrain the Holocene sea level curve for the region below -20 m. Ages from shell material from this study are relatively young compared with the curve.

After the fluvial deltaic deposits were laid down the transgressing shoreline eroded them to the base of the old land surface, except in the deeper depressions and channels where they remain preserved. The unconformity at the base of the shallow shelf sequence represents a wave- and tidal-ravinement surface that was produced as a result of this shoreline reworking. Ages of sediment from cores indicate that open shallow tropical marine conditions were in existence in the southern Gulf at least by 7.5 ka BP. Although this age must be treated with caution due to the relatively disturbed nature of the modern shelf facies (Area A: Facies 5, Area B: Facies 2; Area C: Facies 4A and 4B). Ages around the unconformity at the base of this unit range from 7.5-2.0 ka BP, indicating that large gaps are missing in the sedimentary record. Coralline material <6,000 years old contained in the talus slope next to Reef R1 indicates that the submerged coral reefs were growing in the Gulf of Carpentaria at least at the beginning of the Holocene sea-level highstand, although their morphology indicates that they were likely growing soon after they were submerged (see below).

5.2.2. Development of the Submerged Reefs

The most unexpected discovery in the southern Gulf of Carpentaria was the presence of three living submerged platform reefs. While the submerged reefs were not cored directly and there is no age control on the reefs themselves, insights into their development and growth history can be inferred from available data, namely the high-resolution bathymetry data, shallow seismic profiles, and ages of reefal material collected in the cores.

5.2.2.1. Timing and nature of reef development

The high-resolution bathymetry data reveal that the three reefs comprise six prominent surfaces (Table 5.1), two of which (A and B, Fig. 5.4) occur on more than one reef. These two 'regional' surfaces represent significant phases of carbonate production, most likely formed during a prolonged Quaternary sea level still-stand (Macintyre, 1972; Searle and Harvey, 1982), and are thus palaeo sea-level indicators. The most extensive surface is a central reef platform at 27.3 ± 1.4 m (48.1 km^2) that is well developed on reefs R1 and R2. The second surface at 30.6 ± 0.58 m (7.5 km^2) correlates with terraces on R1 and R2 and the central platform of R3. The shallow seismic data reveal that reef growth occurred over several sea level cycles, as shown by horizontal, sub-surface reflectors unconformably overlying an undulating acoustic basement reflector having positive relief (Fig. 2.7). A series of 3-4 m high marginal ridges on Reef R1 (Fig. 2.3) also indicates that it developed by multiple phases of lateral reef growth. The reefs thus appear similar in their growth history and geomorphic expression to those of the GBR and Caribbean reef provinces (Macintyre, 1972; Searle and Harvey, 1982).

The morphology and depth of the reef surfaces (Table 5.1) indicates that they formed mainly when sea level was 25-27 m below its present position. In the late Quaternary, such low sea level periods occurred at approximately 110-125 kyr BP, 90-102 kyr BP, 76-80 kyr BP, and 10 kyr BP to present (Fig. 5.5). These periods also coincided with cooler and drier climatic conditions than at present (Chivas et al., 2001; Kershaw et al., 2001), when the Gulf of Carpentaria was a large, shallow (<25 m) embayment with only one entrance via the Arafura Sea (Torres Strait was an emergent land bridge). It appears that such periods were more conducive to reef growth than today and that most reefal carbonates were deposited in the Gulf of Carpentaria when sea level was about 25 m lower than present (Fig. 5.5).

The fact that the reefs have not developed to present sea level can not be attributed to

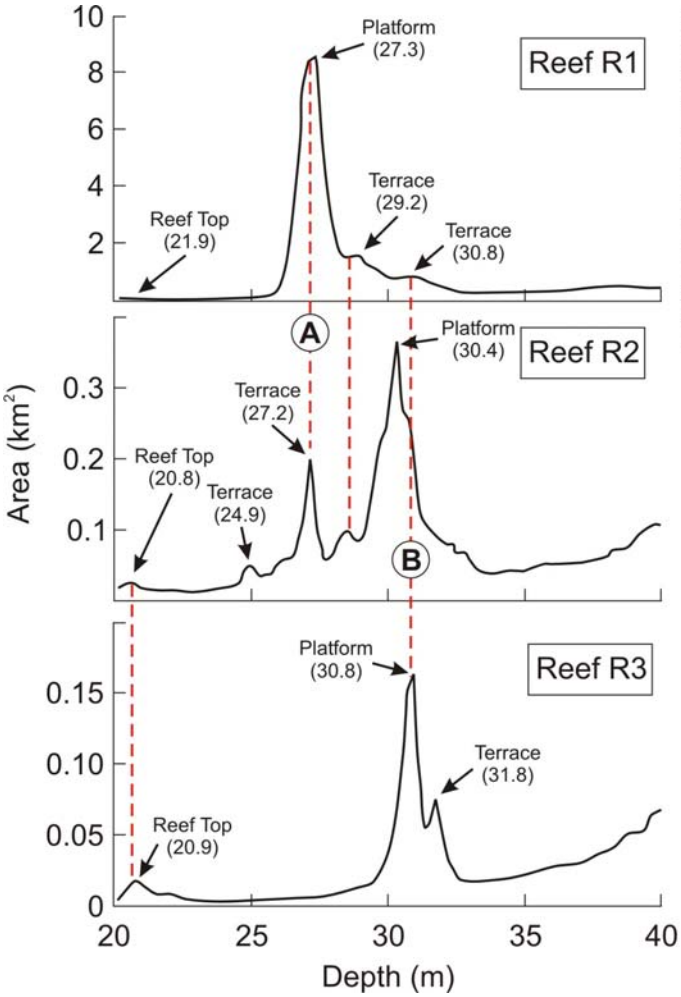

Figure 5.4. Hypsometric curves for reefs R1, R2, and R3 based on 1,008,830 multibeam sonar data points (Table 5.1). The largest peaks, A and B, correspond with horizontal surfaces of extended area (depths in metres shown in brackets) that can be correlated between the reefs. These two surfaces are interpreted to reflect palaeo sea-level still stands and periods of favourable coral reef growth. Smaller peaks represent other surfaces of <1 km² in area specific to individual reefs, and are inferred to reflect carbonate deposition during palaeo sea-level still stands followed by subaerial erosion processes.

Table 5.1. Water depths of reef tops, platforms and terraces measured for the submerged reefs in the southern Gulf of Carpentaria from multibeam sonar data.

Feature	Min. Depth (m)	Max. Depth (m)	Mean Depth (m)	Std. Dev. (m)	No. Data Points	Area (km²)
Reef R1 reef top	20.8	22.4	21.92	1.78	349	0.04
Reef R1 platform	26.6	28.2	27.33	1.37	481,505	48.15
Reef R1 terrace	28.8	29.8	29.24	0.89	75,261	7.53
Reef R1 terrace	30.4	31.2	30.80	0.22	38,724	3.87
Total Reef R1	20.8	(35)*	28.20	0.70	724,848	72.48
Reef R2 reef top	20.2	21.4	20.75	0.61	5,376	0.13
Reef R2 terrace	24.2	25.4	24.89	1.20	1,881	0.22
Reef R2 terrace	26.8	27.6	27.20	2.14	23,945	0.60
Reef R2 platform	29.4	31.6	30.42	0.99	101,294	2.53
Total Reef R2	20.2	(35*)	29.39	0.42	221,656	5.54
Reef R3 reef top	20.4	21.4	20.90	0.92	3,183	0.08
Reef R3 platform	30.2	31.4	30.83	0.07	27,552	0.69
Reef R3 terrace	31.6	32.0	31.79	2.01	7,455	0.19
Total Reef R3	20.2	(35)*	30.24	0.62	62,326	1.56
Grand Total	20.2	(35)*	28.59	0.54	1,008,830	79.59

*Outer reef edge defined as 35 m depth.

high levels of turbidity in the southern Gulf of Carpentaria. Measurements 2 m above the bed over the reefs reached 2.9 mg l^{-1}. This low turbidity is attributed to the nature of the bed sediment, which lacked mud and contained hard coral substrate or coarse carbonate grains.

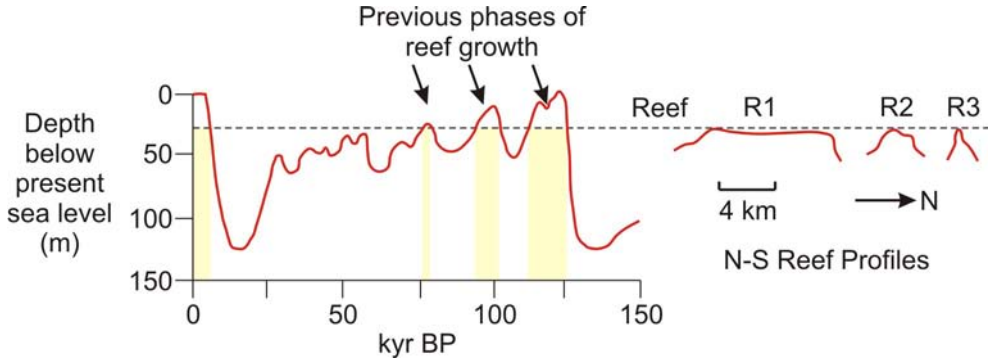

Figure 5.5. Sea level curve for the past 150,000 years (after Chappell et al., 1996) showing the times when the reefs in the southern Gulf of Carpentaria were submerged. Reef growth and main deposition of the reefs probably occurred during the three highstands between 110-125 kyr BP, 90-102 kyr BP, and 76-80 kyr BP.

Although appearing relict, the submerged reefs are mantled by a thin and patchy veneer of living corals. Samples yielded a live specimen of the plate coral *Turbinaria* sp. (Station 82) and abundant hard corals (*Leptoseris* sp.) were observed in video of the seabed on all three reefs. These species are typical of the inner-shelf coral reef association encountered in northern Australia (Veron, 1993; 2000). In addition, species of benthic biota found in the samples from the reefs are commonly found on tropical coral reefs in northern Australia. The species of fan sponge (*Ianthella basta*, *I. flabelliformis*) and one species of barrel sponge (*Xestospongia* sp.) and the gorgonian species are typical of the species commonly encountered on the seabed in channels of Torres Strait and the Great Barrier Reef. Larvae from the Arafura Sea and Torres Strait could be responsible for seeding these modern corals and associated communities (Veron, 1993), carried by a strong clockwise residual current that bring central Gulf waters over the reefs (Wolanski, 1993).

Ages of reefal sediment contained in cores collected adjacent to Reef R1 indicate that that the reefs were active and supporting living corals at least 9,000 years ago, approximately 1,000 years after the youngest lake sediments, as revealed by the ages from cores from the regional survey. The submerged reefs in the southern Gulf of Carpentaria are "give-up" reefs of Neuman and Macintyre (1985). The reasons they have not reached present sea level are because they contain insufficient Holocene coral framework deposition.

5.2.2.2. Implications for Quaternary reef development

The interpretation of the history of reef growth in the Gulf leads to several interesting insights about Quaternary reef growth around Australia. Today, most coral reefs in Australia are found mainly in the Great Barrier Reef and Ningaloo Reef regions. The discovery of well-developed submerged reefs in the southern Gulf of Carpentaria implies that the distribution of coral reefs around Australia for much of the late Quaternary might have been quite different. Indeed, the distribution of fossil reefs found on Lord Howe Island indicates that reef growth on the island has been more extensive than either the Holocene or Last Interglacial reefs on this marginal reef environment (Woodroffe et al., 2005).

While the submerged reefs in the Gulf were flourishing, it is likely that other regions of northern tropical Australia, such as the Timor and Arafura Seas, were similarly home to abundant coral reefs. An assessment of the bathymetry for the southern Gulf of Carpentaria reveals that there could be as many as 50 individual submerged platform reefs located in water depths of between 20-25 m. A follow up survey by Geoscience Australia to investigate

several of these highs (GA Survey 276) was completed in 2005 and revealed that in each casse they were submerged reefs supporting abundant living coral, including one case in the Arafura Sea (Harris et al., in press). The available data indicate that the reef province in the southern Gulf of Carpentaria and rest of northern Australia is much more extensive than previously recognised.

Dating of fossil samples from several submerged reefs could help to constrain palaeo sea level curves derived from uplifted coral terraces (Bard et al., 1990; Gvirtzman et al., 1992; Chappell et al., 1996). The submerged reefs in the Gulf of Carpentaria are located on a comparatively stable continental plate margin, and the extensive horizontal reef surfaces provide vertical reference points that appear to be tied to prolonged phases of lower sea level. Testing of this hypothesis awaits the collection of suitable material for radiometric dating, a principal objective of the follow-up survey conducted in 2005 (GA Survey 276).

Clearly, reef growth is not unique to interglacial periods since the seed stock must have come from somewhere. As such, submerged reefs may be important for regenerating coral assemblages in regions where surface-dwelling corals are subject to bleaching by sea surface temperatures exceeding 30° C. The thicker water column above submerged reefs filters out harmful solar radiation and ameliorates diurnal over-heating of the uppermost surface waters. The submerged reefs in the Gulf of Carpentaria are within the latitudinal belt (10 to 15°) predicted to be most affected by SST warming and coral bleaching (Sheppard, 2003). Sea surface temperatures in the central Gulf range from 28 to 30° C annually (Wolanski, 1993) and the data from this survey indicate that surface water temperatures over the reefs in May-June, 2003 were 28° C (Fig. 4.14). In areas that have suffered substantial bleaching, unaffected submerged reefs like those discovered in the Gulf could provide a refuge for corals and larvae for reseeding. Consequently, mapping of submerged reefs should be a priority for government agencies responsible for the management and protection of these important living marine resources (Hughes et al., 2003).

6. Acknowledgements

We thank the National Facility Steering Committee for making ship time available on the RV *Southern Surveyor*. Financial support for the survey was provided by Geoscience Australia, CSIRO and the Marine National Facility. Technical support for the survey was provided by Pamela Brodie and Steven Thomas (CSIRO), Jon Stratton and Lyndon O'Grady (Geoscience Australia), and Kevin Hooper (James Cook University). Preparation of the radiocarbon samples was undertaken by Dena Mazen (Geoscience Australia). Alex McLachlan, Neil Ramsay, Tony Watson, and Richard Brown of the sedimentology laboratory at Geoscience Australia managed all sample analyses and are thanked for their timely and efficient production of the texture and composition data. The video footage was edited and compiled by Jakob Harris (Geoscience Australia). We also thank Capt. Neil Cheshire, the officers and crew of the RV *Southern Surveyor* for helping us discover something new. The original report benefited from reviews by Drs John Marshall and Kriton Glenn of Geoscience Australia.

7. References

Baldwin, B. and Butler, J.R., 1982. Hamilton's Indonesia map and the Appalachian mountain system. *Journal of Geological Education* **30**, 93-96.

Bard, E., Hamelin, B. and Fairbanks, R.G., 1990. U-Th ages obtained by mass spectrometry in corals from Barbados: sea level during the past 130,000 years. *Nature* **346**, 456-458.

Chappell, J., Omura, A., Esat, T., McCulloch, M., Pandelfi, J., Ota, Y. and Pillans, B., 1996. Reconciliation of Late Quaternary sea levels derived from coral terraces at Huon Peninsula with deep sea oxygen isotope records. *Earth and Planetary Science Letters* **141**, 227-236.

Chivas, A.R., Garcia, A., van der Kaars, S., Coupel, M.J.J., Holt, S., Reeves, J.M., Wheeler, D.J., Switzer, A.D., Murray-Wallace, C.V., Baneriee, D., Price, D.M., Wang, S.X., Pearson, G., Edgar, N.T., Beaufort, L., De Deckker, P., Lawson, E. and Cecil, C.B., 2001. Sea-level and environmental changes since the last interglacial in the Gulf of Carpentaria, Australia: an overview. *Quaternary International* **83-85**, 19-46.

Damuth, J.E., 1980. Use of high-frequency (3.5-12 kHz) echograms in the study of near-bottom sedimentation processes in the deep-sea: a review. *Marine Geology* **38**, 51-75.

Dott, R.H. and Batten, R.L., 1976. *Evolution of the Earth*. McGraw-Hill, New York. 643p.

Edgar, N.T., Cecil, C.B., Mattick, R.E., Chivas, A.R., De Deckker, P. and Djajadihardja, Y.S., 2003. A modern analogue for tectonic, eustatic, and climate processes in cratonic basins: Gulf of Carpentaria, northern Australia. *In*: Cecil, C.B. & Edgar, N.T., (Eds.), *Climate Controls on Stratigraphy*, pp. 193-205. SEPM Special Publication **77**, Tulsa.

Edgar, N.T., Cecil, C.B., Grim, M.S. and Chappell, J., 1994. Allocyclic stratigraphy beneath the floor of the Gulf of Carpentaria, Northern Australia, based on high resolution seismic survey. *Geological Society of America Abstracts with Programs* **26**, A-229.

Gvirtzman, G., Kronfeld, J. and Buchbinder, B., 1992. Dated coral reefs of the southern Sinai (Red Sea) and their implication to late Quaternary sea levels. *Marine Geology* **108**, 29-37.

Harris, P.T., 1994. Comparison of tropical, carbonate and temperate, siliciclastic tidally dominated sedimentary deposits: examples from the Australian continental shelf. *Australian Journal of Earth Science* **41**, 241-254.

Harris, P.T., Heap, A.D., Marshall J., Hemer, M., Daniell, J., Hancock, A., Buchanan, C., Post, A., Passlow, V., Brewer, D., and Heales, D., in press. Submerged coral reefs and benthic habitats of the southern Gulf of Carpentaria - post survey report. Geoscience Australia, Record. Geoscience Australia, Canberra.

Harris, P.T., Heap, A.D., Passlow, V.L., Sbaffi, L., Fellows, M., Porter-Smith, R., Buchanan, C. and Daniell, J., 2004. Geomorphic features of the continental margin of Australia. *Geoscience Australia Record* **2003/30**. 146pp.

Harris, P.T., Baker, E.K. and Cole, A.R., 1991. Physical sedimentology of the Australian continental shelf, with emphasis on Late Quaternary deposits in major shipping channels, port approaches and choke points. *Ocean Sciences Institute, University of Sydney, Report No. 51*. 505pp.

Heap, A.D., Dickens, G.R. and Stewart, L.K., 2001. Late Holocene sediment in Nara Inlet, central Great Barrier Reef platform, Australia: sediment accumulation on the middle shelf of a tropical mixed clastic/carbonate system. *Marine Geology* **176**, 39-54.

Heap, A.D., Larcombe, P. and Woolfe, K.J., 1999. Storm-dominated sedimentation in a protected basin fringed by coral reefs, Nara Inlet, Whitsunday Islands, Great Barrier Reef, Australia. *Australian Journal of Earth Sciences* **46**, 443-451.

Hughes, T.P., Baird, A.H., Bellwood, D.R., Card, M., Connolly, S.R., Folke, C., Grosberg, R., Hoegh-Guldberg, O., Jackson, J.B.C., Kleypas, J., Lough, J.M., Marshall, P., Nystrom, M., Palumbi, S.R., Pandolfi, J.M., Rosen, B. and Roughgarden, J., 2003. Climate change, human impacts, and the resilience of coral reefs. *Science* **301**, 929-933.

Jones, B.G., Woodroffe, C.D. and Martin, G.R., 2003. Deltas in the Gulf of Carpentaria, Australia: forms, processes, and products. *In*: Sidi, F.H., Nummedal, D., Imbert, P., Darman, H. & Posamentier, H.W., (Eds.), *Tropical Deltas of Southeast Asia - Sedimentology, Stratigraphy, and Petroleum Geology*, pp.21-43. SEPM Special Publication **76**, Tulsa.

Jones, M.R., 1987. Surficial sediments of the western Gulf of Carpentaria. *Australian Journal of Marine and Freshwater Research* **38**, 151-167.

Jones, M.R., 1986. Surfical sediments of the central Gulf of Carpentaria. *Queensland Geological Survey Record* **1986/40**. 36pp.

Jones, M.R. and Torgersen, T., 1988. Late Quaternary evolution of Lake Carpentaria on the Australia-New Guinea continental shelf. *Australian Journal of Earth Sciences* **35**, 313-324.

Kershaw, A.P., van der Kaars, S. and Moss, P.T., 2001. Late Quaternary Milankovitch-scale climate change and variability and its impact on monsoonal Australasia. *Marine Geology* **201**, 81-95.

Macintyre, I.G., 1972. Submerged reefs of the eastern Carribean. *American Association of Petroleum Geologists Bulletin* **5**, 49-53.

Muller, G. and Gastner, M., 1971. The "Karbonate-Bombe", a simple device for the determination of the carbonate content in sediments, soils, and other materials. *Neues Jahrbuch fuer Mineraliogie* **10**, 466-469.

Neumann, A.C. and Macintyre, I.G., 1985. *Reef response to sea level rise: keep-up, catch-up, or give-up*. 5th International Coral Reef Congress, Tahiti. International Coral Reef Society, pp.105-110.

Phipps, C.V.G., 1980. The Carpentaria Plains. *In*: Henderson, R.A. & Stephenson, P.J., (Eds.), *The Geology and Geophysics of Northeastern Australia*, pp. 382-386. Geological Society of Australia, Brisbane.

Phipps, C.V.G., 1970. Dating of eustatic events from cores taken in the Gulf of Carpentaria and samples from the New South Wales continental shelf. *Australian Journal of Science* **32**, 329-331.

Searle, D.E. and Harvey, N., 1982. Interpretation of inter-reefal seismic data: a case study from Michaelmas Reef, Australia. *Marine Geology* **46**, M9-M16.

Shepard, C.R.C., 2003. Predicted recurrences of mass coral mortality in the Indian Ocean. *Nature* **425**, 294-297.

Stuiver, M., Pearson, G.W. and Braziunas, T.F., 1986. Radiocarbon age calibration of marine samples back to 9000 cal yr BP. *Radiocarbon* **28**, 980-1021.

Torgersen, T., Hutchinson, M.F., Searle, D.E. and Nix, H.A., 1983. General bathymetry of the Gulf of Carpentaria and the Quaternary physiography of Lake Carpentaria. *Palaeogeography, Palaeoclimatology, Palaeoecology* **41**, 207-225.

Veron, J.E.N., 1993. A Biogeographic Database of Hermatypic Corals: Species of the Central Indo-Pacific, Genera of the World. Monograph Series-Australian Institute of Marine Science, vol. 10. 433pp.

Veron, J.E.N., 2003. Corals of the World. Australian Institute of Marine Science, Townsville. 1410pp.

Wasson, R.J., Olive, L.J. and Rosewell, C.J., 1996. Rates of erosion and sediment transport in Australia. *In*: Walling, D.E. & Webb, B.W., (Eds.), *Erosion and Sediment Yield: Global and Regional Perspectives*, pp. 139-148. IAHS Publication **236**, Oxfordshire.

Wolanski, E., 1993. Water circulation in the Gulf of Carpentaria. *Journal of Marine Systems* **4**, 401-420.

8. Appendices

8.1. Appendix A – Survey Leaders Log

Geoscience Australia Survey 238 (SS04/2003), Gulf of Carpentaria 2003
Survey Leaders Log
RV *Southern Surveyor*

Friday, 9 May 2003. RV *Southern Surveyor* sailed from Cairns Slipways @ 0700 UTC, as per schedule and without incident. Scientific party were taken on a tour of the ship by the first mate John Boyes.

Saturday, 10 May 2003. Transit to start of survey. A presentation of the voyage scientific plan was given by the Chief Scientist (Peter Harris) @ 1030 UTC. A proposed list of stations for the first phase of the survey was delivered to the bridge.

Sunday, 11 May 2003. Fire drill @ 1030 UTC. John Stratton advised that the Boomer digital acquisition system was damaged during a power outage on the ship on the 10/05/03. Discovered that EPC recorder hired from Seismic Supply in Brisbane was faulty and was returned 2 weeks ago for repairs but was not sent back in time for our departure.

Monday, 12 Mary 2003. Arrived at the first station @ 0020 UTC. Station operations were CTD, camera, grab and dredge. Station 2 completed @ 1000 UTC. Station 5 completed @ 2350 UTC. In traversing the assumed location of the Lake Carpentaria shoreline at 55 m water depth we did not see any indication of a beach or coastline depositional system in the chirp or side scan image. The un-named shoal appears to be a (Holocene?) sedimentary deposit as a positive relief feature was seen to overlie a horizontal reflector. This may be the new objective of the Area C survey. Kevin Hooper has managed to rig up another EPC recorder from JCU so that we can print the Chirp data as we survey – this will greatly improve our ability to monitor changes in the subsurface and plan our eventual coring stations.

Tuesday, 13 May 2003. Deployed the current meter frame BRUCE this evening and mapped three test-trawl survey areas under investigation by the CSIRO. The seabed in the BRUCE area has some rocky features and bedforms. The CSIRO trawl areas appeared to be flat and featureless and we could see no indication of trawl marks on the seabed in our side scan sonar images.

Wednesday, 14 May 2003. Continued long survey, finishing line 2 and started line 3. Encountered some muddy deltaic sediments along Line 2 and first indication of anoxic (H_2S) sediments at Station 12.

Thursday, 15 May 2003. Completed Line 3 and Station 16 this evening. Sediments at station 15, SE of Mornington Island are well-sorted, fine muddy sand. The relict Norman River channel is evident in our seismic data and has been crossed on all lines so far. It is best developed on the western edge of line 3. Based on the crossing of the proposed position of Area A and its flat, uninteresting character, I have consulted with Andrew Heap and we decided to forgo the detailed multibeam survey here and to collect a set of vibrocores over a broad area instead, to compliment the seismic data. We intend to complete a multibeam survey of Area B as planned.

Friday, 16 May 2003. Continued multibeam (swath) mapping and station work. Two extra stations and a new section of multibeam/seismic survey were added, with the aim of arriving at the first vibrocore station in the morning. A total of ~900 line km of multibeam/chirp survey have been completed so far.

Saturday, 17 May 2003. First vibrocore completed @ 1000 UTC and second core before lunch. Delay to first core of ~2UTC was caused by faulty wiring of the power cable termination. Fortunately a second back-up cable had been prepared by the science technicians otherwise a much longer delay would have occurred. By midnight 6 vibrocores up to 4.5 m in length were completed. The new GA vibrocore system, with modified deck-trolly has performed very well. It is now much safer and more reliable than the older version. I am also impressed with the performance of the GA vibrocore tower, although its legs drag on the trawl deck doors and could hang-up on them. The very calm sea conditions have continued, making our work much easier.

Sunday, 18 May 2003. Eight more vibrocores collected today, along with CTD, camera, grab and dredging operations.

Monday, 19 May 2003. The 18th vibrocore was collected today @ 1100 UTC, completing the sampling work for this part of the survey. Transit to area B to start swath mapping, which commenced @ 1400 UTC. Sighted the surface floats for BRUCE, with only yellow and two white floats showing, the rest submerged below a strong southerly tidal current.

Tuesday, 20 May 2003. Swath mapping of Area B continues. Completed about twenty 10 km lines in the first 24 hours, so are on target to complete ~100 lines in 5 days. Meanwhile, the science technicians have completed repairs to the cable for the underwater camera, which had been broken.

Wednesday, 21 May 2003. Swath mapping of Area B continues. Today we saw the first gridded bathymetry map generated using the new data, which showed what appears to be a relict reef in about 30 m depth, with a distinctive flat top and doline Karst features (sink holes). It is surrounded by two channels up to 45 m in depth. The reef was part of what may have been a much larger reef complex that grew in the Gulf of Carpentaria when sea level was 30 m lower than present during the late Plesitocene period. If this hypothesis is correct, it could be a major finding of our voyage. Sampling of the features to prove their reefal origins has become a major goal of the sampling program.

Thursday, 22 May 2003. Swath mapping of Area B continues. Today we completed our 78th 10 km line.

Friday, 23 May 2003. Swath mapping of Area B continues. Completed E-W swath lines and started N-S lines.

Saturday, 24 May 2003. Completed swath mapping of Area B @ 0600 UTC (1,820 line-km completed on voyage so far). Commenced sampling program.

Sunday, 25 May 2003. Commenced sampling in Area B. Strong wind from 0500 UTC onwards forced a stop of work in the morning shift. However, wind had died down by 1100 UTC. Our 27th vibrocore and 4th rock dredge was collected today and station 61 completed. Sampling has confirmed the reef feature is a relict carbonate deposit of

unknown age. Several samples of weathered and iron stained limestone (packstone/boundstone) have been recovered in dredge and grab samples. The banks appear to be comprised mainly of molluscs (pearl shell) and bryozoans. Interestingly, no living pearl shells have been recovered in any of our benthic sleds. Vibrocoring has produced mainly short core samples terminating in hard clay or sand. On one reef-top station a plug of hard lime sand was in the core cutter. Another break in the new camera cable has caused us to abandon use of the camera winch and to deploy via the main coring winch, using cable ties to attach the camera cable. This has slowed the camera deployment and removes our ability to remotely operate the winch from the video monitor station.

Monday, 26 May 2003. Sampling continues in Area B. Strong wind up to 35 knots from 0500 UTC onwards again forced a stop of work in the morning shift. Wind had died down by 1100 UTC and sea conditions abated so sampling could continue. An electrical fault in the main winch stopped the work program for 4 hours @ 1630 UTC. The winch paid out wire and then pulled it in without command from the winch operator. No fault could be detected but because the system is unreliable, it has been decided that henceforth the winches will be operated manually. Station 70 was completed today.

Tuesday, 27 May 2003. Station 75 completed this morning before strong winds forced us to stop the sampling program @ 0600 UTC. It was decided to continue swath mapping the southern part of Area B. At 1600 UTC we successfully recovered the current meter frame BRUCE and began the transit to Area C.

Wednesday, 28 May 2003. Started long survey lines in Area C @ 0100 UTC and discovered that the un-named shoal is also comprised of flat-topped, reef-like features. Completed long lines @ 0700 UTC and selected a 10x10 km grid for detailed swath survey. Lines were extended to 11.5 km length after it was seen the feature would extend beyond 10 km in length.

Thursday, 29 May 2003. Continued swath survey of Area C. Completed 21 lines before breaking off the survey to head for Weipa @ 1330 UTC for refuelling. Based on the opaque seismic character of the reef top, it was decided to try using the Sparker system when we return, to attempt to see through to the basement structure.

Friday, 30 May 2003. Port call to Weipa. The vessel arrived offshore of the port @ 0700 UTC and took aboard the pilot @ 0800 UTC. Along side the jetty @ 0930 UTC. The scientific party had a pleasant interlude ashore. Local fisherman informed us the unofficial name of the reefs we are mapping in Area C is "The Lost City", presumably because the flat-tops and vertical walls of the reefs appear like submerged buildings on an echo sounder. After loading 35 tonnes of fuel, ship departed Weipa @ 1500 UTC and headed back to Area C.

Saturday, 31 May 2003. Continued mapping Area C on our arrival from Weipa, @ 0730 UTC. By 2400 UTC we had completed the 32nd line in this area.

Sunday, 1 June 2003. Continued mapping Area C. Completed 2,597 line-km of swath sonar by 1600 UTC.

Monday, 2 June 2003. Continued mapping Area C. Saw the first print-out of Area C and spent some time with Andrew Heap selecting sampling stations. We plan to start the

sampling work by mid-day tomorrow. Sparker data has revealed a sub-surface reflector exhibiting positive relief under the reefal mound. Sad news today when we learned of the death of the 8 yr old niece of Chris McGuire (2nd Mate). Options are being considered to drop Chris off at a port nearby or along route.

Tuesday, 3 June 2003. Completed swath mapping Area C @ 1900 UTC and commenced sampling program.

Wednesday, 4 June 2003. A major discovery! Sampling of the reef top has confirmed that this is indeed a coral reef, but it is a living reef, with luxuriant coral growth on elevated surfaces and even within the flat reef top (relict lagoon). It appears to be the largest continuous area of modern reef growth discovered in Australia outside of the Great Barrier Reef and Ningiloo Reef complexes.

Thursday, 5 June 2003. Sampling work completed @ 1700 UTC. A 4.2 m long vibrocore was collected from an area of wavy surface adjacent to the southern flank of the reef and was found to be unconsolidated muddy carbonate sand throughout. This appears to be an important sediment sink for the reef system. Commenced final phases of swath mapping @ 1800 of two smaller reef features to the SW.

Friday, 6 June 2003. Completed swath mapping of two smaller reefs @ 1900 UTC. Sparker data has revealed a sub-surface reflector exhibiting positive relief under both of the reefal mounds. Camera and grabs show that the smallest, SW-most reef in the group appear to have had hard corals growing on it in the recent past based on samples in the grabs, but we saw little evidence for modern corals in the video imagery. Instead there is mainly soft corals, sponges, crinoids and hydroids living here. The middle-reef supports luxuriant hard corals on its uppermost surface but mainly soft corals, sponges and hydroids elsewhere.

Saturday, 7 June 2003. Completed sampling work @ 0415 UTC. Transit to Gove, where we will disembark the second mate, Chris McGuire, for compassionate leave, before sailing on to Darwin. The scientific part of the survey is now completed after 117 stations being completed, including 108 grab samples, 101 camera deployments, 62 benthic sleds, 58 CTDs, 40 vibrocores and 11 rock dredges. We have collected 3,275 line-km of swath sonar and Chirp seismic data plus some 400 line-km of sparker data. In our survey we have mapped about 0.01% of the Gulf of Carpentaria, which means it would take us another 830 years to map the rest!

Sunday, 8 June 2003. Arrived in Gove Harbour @ 0700 UTC and dropped off the 2nd mate. On our way to Darwin. Packing up computers and sampling equipment.

Monday, 9 June 2003. Continued transit to Darwin.

Tuesday, 10 June 2003. Arrived in Darwin harbour @ 0800 UTC. Demobilisation of ship.

Wednesday, 11 June 2003. Science and technical parties depart for Canberra.

8.2. Appendix B – Shallow Seismic Reflection Profiles

Figures showing the shallow seismic reflection profiles are provided on the data DVD in Windows JPEG format. The figures are obtained from the seismic viewing program SeiSee, a freeware package produced by the Russian geophysical company DMNG. The filenames follow the convention: *GA survey number_Area_Line Number*. (e.g., 238_AreaA_400). The line numbers indicate the distance in metres from the northern-most line. The latitudes and longitudes and shot points for the beginning and end of the lines are contained in the accompanying Excel spreadsheet called "line_locations.xls".

8.3. Appendix C – Photographs of the BRUCE Mooring

Photos of the BRUCE mooring are provided on the data DVD in jpg format.

8.4. Appendix D – Digital Video Footage

Excerpts of the digital video footage for select sites are provided on the data DVD in mpeg format. The filenames follow the convention: *GA Survey Number_Station Number, Operation Type* and *Operation Number* (e.g., 238_11CAM11).

8.5. Appendix E – Scheffe's Test Results for CTD Data

Tables showing the probabilities for the post-hoc Scheffe's Tests are provided on the data DVD in Microsoft Excel format. Statistically significant probabilities at 95% confidence are italicised and highlighted in red.

8.6. Appendix F – Photographs of Benthic Biota

Photos of the biota collected in the benthic sleds, surface grabs, and dredges are provided on the data DVD in jpg format. The filenames follow the convention: *GA Survey Number_Station Number, Operation Type* and *Operation Number* (e.g., 238_01BS01; 238_39GR38, 238_43DR01). Some file names contain a letter suffix that refers to the sub-sample that was collected for biology (e.g., 238_06BS06A).

8.7. Appendix G –Textural Characteristics of Surface Sediments

The tables below show the textural data for each surface sample based on sieve analysis and carbonate bomb analysis, and are thus expressed as weight percents. Grainsize distribution graphs and associated data from the Malvern™ Mastersizer-2000 laser particle analyser are contained on the data DVD in pdf format. The filenames of the graphs follow the convention: 5-*digit Lab* Number, *Survey Number*, *Station Number*, *Operation Type*, and *Operation Number* (e.g., 22484_238/1GR01).

Table 8.1a. Textural characteristics of surface sediment samples collected in Area A: Regional Survey.

Sample Id	Latitude	Longitude	%Gravel	%Sand	%Mud	$\%CaCO_3$ (Bulk)	$\%CaCO_3$ (Sand)	$\%CaCO_3$ (Mud)
238/1GR1	-14.160	140.201	8.54	60.38	31.08	59.79	82.11	30.36
238/2GR2	-14.505	140.201	6.70	50.79	42.50	60.81	90.23	28.34
238/3GR3	-14.834	140.201	2.38	80.11	17.50	18.19	22.25	30.36
238/4GR4A	-15.166	140.200	3.91	76.31	19.77	28.34	35.44	35.44
238/5GR5A	-15.399	140.199	2.97	90.09	6.93	40.51	46.60	35.44

238/6GR6A	-15.084	140.200	5.61	70.32	24.07	41.02	48.63	33.41
238/7GR7A	-16.167	140.200	7.99	74.67	17.34	37.47	35.44	28.34
238/8GR8A	-16.500	140.201	4.24	86.53	9.23	31.89	38.48	23.26
238/9GR9A	-16.499	139.935	20.54	70.49	8.97	31.4	17.2	15.1
238/10GR10	-16.835	140.199	3.67	81.93	14.40	27.32	30.36	17.17
238/11GR11A	-17.216	140.199	3.11	78.82	18.07	19.20	22.25	18.19
238/12GR12	-17.046	140.498	5.29	77.74	16.97	25.29	30.36	18.19
238/13GR13A	-16.862	140.830	4.80	78.05	17.14	12.10	10.07	17.17
238/14GR14A	-16.851	140.501	4.88	79.09	16.03	32.39	37.47	23.26
238/15GR15A	-16.849	139.790	0.14	88.54	11.32	11.09	15.14	13.11
238/16GR16A	-16.708	140.000	12.58	73.18	14.23	42.54	41.53	24.28
238/17GR17A	-16.613	140.567	2.22	89.65	8.13	32.39	35.44	25.29
238/18GR18A	-16.500	140.932	0.11	97.59	2.30	14.13	17.17	I/S
238/19GR19A	-16.501	140.567	8.83	90.56	0.61	62.83	64.86	I/S
238/20GR20A	-16.749	139.882	15.58	76.07	8.35	18.19	14.13	15.14
238/21GR21A	-17.000	139.884	2.31	83.42	14.26	22.25	43.56	16.16
238/22GR22A	-16.850	139.885	5.63	82.84	11.53	24.28	39.50	15.14
238/23GR23A	-16.849	139.909	3.32	84.77	11.92	27.32	36.45	15.14
238/24GR24A	-17.204	140.221	3.34	75.61	21.05	18.19	21.23	19.20
238/25GR25A	-17.206	140.215	3.89	76.34	19.77	22.25	30.36	18.19
238/26GR26A	-17.107	140.396	3.72	72.28	24.00	26.31	35.44	24.28
238/27GR27	-17.102	140.403	4.47	73.87	21.66	23.26	36.45	18.19
238/28GR28A	-17.098	140.411	2.21	75.34	22.45	24.28	32.39	22.25
238/29GR29A	-16.851	140.322	3.38	81.28	15.34	30.36	30.36	24.78
238/30GR30A	-16.851	140.336	2.64	77.65	19.71	30.36	33.41	23.26
238/32GR31A	-16.556	140.751	13.26	84.16	2.58	45.58	63.85	I/S
238/33GR32A	-16.501	140.522	6.01	86.20	7.79	46.60	51.67	26.31
238/34GR33A	-16.615	140.562	9.14	87.01	3.85	45.58	50.66	I/S
238/35GR34A	-16.707	140.261	5.93	81.17	12.90	31.38	43.56	21.74
238/36GR35A	-16.710	140.251	11.91	72.66	15.43	40.51	42.54	24.28
238/37GR36A	-16.681	140.200	7.73	77.72	14.55	27.32	33.41	23.26
238/38GR37A	-16.808	139.928	4.15	86.11	9.74	24.28	41.53	16.16
238/39GR38A	-16.818	139.897	3.55	95.80	0.64	20.22	28.34	I/S
238/22VC1/0-2	-16.850	139.885	3.46	84.57	11.97	24.28	30.36	14.64
238/23VC2	-16.850	139.909	2.85	83.84	13.30	28.02	31.89	I/S
238/24VC3	-17.204	140.221	3.44	81.22	15.34	22.25	19.20	I/S
238/25VC4	-17.206	140.215	2.26	76.57	21.18	18.19	21.74	18.19
238/26VC5	-17.107	140.396	2.01	79.08	18.91	27.32	32.39	19.71

Table 8.1b. Textural characteristics of surface sediment samples collected in Area B: Bryomol Reef.

Sample Id	Latitude	Longitude	%Gravel	%Sand	%Mud	$\%CaCO_3$ (Bulk)	$\%CaCO_3$ (Sand)	$\%CaCO_3$ (Mud)
238/41GR39A	-16.512	139.909	19.78	71.77	8.45	27.3	32.4	16.2
238/42GR40A	-16.513	139.898	29.47	56.69	13.84	62.8	76.0	17.2
238/43GR41A	-16.497	139.915	47.75	44.86	7.39	53.7	57.8	17.2

238/44GR42A	-16.485	139.923	64.25	31.88	3.87	57.8	55.7	I/S
238/45GR43A	-16.510	139.948	30.42	57.47	12.10	41.5	39.5	12.1
238/46GR44A	-16.516	139.945	19.85	60.61	19.54	35.4	39.5	13.1
238/47GR45A	-16.487	139.941	26.25	54.57	19.18	25.8	14.1	7.0
238/48GR46	-16.480	139.886	17.20	82.71	0.09	74.0	87.2	I/S
238/49GR47A	-16.497	139.893	38.48	60.92	0.61	61.8	61.8	I/S
238/49GR48A	-16.497	139.893	37.24	61.85	0.91	74.0	80.1	I/S
238/50GR49A	-16.501	139.889	39.76	48.85	11.38	67.9	67.9	17.2
238/51GR50A	-16.526	139.876	37.56	57.86	4.58	62.8	76.0	I/S
238/52GR51	-16.534	139.879	42.32	52.23	5.44	69.9	67.9	15.1
238/53GR52	-16.546	139.892	21.69	53.98	24.34	41.5	50.7	9.6
238/54GR53A	-16.514	139.869	33.75	64.54	1.71	73.0	73.0	I/S
238/55GR54A	-16.487	139.884	25.07	66.44	8.48	65.9	73.0	20.2
238/58GR55A	-16.542	139.963	33.17	60.21	6.62	42.5	52.7	I/S
238/59GR56A	-16.529	139.940	36.80	52.98	10.22	56.7	71.0	17.2
238/60GR57A	-16.469	139.927	41.94	54.85	3.21	73.0	84.1	I/S
238/61GR58	-16.475	139.925	36.31	44.06	19.63	61.8	47.6	16.2
238/62GR59A	-16.451	139.902	43.44	54.68	1.87	79.6	72.0	I/S
238/63GR60A	-16.433	139.958	25.40	62.39	12.21	39.5	50.7	18.2
238/64GR61	-16.449	139.931	31.12	47.78	21.09	50.7	63.8	15.1
238/65GR62A	-16.442	139.916	31.50	54.97	13.52	53.7	55.7	18.2
238/66GR63A	-16.494	139.888	19.89	78.21	1.90	55.7	53.7	I/S
238/67GR64A	-16.439	139.879	34.53	61.55	3.93	55.7	39.5	I/S
238/67GR65A	-16.439	139.872	70.14	27.94	1.92	66.9	56.7	I/S
238/68GR66A	-16.443	139.847	17.69	82.21	0.10	78.1	85.2	I/S
238/69GR67A	-16.445	139.866	18.82	80.83	0.35	77.0	84.1	I/S
238/70GR68A	-16.452	139.879	20.99	70.48	8.53	45.6	59.8	16.2
238/71GR69A	-16.461	139.905	32.12	65.16	2.72	71.0	77.0	I/S
238/72GR70A	-16.493	139.884	56.96	38.31	4.73	52.7	38.5	17.2
238/73GR71A	-16.458	139.850	23.52	76.19	0.29	72.0	79.1	I/S
238/74GR72A	-16.481	139.907	43.17	51.33	5.50	20.2	29.3	17.2
238/75GR73A	-16.526	139.910	31.52	57.32	11.17	41.5	55.7	17.2

Table 8.1c. Textural characteristics of surface sediment samples collected in Area C: Reef R1.

Sample Id	Latitude	Longitude	%Gravel	%Sand	%Mud	$\%CaCO_3$ (Bulk)	$\%CaCO_3$ (Sand)	$\%CaCO_3$ (Mud)
238/79GR74	-15.262	140.382	3.52	76.55	19.93	34.4	38.5	32.4
238/80GR75A	-15.349	140.382	23.86	55.10	21.05	58.8	72.0	36.5
238/81GR76	-15.351	140.341	0.39	76.64	22.97	62.8	83.1	38.5
238/82GR77A	-15.333	140.330	24.98	74.46	0.56	91.2	93.3	I/S
238/83GR78A	-15.302	140.340	14.35	84.97	0.68	90.2	92.3	I/S
238/85GR79A	-15.266	140.347	4.17	76.68	19.15	42.5	56.7	40.5
238/86GR80A	-15.285	140.339	24.63	73.88	1.48	91.2	94.3	I/S
238/87GR81A	-15.295	140.325	20.96	77.91	1.13	90.2	92.3	I/S
238/88GR82A	-15.268	140.319	91.35	7.88	0.77	85.2	92.3	I/S
238/89GR83	-15.255	140.329	5.23	69.17	25.60	49.6	56.7	35.4

238/90GR84	-15.265	140.291	23.64	64.69	11.66	81.1	94.3	36.5
238/91GR85	-15.280	140.285	17.48	66.65	15.87	81.1	98.3	34.4
238/93GR87A	-15.249	140.307	28.45	58.97	12.57	75.0	87.2	38.5
238/94GR88A	-15.305	140.299	9.71	89.46	0.83	90.2	92.3	I/S
238/96GR89A	-15.326	140.297	31.35	68.25	0.39	92.3	92.3	I/S
238/97GR90A	-15.329	140.295	16.75	82.53	0.72	92.3	91.2	I/S
238/98GR91A	-15.324	140.284	26.04	71.07	2.88	88.2	90.2	I/S
238/99GR92A	-15.329	140.280	15.54	81.79	2.68	86.2	88.2	I/S
238/100GR93A	-15.338	140.275	15.09	73.21	11.70	71.0	75.0	37.5
238/102GR94A	-15.341	140.284	4.29	86.93	8.78	77.0	86.2	36.5
238/103GR95A	-15.353	140.288	1.17	84.56	14.27	72.0	80.1	39.5
238/104GR96A	-15.343	140.308	0.33	93.66	6.01	84.1	89.2	44.6
238/105GR97A	-15.341	140.374	28.51	59.02	12.47	75.0	86.2	37.5
238/80VC29	-15.349	140.382	30.30	49.99	19.71	72.5	75.5	36.1
238/81VC30	-15.351	140.341	0.78	73.05	26.17	64.9	78.1	39.5
238/90VC34	-15.264	140.291	19.69	70.77	9.54	85.2	93.3	43.0
238/100VC37	-15.338	140.275	13.57	70.21	16.21	71.0	80.1	I/S
238/104VC40	-15.343	140.308	0.00	90.51	9.49	85.7	90.7	I/S

Table 8.1d. Textural characteristics of surface sediment samples collected in Area D: Reef R2.

Sample Id	Latitude	Longitude	%Gravel	%Sand	%Mud	%$CaCO_3$ (Bulk)	%$CaCO_3$ (Sand)	%$CaCO_3$ (Mud)
238/112GR104A	-15.464	140.169	7.68	79.36	12.96	82.1	92.3	38.5
238/114GR105	-15.445	140.176	32.51	66.24	1.25	91.2	94.3	I/S
238/115GR106A	-15.447	140.165	14.08	65.97	19.96	71.0	91.2	37.5
238/116GR107	-15.445	140.187	19.65	78.00	2.35	69.9	75.0	I/S
238/117GR108A	-15.432	140.175	24.27	61.78	13.96	55.7	65.9	34.4

Table 8.1e. Textural characteristics of surface sediment samples collected in Area E: Reef R3.

Sample Id	Latitude	Longitude	%Gravel	%Sand	%Mud	%CaCO3 (Bulk)	%CaCO3 (Sand)	%CaCO3 (Mud)
238/106GR98	-15.528	140.107	17.85	68.04	14.11	81.1	94.3	32.4
238/108GR100A	-15.525	140.113	14.61	83.92	1.47	92.3	91.2	I/S
238/111GR103	-15.510	140.115	12.40	59.91	27.68	50.7	59.8	29.3

I/S = insufficient sample for analysis.

8.8. Appendix H – Core Logs

The core logs contain the physical property data (Bulk Density, Fractional Porosity, and colour), texture and composition information, visual log (including digital images) and comments on specific features. The core logs are contained on the data DVD in jpg format. The filenames follow the convention: *GA Survey Number_Station Number, Operation Type, Operation Number* (e.g., 238_45VC19). High-resolution digital photographs of the cores are also contained in the Appendix. The filenames follow the convention: *GA Survey Number_Station Number, Operation Type, Operation Number*, and *Interval Depth* (e.g., 238_22VC01_0-33cm).

8.9. Appendix I – Textural Characteristics of Subsurface Sediments

The tables below show the textural data for the sub-samples collected from the vibrocores. The data are based on sieve analysis and carbonate bomb analysis, and are thus expressed as weight percents. Grain size distributions for all of the subsurface samples are expressed as volume percentages measured from the Malvern™ Mastersizer-2000 laser particle analyser can be found on the accompanying data DVD. Grainsize distribution graphs and associated data from the Malvern are contained on the data DVD in pdf format. The filenames follow the convention: 5-*digit Lab Number*, *GA Survey Number*, *Station Number, Operation Type, Operation Number*, and *Sub-sample Depth Interval* (e.g., 24213 238/104VC40 0-2). Histograms of the colour spectrum from the digital scans of the cores are also included on the data DVD. The histograms are broken down by area and show the distribution of pixel intensities for the red, green and blue phases for each facies.